UNIVERSIDADE D
COIMBRA

Miguel Ângelo Reis Pereira

CRITICAL ANALYSIS OF THE WELDING PARAMETERS BY FRICTION STIR WELDING OF POLYMERIC MATERIALS

Dissertação no âmbito do Mestrado Integrado em Engenharia Mecânica, no ramo de produção e projeto orientada pela Professora Doutora Ana Paula Bettencourt Martins Amaro e Professor Doutor Paulo Nobre Balbis dos Reis apresentada ao Departamento de Engenharia Mecânica da Universidade de Coimbra.

Setembro de 2020

1 2 9 0

FACULDADE DE CIÊNCIAS E TECNOLOGIA
UNIVERSIDADE D COIMBRA

Critical analysis of the welding parameters by friction stir welding of polymeric materials

Submitted in Partial Fulfilment of the Requirements for the Degree of Master in Mechanical Engineering in the speciality of Production and Project

Análise crítica dos parâmetros de soldadura por fricção linear na ligação de materiais poliméricos

Author

Miguel Ângelo Reis Pereira

Advisors

Ana Paula Bettencourt Martins Amaro

Paulo Nobre Balbis dos Reis

Jury

President	**Professor Doutor Altino de Jesus Roque Loureiro** **Professor Catedrático da Universidade de Coimbra**
Vowel	**Professor Doutor Rui Manuel Ferreira Leal** **Professor Adjunto do Instituto Politécnico de Leiria**
Advisor	**Professora Doutora Ana Paula Bettencourt Martins Amaro** **Professora Auxiliar da Universidade de Coimbra**

Coimbra, September, 2020

ACKNOWLEDGEMENTS

The work presented here was only possible thanks to the collaboration of some people, to whom I cannot but thank.

First, I would like to express my sincere gratitude to my advisors Prof. Dr. Ana Paula Bettencourt Martins Amaro and Prof. Dr. Paulo Nobre Balbis dos Reis for having supported and motivated me throughout my entire thesis.

Secondly, I would like to thank my parents, my grandparents and my sister from the bottom of my heart to whom I owe everything I am as a person and who, despite not gathering the scientific knowledge to help me in the elaboration of the thesis, never stopped giving me support, affection and love throughout this journey.

Finally, I would like to thank my girlfriend Carolina for her patience and for having accompanied me in all the important moments.

Abstract

The work presented here corresponds to a bibliographic review on the union of polymeric materials by friction stir welding (FSW), with special focus on the analysis of the different parameters involved in this welding process.

Due to the greater difficulty in obtaining strong joints with the conventional FSW method in polymeric materials, new tools and changes on the original process were developed, which were also presented and explained in this work.

The main focus of this work was on the study of the influence of the different parameters on the quality of the welding, so that as much information as possible was gathered regarding the optimal values for each parameter and the way in which its variation affected the performance of the process.

The studied parameters were the rotational speed, the welding speed, the axial force, the plunge depth, the tilt angle, the geometry and the size of the different components of the tool and also the heating and preheating temperatures of the tool and of the material.

The comparison between the results obtained by the different researchers revealed that the optimal value for each parameter is dependent on too many factors and that, therefore, it is impossible to point to specific values. Based on the information collected in the literature on the joining of polymeric materials by FSW, the concentration of the optimum values was found for rotational speed between 300 and 3000 rpm, welding speed between 10 and 105 mm/min , axial force between 950 and 1500 N, plunge depth between 0.5 and 1.2 mm, tilt angle between 1º and 2º and heating temperature between 45 and 177ºC. It was also found that in most cases, the threaded pin tool led to better welds, as well as the use of stationary shoulder tools.

Keywords Friction Stir Welding (FSW), Polymeric Materials, Welding Parameters.

Resumo

O trabalho aqui apresentado corresponde a uma revisão bibliográfica sobre a união de materiais poliméricos recorrendo à soldadura por fricção linear (FSW, do inglês Friction Stir Welding), com especial foco na análise dos diferentes parâmetros envolvidos neste processo de soldadura.

Pela maior dificuldade em obter ligações fortes com o método de FSW convencional em materiais poliméricos, foram desenvolvidas novas ferramentas e sugeridas alterações ao processo original, as quais também foram apresentadas e explicadas neste trabalho.

O grande foco deste trabalho centrou-se no estudo da influência dos diferentes parâmetros na qualidade da soldadura, pelo que se tentou reunir o máximo de informação relativa aos valores ótimos para cada parâmetro e avaliar a forma de como a sua variação afetou o desempenho do processo.

Os parâmetros estudados foram a velocidade de rotação, a velocidade de soldadura, a força axial, a profundidade de penetração, o ângulo de ataque, a geometria e o tamanho dos diferentes componentes da ferramenta e ainda a temperatura de aquecimento e pré-aquecimento da ferramenta e do material.

A comparação entre os resultados obtidos pelos diferentes investigadores revelou que o valor ótimo para cada parâmetro está dependente de demasiados fatores e que por isso, é impossível apontar valores específicos. Com base na informação recolhida da literatura sobre a união de materiais poliméricos por FSW, verificou-se a concentração dos valores ótimos de velocidade de rotação entre 300 e 3000 rpm, de velocidades de soldadura entre 10 e 105 mm/min, de força axial entre 950 e 1500 N, de profundidades de penetração entre 0.5 e 1.2 mm, de ângulo de ataque entre 1º e 2º e de temperaturas de aquecimento entre 45 e 177ºC. Também se verificou que na maioria dos casos a ferramenta de pino roscado permitiu a obtenção de melhores soldaduras, assim como a utilização de bases estacionárias.

Palavras-chave: Soldadura por Fricção Linear (FSW), Materiais Poliméricos, Parâmetros de Soldadura.

Contents

LIST OF FIGURES ix
LIST OF TABLES xiii
LIST OF ACRONYMS/ABBREVIATIONS xv
1. INTRODUCTION 1
2. FSW IN CONTEXT OF JOINING METHODS 3
3. MAIN CHARACTERISTICS OF THE FSW PROCESS 7
4. EFFECT OF DIFFERENT PARAMETERS ON FSW 19
4.1. Introduction 19
4.2. Rotational speed effect 21
4.2.1. Polyethylene (PE) 21
4.2.2. Polypropylene (PP) 26
4.2.3. Acrylonitrile butadiene styrene (ABS) 27
4.2.4. Polyamides (PA) 29
4.2.5. Other materials 31
4.2.6. Joints with dissimilar materials 32
4.3. Welding speed effect 33
4.3.1. Polyethylene (PE) 33
4.3.2. Polypropylene (PP) 36
4.3.3. Acrylonitrile butadiene styrene (ABS) 37
4.3.4. Polyamide (PA) 39
4.3.5. Other materials 40
4.3.6. Joints with dissimilar materials 42
4.4. Axial force effect 44
4.5. Plunge depth effect 45
4.6. Tilt angle effect 47
4.7. Pin geometry and size effect 50
4.7.1. SRFSW – pin geometry 56
4.8. Shoulder geometry and size effect 56
4.9. Material preheating temperature effect 58
4.10. Tool temperature effect 59
5. CONCLUSIONS AND SUGGESTIONS FOR FUTURE WORKS 65
5.1. Conclusions 70
5.2. Suggestions for future works 73
BIBLIOGRAPHY 75

LIST OF FIGURES

Figure 2.1. Diagram of the main polymer bonding methods, adapted from [3], [4]. 3

Figure 3.1. (a) Schematic illustration of the FSW process with conventional tool. (b) Real image of a conventional tool used on FSW [16]. 7

Figure 3.2. (a) FSW in: butt joint configuration, (b) lap join configuration [16]and T-joint configuration [19]. 7

Figure 3.3. Schematic illustration of the different regions of the microstructure and of the AS and RS [25]..... 9

Figure 3.4. Root defect: (a) schematic illustration adapted from [28] and (b) real example [29]. 9

Figure 3.5. Real example of flash defect produced by FSW [30]. 10

Figure 3.6. Presence of empty spaces within the WN [31]. 10

Figure 3.7. (a) Clean pin before FSW, (b) formation of BUE around the pin and (c) formation of BUE around the pin and under the shoulder [32]..... 11

Figure 3.8. (a) Temperature measured at the beginning (i-P), at the middle (m-P) and at the end (f-P) points of the weld. (b) Face bending strength of the material from the different zones [34]. 11

Figure 3.9. Axial force measurements during FSW process with: (a) conventional tool [35] and (b) conventional and stationary shoulder tool [36]..... 12

Figure 3.10. Schematic illustration of the cross section of the joint produced by FSW with double side pass of the tool [27]..... 12

Figure 3.11. Illustration of the exploded view of the tool used in the SRFSW [40]. 13

Figure 3.12. Example of the assembly of a stationary shoulder tool[41]. 14

Figure 3.13. Stationary shoulder tool with bronze sleeve: (a) schematic illustration and (b) real image [36]..... 15

Figure 3.14. Schematic drawing of the construction of a common heated shoe [46]. Hot shoe used by Mendes et al. (2014) [45]..... 16

Figure 3.15. (a) Schematic illustration of the tool used on i-FSW. (b) Experimental set-up for i-FSW [30]. (c) Schematic illustration of a new heated tool by electric resistance [46]..... 17

Figure 3.16. (a) Schematic illustration of the new developed tool heated by a hot air gun. (b) Welding assembly during the process [47]..... 17

Figure 3.17. Effect on the surface finish of the weld with an hot shoe: (a) without coating and (b) with PTFE coating [48]..... 18

Figure 4.1. FSW stages [51]. 19

Figure 4.2. Schematic illustration of: (a) rotational speed, welding speed and axial force, adapted from [53] and (b) plunge depth and tilt angle, adapted from [54]. 20

Figure 4.3. Influence of different rotational speeds for single and double pass of the tool on: (a) tensile strength and (b) elongation [23]. 22

Figure 4.4. Burned material due to high rotational speeds used, adapted from [59]. 23

Figure 4.5. Effect of the rotational speed on the tensile strength for different welding speeds [1]. 24

Figure 4.6. Influence of different rotational speeds with different welding speeds for a tilt angle of: (a) 1º and (b) 2º [62]..... 25

Figure 4.7. Effect of rotational speed on tensile strength and on percentage of elongation [47]. 27

Figure 4.8. Morphology of the weld crown with rotational speeds of: (a) 1000 rpm, (b) 1250 rpm and (c) 1500 rpm [57]. 28

Figure 4.9. Micrographs of the cross section of the welds produced with rotational speeds of: (a) 1000 rpm, (b) 1250 rpm and (c) 1500 rpm [57]. 29

Figure 4.10. Effect of rotational speed for different welding speeds on: (a) tensile strength and (b) impact strength [69]. 30

Figure 4.11. Cross section of the welds produced with rotational speeds of: (a) 300 rpm, (b) 400 rpm and (c) 500 rpm, adapted from [71]. 30

Figure 4.12. Effect of rotational speed for different welding speeds on the tensile strength with: (a) cylindrical pin, (b) threaded cylindrical pin and (c) conical pin [75]..... 32

Figure 4.13. External voids and deformations on the weld surface, adapted from [59]. 33

Figure 4.14. (a) Effect of the welding speed on the tensile strength for different rotational speeds. (b) Peeling defect [1]. 34

Figure 4.15. Milling effect during FSW due to the use of high welding speeds [62]. 35

Figure 4.16. (a) Effect of different rotational and welding speeds on: (a) the tensile strength and (b) average axial force [35]. 37

Figure 4.17. Effect of welding speed on tensile strength and on the percentage of elongation [47]. 37

Figure 4.18. External voids and deformations produced under high welding speeds [67]. 38

Figure 4.19. Morphology of the weld crown with rotational speeds of : (a) 50 mm/min, (b) 100 mm/min and (c) 200 mm/min [57]. 38

Figure 4.20. Effect of welding speed on: (a) tensile strength and (b) strain at brake [45].. 39

Figure 4.21. Defects produced with welding speeds: (a) above 30 mm/min and (b) below 20 mm/min [49]. 40

Figure 4.22. Effect of welding speed during conventional FSW of PP plates on: (a) tensile strength, (b) flexural strength and (c) impact energy, adapted from [72]. 41

Figure 4.23. Force-displacement curves of PP joint made by conventional FSW for different values of welding speed [79]. 41

Figure 4.24. Effect of welding speed for different rotational speeds on the tensile strength of welds obtained with: (a) cylindrical pin, (b) threaded cylindrical pin and (c) conical pin [75]. 42

Figure 4.25. Microstructure obtained with welding speeds of: (a) 12.5 mm/min and (b) 8 mm/min [77]. 43

Figure 4.26. Effect of axial force on: (a) tensile strength and (b) strain at brake [45]. 45

Figure 4.27. Effect of axial force on the macrostructure of the weld cross section with values of: (a) 1 kN, (b) 1.5 kN and (c) 2 kN [45]. 45

Figure 4.28. Effect of plunge depth during conventional FSW of PP plates on: (a) temperature, (b) thickness of HAZ and (c) SZ dimension, adapted from [72]. 46

Figure 4.29. Effect of plunge depth during conventional FSW of PP plates on: (a) tensile strength, (b) flexural strength and (c) impact energy, adapted from [72]. 46

Figure 4.30. Influence of different tilt angles with different rotational speeds on: (a) tensile strength and (b) percent of elongation [61]. 48

Figure 4.31. Effect of tilt angle during conventional FSW of PP plates on: (a) temperature, (b) thickness of HAZ and (c) SZ dimension, adapted from [72]. 49

Figure 4.32. Effect of tilt angle during conventional FSW of PP plates on: (a) tensile strength, (b) flexural strength and (c) impact energy, adapted from [72]. 49

Figure 4.33. Conventional milling tools used in the FSW of PP plates [54]. 51

Figure 4.34. Schematic illustration of the process with left hand threaded pin with: (a) clockwise and (b) counterclockwise rotation [80]. 51

Figure 4.35. Cross section of the welds produced with a left hand threaded pin with: (a) clockwise direction and (b) counterclockwise direction, adapted from [80]. 52

Figure 4.36. Weld with poor finish and reduced tensile strength obtained by FSW with conical pin tool [35]. 55

Figure 4.37. Pin geometries used to weld PMMA plates with conventional FSW: (a) cone frustum, (b) square frustum and (c) triangle frustum [73]. 55

Figure 4.38. Tools used to weld 6 mm thick PLA in butt joint configuration by FSW [75]. 56

Figure 4.39. Pin geometry: (a) simple and (b) convex. (c) Effect of pin geometry on the tensile strength of the material in the SRFSW [40]. 56

Figure 4.40. Distortion of the welded material [35]. 57

Figure 4.41. Result of welding performed with shoe temperature below 70ºC, adapted from [59]. 60

Figure 4.42. Join efficiency for different values of rotational speed and tool temperatures with i-FSW [30]. 60

Figure 4.43. Efect of rotational speed with and without heating the tool on: (a) tensile strength and (b) Percentage of elongation [46]. 61

Figure 4.44. Weld surface of PP plates welded with: (a) non-heated tool and (b) heated tool. (c) Effect of tool temperature on tensile strength and on the percentage of elongation of joints [47] 62

Figure 4.45. Surface finish of welds produced with hot shoe temperatures of: (a) 90ºC, (b) 115ºC and (c) 130ºC [45]. 63

Figure 4.46. Poor surface wiring resulting from excessive operating temperature and loss of shoe coating quality [49]. 63

LIST OF TABLES

Table 5.1. Resume of the researches carried out on FSW in polymeric materials..... 65

LIST OF ACRONYMS/ABBREVIATIONS

ABS – Acrylonitrile Butadiene Styrene

AS – Advancing Side

BBD – Box-Behnken Design

BM – Base Material

BUE - Built-Up Edge

BYU – Brigham Young University

FSLW – Friction Stir Lap Welding

FSW – Friction Stir Welding

HAZ – Heat Affected Zone

HDPE – High Density Polyethylene

HMW-PE – High Molecular Weight Polyethylene

i-FSW – Induction Friction Stir Welding

MDPE – Medium Density Polyethylene

PA – Polyamide

PC – Polycarbonate

PE – Polyethylene

PETG – Polyethylene Terephthalate Glycol

PLA – Polylactic Acid

PMMA – Polymethylmethacrylate

PP – Polypropylene

PS – Polystyrene

PTFE – Polytetrafluoroethylene

PVC – Polyvinyl Chloride

RS – Retreating Side

RSM – Response Surface Methodology

SRFSW – Self-Reacting Friction Stir Welding

SZ – Stirred Zone

TMAZ – Thermomechanical Affected Zone

TWI – The Welding Institute

UHMW-PE – Ultra High Molecular Weight Polyethylene

WN – Weld Nugget

1. INTRODUCTION

Friction Stir Welding (FSW) is a simple welding process in which the joint material is softened and mixed by friction when it contacts with the tool at high rotational speed. It is a process in which there is no need for adding material and no emission of toxic gases and UV radiation or splashes of molten material. The FSW can be done in any joint configuration and with low associated costs. These characteristics made this welding method known as safe, eco-friendly and economic when compared to other joining methods. As if these characteristics were not enough to raise the interest of several researchers around the world, this type of welding also allows the union between materials of different categories, such as the polymer-metal or metal-composite.

The work presented here aimed to gather published studies on the applicability and optimization of the FSW in the joining of polymeric materials. The analysis of the literature on this subject allowed to understand the operation of this welding technique, the innovations developed for the optimization of polymeric joints by FSW, the different parameters that influence the process and the way in which the quality of the welding varies with the alteration of these parameters.

In addition to this introductory chapter, this dissertation was divided into four more chapters, being FSW in context of joining methods, main characteristics of the FSW on polymeric materials, influence of the different parameters on the FSW of polymeric materials, and conclusions and suggestions for future works. In the FSW in context of joining methods chapter, the main methods of joining polymeric materials will be discussed and the emergence of FSW, its main characteristics and the polymeric materials normally united by this technique will be presented. In the next chapter, it will be presented the main elements of the conventional tool, the most used joint configurations, the stages of the process, the different welding parameters, the different areas of the micro and macrostructure, the most common defects formed during welding and the main innovations brought to the union of polymers. The fourth chapter is focused on studying the influence of each of the parameters on the final performance of the process. In addition to presenting the optimal values determined by each of the studies for each of the parameters, the way in which the variation

of the value of each parameter affected the quality of the union will also be analyzed. In the last chapter, the main conclusions about this bibliographic review study will be presented and some themes for future studies will also be proposed.

2. FSW IN CONTEXT OF JOINING METHODS

The application of polymeric materials has grown significantly in the industry. Low density, good moldability, excellent resistance to corrosion and low production costs were some of the characteristics that led to the substitution of metallic materials by polymers in several sectors of industry, especially in automobile, naval and aerospace sectors [1].

Even in the most banal everyday objects, there are countless cases in which it is not possible to manufacture the item in one single piece. Factors such as size, geometry, the coexistence of different materials or even due to the product's own mode of operation require the division of production into more than one component and, subsequently, the union of these to arrive to the final product [2]. In the case of polymeric materials, Figure 2.1 reports the main joining methods, which are divided into mechanical fastening, adhesive bounding and welding.

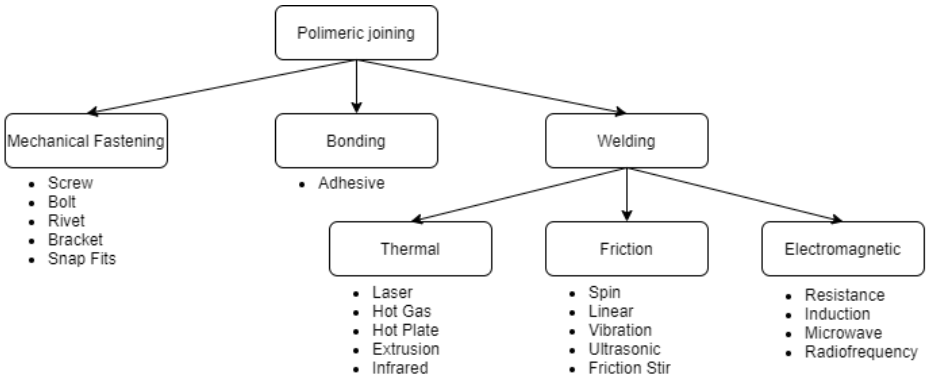

Figure 2.1. Diagram of the main polymer bonding methods, adapted from [3], [4].

Mechanical fastening consists of using mechanical components to join different parts. These components are usually screws, rivets, clamps and, in this context, the mechanical joints can be permanent or not [5]. In certain cases, the mechanical component can be removed for disassembly or maintenance purposes, making it a great advantage over other joining processes. On the other hand, for the connection to be established, the mechanical component normally requires the existence of a hole in the parts to be joined. The existence of this hole ends up bringing the biggest disadvantage of the process since it

represents a zone of stress concentration [3]. Another major disadvantage of this joining method is the addition of weight by adding the mechanical components. In summary, the mechanical connection can be very interesting in structures that require replacement or repair of components, but it is not suitable when looking for lightweight structures with great resistance.

The adhesive bonding allows the joining of almost any material as long as the adhesive is chosen correctly [3]. In certain situations, adhesive bonding may be the only applicable method, especially when it is necessary to join profiles with a very small cross section. Unlike mechanical fastening, the adhesive connection has low values of stress concentration, because it does not require holes [6]. In this case, the stress concentration values observed in the adhesive joints are lower due to an uniform stress distribution. The adhesive can also act as a sealant and prevent the appearance of galvanic corrosion between different materials. Despite this, adhesive bounding also has disadvantages. The fact that it is an irreversible process means that disunity processes can be expensive and in most cases impossible, leading to the destruction of the material around the glued area [7]. The use of adhesives always requires a cure period. This period can vary between a few seconds and many hours and may also require the application of heat and pressure. Other disadvantages of using adhesives are found in the release of toxic fumes during use and cure processes and also the need of surface preparation to ensure the effectiveness of the process [5]. Fatigue stresses in an aqueous environment can also cause the adhesive bond to degrade faster [4]. This joining process can be a very interesting and useful method, but sometimes it is a complex process that takes very long production times, and therefore, in some cases it is not practical to apply it in the industrial environment.

In welding, the bonding material corresponds to the portion of material previously heated to a viscous or molten state which, when solidified, creates a permanent joint [2], [8]. Cooling of the molten portion is usually accompanied by the application of pressure in order to improve the quality of the joint [4]. The welded joint can be made either by adding molten material or by melting the interfaces to be joined. As the use of polymeric materials for reasons of mass minimization is important in the industry, so the welded joints stand out at this point because they can be carried out without adding material, contributing to obtain lighter structures. Although there is the possibility of creating residual stresses during this process due to heating cycles, the concentration of stresses is normally much

lower than the stress concentration created by the characteristic holes of mechanical fastening [9]. Therefore, there are different ways to carry out the fusion process, welded joints can be divided into three different categories. Each category groups processes that use the same operating principles for melting the material. Consequently, as reported in Figure 2.1, the welding methods are divided into thermal welding, friction welding and electromagnetic welding [3], [4]. The FSW is one of the welding methods that is inserted into friction welded joints category, as it uses friction between the base material and the tool to generate the heat necessary to melt the material of the joint [5]. The consequent plastic deformation of the material also contributes to the increase in the total heat of the process, but with less impact than the heat produced by friction [10].

The FSW process was developed, demonstrated and patented by The Welding Institute (TWI) in England for the first time by Thomas et al. (1991) [11], [12]. This welding method was developed to overcome the difficulties of traditional welding technics when applied to lightweight alloys and was initially used to weld aluminum alloys. After proving its potential, FSW was also applied to other metals and their alloys, such as magnesium, copper, titanium and steel [13].

In the majority of the cases, FSW is a relatively simple process [10] and does not require the addition of material, protective atmosphere or joint preparation [12]. Since during the process there are no toxic fumes or UV radiation emissions, it can be said that this type of welding is safer and environmentally friendlier than other welding processes [14]. Because the main source of heat of the FSW process is the friction between the base material and the tool, it makes this welding process an economic and energy efficient process compared to others that traditionally consume higher energy levels [15].

With the good results achieved on joining metallic materials, FSW started to be studied on polymeric materials in 1998 at the Brigham Young University (BYU) [5]. Since then, studies have been carried out in acrylonitrile butadiene styrene (ABS), polyamide (PA), polycarbonate (PC), polyetherimide (PEI), polyethylene (PE), polymethylmethacrylate (PMMA), polypropylene (PP), polystyrene (PS), polyvinyl chloride (PVC) and polylactic acid (PLA).

3. MAIN CHARACTERISTICS OF THE FSW PROCESS

In the FSW process the conventional tool consists of two fundamental non-consumable elements: the pin, also known as probe, and the shoulder [10]. As shown in Figure 3.1, the pin and shoulder rotate simultaneously because the tool is composed of a single piece. For this reason, both are responsible for the generation of heat due to the friction that in turn leads to the softening of the base material. The pin is also responsible for mixing the softened material in the weld seam, while the shoulder is responsible for avoiding the projection of material out of the welding zone [1].

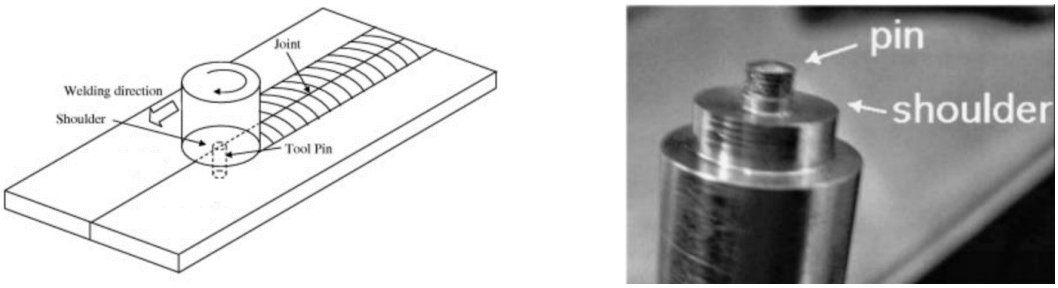

(a) (b)

Figure 3.1. (a) Schematic illustration of the FSW process with conventional tool. (b) Real image of a conventional tool used on FSW [16].

One of the biggest advantages of FSW is that it is applicable to almost any joint configuration. Despite its versatility, the most studied configuration in the development of FSW is the butt joint configuration, but there are also a few studies in lap joint configuration [1], [16], and in T-joint configuration [17] (see Figure 3.2). The FSW on lap joint configuration is known as Friction Stir Lap Welding (FSLW) [18].

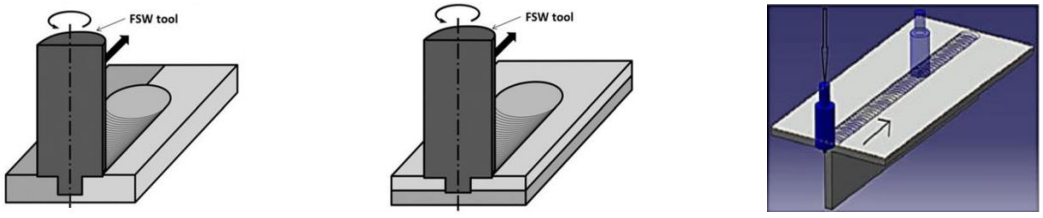

(a) (b) (c)

Figure 3.2. (a) FSW in: butt joint configuration, (b) lap join configuration [16] and T-joint configuration [19].

Therefore, independently of the joint, it is necessary to understand the physical state of the process, the different zones and respective defects. Originally developed for welding lightweight alloys, FSW was defined as a solid-state welding process. This designation was popularized since, typically, the melting temperature is not reached during the FSW with metallic materials [20].

Inaniwa et al. (2013) [21], during the study of the weldability by FSW of 5 mm thick plates of HDPE, PA 6 and PVC in butt joint configuration, monitored the pin temperature throughout the process. Since the temperature obtained was always lower than the melting temperature of each polymer, the researchers concluded that FSW occurred in the solid state and without the consequent degradation of the polymer.

However, Strand (2004) [5] argued that the FSW of polymers is not a process that occurs exclusively in the solid state. While metals have a specific fusion temperature, in polymeric materials, normally, there is not a single value, but a temperature range in which the change from solid to liquid state occurs. This phenomenon happens because polymers are composed by molecular chains with different lengths and molecular weights and therefore, with different melting temperatures. According to this researcher, during polymeric FSW the shortest molecular chains reach the melting temperature, while the largest do not. For this reason, FSW in polymeric materials was redefined as a welding process in which there are portions of solid material suspended in a molten polymeric matrix. Rezgui et al. (2010) [20] studied the influence of several parameters on the optimization of the FSW process on 15 mm thick HDPE plates in but joint configuration. During this study, the temperatures of the process were measured and values between 120 and 180ºC were obtained. These temperatures confirm that FSW is not a process that occurs exclusively in the solid state, because at these temperatures the HDPE used in this study is above the melting temperature and, for this reason, completely in the liquid state. Eslami et al. (2018) [22] during the study of FSW in 3 mm thick high molecular weight polyethylene (HMW-PE) plates in butt joint configuration, also found that the temperatures measured were higher than the melting temperature of this polymer which reinforced the theory of Strand [5].

However, through the analysis of cross-section and surface appearance of the weld, it appears that in most cases the two sides of the joint have different characteristics. The side of the weld where the direction of the rotational speed is the same of the direction of travel of the tool is called the advancing side (AS). The side of the weld on which the

direction of the rotational speed is opposite to the direction of travel of the tool is called the retreating side (RS) [16] (see Figure 3.3). The analysis of the cross-section also shows that it is possible to identify 4 different regions of the microstructure. In addition to the base material (BM), it is possible to distinguish the weld nugget (WN), the heat affected zone (HAZ) and thermo mechanically affected zone (TMAZ) [23], [24], as shown in Figure 3.3. However, some authors merge the WN and TMAZ zones into stirred zone (SZ).

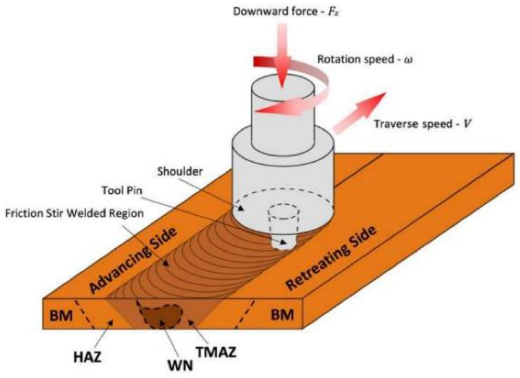

Figure 3.3. Schematic illustration of the different regions of the microstructure and of the AS and RS [25].

With a simple analysis of the different microscopic regions, many of the phenomena that happen during FSW can be better understood. For example, Kiss and Czigány (2012) [26] stated that the width of the HAZ exhibits a strong correlation with the mechanical properties of the joint and that by measuring this width the weld could be well qualified. Most of the researchers analyzed the microstructure of the cross section of the welds to search for welding defects that could justify the mechanical behavior of the joints produced.

Nevertheless, in order to better understand the influence of each parameters on the FSW performance, it is necessary to identify some of the most common defects. The root defect, illustrated in Figure 3.4, corresponds to the existence of an area at the bottom of the join that is not welded [5]. Therefore, the absence of welding at the root of the joint results in the decrease on the tensile and flexural strengths of the weld [27].

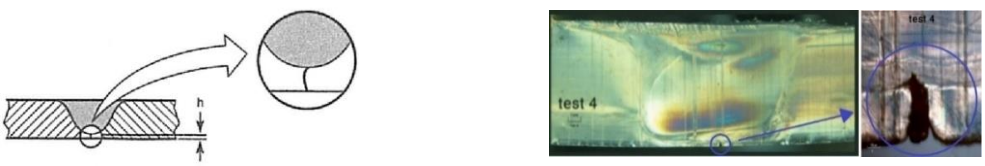

(a) (b)

Figure 3.4. Root defect: (a) schematic illustration adapted from [28] and (b) real example [29].

The flash defect shown in Figure 3.5 corresponds to the formation of burr during the welding process,. The cause for this defect is most of the times related with high material temperatures and turbulent flows. Although it appears to be only an aesthetic defect, the burr ends up symbolizing the waste of material and the reduction of the joints thickness. This defect generally implies the loss of mechanical strength of the welded joint and therefore should always be avoided.

Figure 3.5. Real example of flash defect produced by FSW [30].

The existence of empty spaces within the weld seam, reported in Figure 3.6, also corresponds to a common and undesirable defect that is formed by the incorrect choice of welding parameters. The formation of these defects can have several associated causes. Voids and cavities are examples of empty spaces within the weld and according to Strand (2004) [5] the formation of these defects occur due to the quicker cooling rate of the outer material and due to the natural material shrinkage during the cooling phase. If the empty space extends continuously along the welding direction, it is called a tunnel defect. On the other hand, if the empty space extends along the welding direction but intermittently, can also be called a wormhole defect. When a tunnel defect forms near the surface of the weld it is called a groove defect [31].

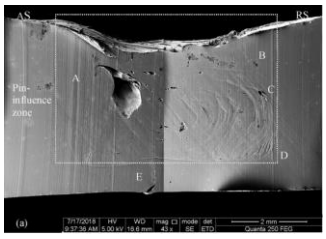

Figure 3.6. Presence of empty spaces within the WN [31].

The built-up edge (BUE) shown in Figure 3.7 corresponds to the accumulation of material from the joint on the tool and is a characteristic defect of machining processes. It is a defect because its existence leads to a change in the geometry of the tool and the creation of other defects such as the projection of material out of the weld and the consequent reduction in the thickness of the weld [32] and is usually associated with the presence of unstable material flows [33].

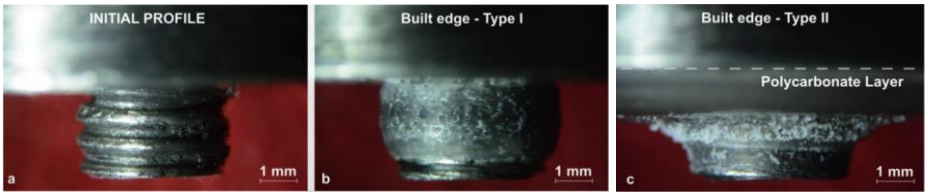

Figure 3.7. (a) Clean pin before FSW, (b) formation of BUE around the pin and (c) formation of BUE around the pin and under the shoulder [32].

In addition to the previously mentioned defects, which are directly related to the FSW process, others can be mentioned as arising from this technique. Kusharjanta et al. (2016) [34], for example, investigated the evolution of the temperature at the initial, middle and final points of the FSW of 6 mm thick PP plates in butt joint configuration. The study showed that the highest temperature measured was obtained in the middle of the process and the lowest temperature at the end, as shown in Figure 3.8. According with Figure 3.8b the bending tests demonstrated the existence of a relationship between strength and temperature, where the highest value was obtained on the central zone and the lowest at the end of the welding zone.

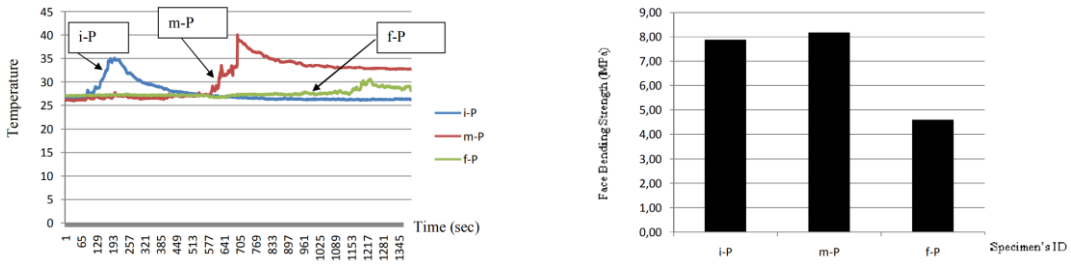

Figure 3.8. (a) Temperature measured at the beginning (i-P), at the middle (m-P) and at the end (f-P) points of the weld. (b) Face bending strength of the material from the different zones [34].

In terms of axial force, Sahu et al. (2018) [35] measured its during the conventional FSW process carried out with a conventional tool. Figure 3.9a shows the graphic obtained, which is divided into 5 stages. The first stage corresponds to the machine starting. The second stage corresponds to the penetration phase, where in the initial moment the axial force increases to allow the beginning of the penetration of the pin in the polymer. With the penetration of the pin, the required force slowly decreased due to the softening of the material. At the end of the penetration phase, there was a very fast increase of the force measured due to the contact of the shoulder on the material surface. The third phase is

characterized by the end of the downward movement of the tool, which led to the axial force measured to drop. The fourth phase corresponds to the welding phase itself and is characterized by an approximately constant force. The last stage corresponds to the tool removal step so that the axial force decreased again. Similar curves to those described above were obtained by Mishra et al. (2019) [1] in a study developed on HDPE plates with 6 mm of thickness. Finally, Eslami et al. (2015) [36] also studied the axial force on PE and PP plates with 2 and 1.2 mm of thickness, respectively. They used position controllers to analyze the evolution of axial force with a conventional tool and with a new developed tool with a stationary shoulder. The results showed that with the stationary shoulder tool the axial force measured remained approximately constant during the process, as shown in Figure 3.9b.

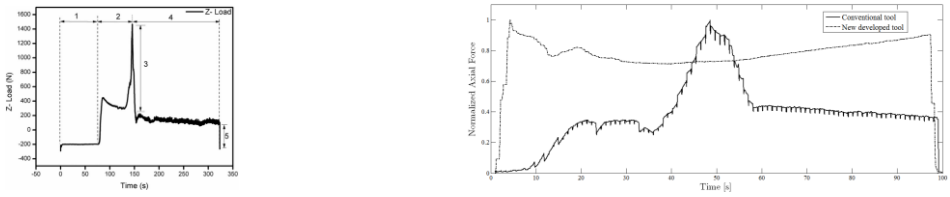

(a) (b)

Figure 3.9. Axial force measurements during FSW process with: (a) conventional tool [35] and (b) conventional and stationary shoulder tool [36].

In order to improve the efficiency of the FSW process and, simultaneously, to eliminate some defects referred above, literature reports some innovations. For example, the double side pass of the tool is one of the methods found to eliminate the root effect formed during the welding process. This method consists of making a first passage by welding approximately half of the thickness of the joint and a second passage on the reverse side in order to weld the remaining unwelded half (see Figure 3.10). Therefore, it is possible to guarantee the weld of the entire thickness of the joint and effectively eliminating the root defect. The biggest disadvantage of this method results from the fact that it takes twice the time to perform the welding and obliges accessibility to both sides of the material.

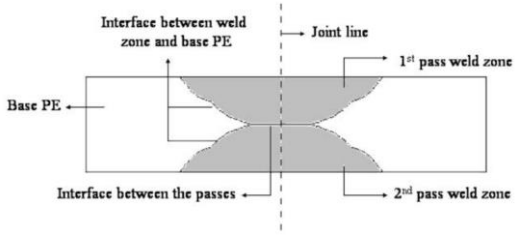

Figure 3.10. Schematic illustration of the cross section of the joint produced by FSW with double side pass of the tool [27].

Arici and Sinmaz (2005) [27] verified that the conventional FSW, i.e., with single passage of the tool in 3 mm thick medium density polyethylene (MDPE) plates in butt joint configuration, led to the formation of root defect. The thickness of these defect was 0.2 mm, which was equal to the difference between the thickness of the plate and the length of the pin (2.8 mm). Due to the existence of the root defect, the joints easily failed, and could even be broken by hand. To evaluate the potential of the double side passage of the tool to eliminate the root defect, Arici and Sinmaz used 5 mm thick HDPE plates and the same tool with a 2.8 mm pin length and 5 mm pin diameter. The study proved that the root defect can be eliminated by double-passing the tool. All the welds performed by these researchers with double pass achieved joint efficiencies above 79% of the base material strength. Arici and Selale (2007) [37] also studied the FSW with double side pass of the tool in MDPE plates with 5 mm of thickness and achieved a joint efficiency of 87% of the base material strength. Saeedy and Givi (2010) [23] studied the effect of the double side pass of the tool on 8 mm thick HDPE plates in butt joint configuration, in order to optimize the welding process of FSW. This study demonstrated, one more time, that the root defect was eliminated by double-passing the tool. Consequently, tensile strength, elongation and impact resistance were always higher than those obtained with a single side pass.

The Self-Reacting Friction Stir Welding (SRFSW), is a variant of the conventional FSW that is distinguished by the existence of a pin that runs the entire thickness of the joint and two stationary shoulder, one at the top and another on the opposite side, as can be seen in Figure 3.11. The process was patented by Carter (2004) [38], but there were already published studies prior to the patent on SRFSW, such as that of Bjorkman et al. (2003) [39]. Pirizadeh et al. (2014) [40] studied the potential of SRFSW to join ABS plates with 5 mm of thickness in butt joint configuration and observed that the root defect and the back slit of the welded parts were eliminated and a maximum joint efficiency of 60.63% was achieved.

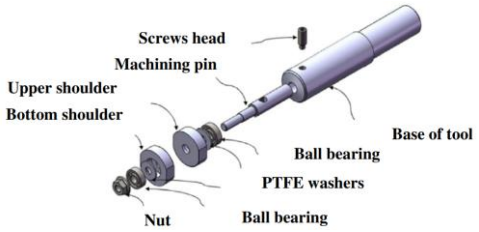

Figure 3.11. Illustration of the exploded view of the tool used in the SRFSW [40].

Another innovation related with the FSW of polymeric materials was the introduction of stationary shoulders. According to Strand (2004) [5], a tool with a rotating shoulder is not able to retain the polymeric material inside the weld seam as it happens in the FSW of metals. Stationary shoulder tools have been developed to eliminate this phenomenon. The solution found consists in the application of bearings between the shoulder and pin, which allows the pin to be the unique rotating element and the shoulder to slide smoothly through the weld surface. With the introduction of non-rotating shoulders, it was possible to reduce the amount of material pushed out of the weld volume and significantly improve the surface finish of the weld. Eslami et al. (2015) [41], during the study of the FSW of dissimilar materials in lap joint configuration, joined PS and PP plates with 2.6 and 1.5 mm of thickness, respectively, and compared different conventional tools and stationary shoulder tools. The tools with rotating shoulders obtained worse surface finishes, bad mixture of the polymer and in some cases, burned material under the tool. With the stationary shoulder tool proposed, as shown in Figure 3.12, these defects were reduced and the quality of the joints improved. Consequently, an increase around 40% of the tensile strength was observed.

Figure 3.12. Example of the assembly of a stationary shoulder tool [41].

Romero et al. (2018) [42] also carried out the comparison between conventional FSW and FSW with a stationary shoulder tool for joining of 8.5 mm thick HDPE plates in the lap joint configuration. Welding with a conventional tool resulted in discontinuous welds with large burrs. Higher welding speed led to the aggravation of these defects. On the other hand, welds carried out with a stationary shoulder were continuous and with much less defects. Eslami et al. (2015) [36] also found that the introduction of a bronze sleeve was beneficial to the process, not only to avoid the injection of melted material inside the shoulder, but also to conduct and distribute heat in the front area of the pin. Therefore, the bronze sleeve allowed the material to be preheated before the action of the pin itself. These researchers also observed that when the shoulder is stationary allowed the material to cool under pressure, reducing the possibility of defects formed at this stage. With this solution, in

certain cases, the surface finish reached such a high quality that according to these researchers it was difficult to distinguish the separation between the base material and the weld surface. The tool used in this research is presented in Figure 3.13.

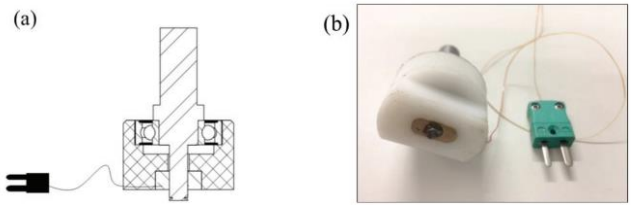

Figure 3.13. Stationary shoulder tool with bronze sleeve: (a) schematic illustration and (b) real image [36].

Because FSW operates at lower temperatures than conventional welding methods, diffusion plays a very important role in the performance of this process. Since most metals have good thermal conductivity, it is easier to transmit the heat generated during the process to the material close to the tool during FSW. This characteristic makes metallic materials very easy to join by conventional FSW and to obtain strong joints. On the other hand, polymers have lower thermal conductivity values, mainly due to their molecular structures. For this reason, heat diffusion in polymeric materials is less efficient, so FSW is much more complex, which makes it difficult to achieve strong joints [10]. To overcome this difficulty and to improve the efficiency of the process in polymeric materials, new techniques have emerged that resort on the implementation of external sources of heat.

Squeo et al. (2009) [10] studied the FSW on 3 mm thick HDPE plates in butt joint configuration and tested the effect of preheating the pin with a hot air gun and of preheating the material with a heater plate. The results obtained by preheating the pin with a hot air gun showed the potential of introducing an external heat source in the process, even with only minor improvements. By preheating the material, tensile strengths close to the base material strength were achieved. Aydin (2010) [2], during the study of FSW in 4 mm thick ultra high molecular density polyethylene (UHMW-PE) plates in butt joint configuration also tested the effect of preheating the material and achieved a maximum joint efficiency of 89%.

The hot shoe tool was another solution found to solve the problems related with the formation of empty spaces within the weld seam and to improve the mixing of the molten material in the FSW of polymeric materials [43]. This tool was developed and patented by Nelson et al. (2004) [44] in the BYU. The hot shoe consists of a long rectangular stationary

shoulder, a rotating pin and a heating system inserted inside the shoulder [29], Figure 3.14 (a). According to Strand (2004) [5], it is important to guarantee a uniform cooling rate in order to avoid the formation of defects during the solidification phase. If the outer material cools faster than the inner material, a hard shell with a core still softened is formed. During the solidification, the inner layers contract and the contracted material moves away from the rigid shell creating voids. With the implementation of the hot shoe in the process, cooling and solidification occurred under pressure and in a longer period. Thus, the natural contraction of the material is reduced and, therefore, there is less probability for the formation of voids. Mendes et al. (2014) [45], used a new heated shoe design in the study of the FSW of 6 mm thick ABS plates in butt joint configuration. The proposed tool was distinguished by the fact that the rotating pin was in the center of the rectangular stationary shoulder. This innovation allowed the material to be preheated before the pin action (see Figure 3.14b).

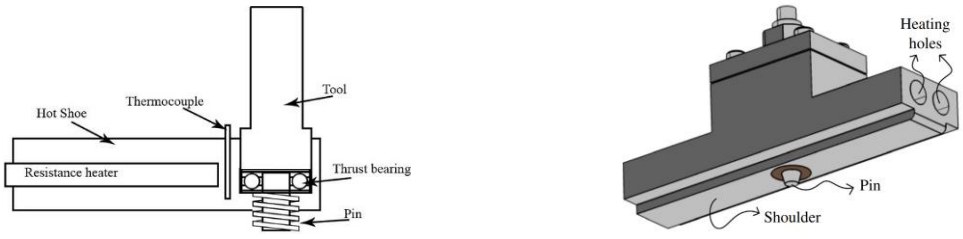

(a) (b)

Figure 3.14. Schematic drawing of the construction of a common heated shoe [46]. Hot shoe used by Mendes et al. (2014) [45].

The induction friction stir welding (i-FSW) is another hot tool FSW technic and consists of the introduction of an induction coil around the tool for heating it. This technic was developed to combat the limitations of existing methods because, for example, allows the welding in curvilinear joints and hot shoes do not and do not has the drop in temperature that preheated tools have in long welds. As shown in Figure 3.15, the assembly of the system generally implies the association of a temperature control system [30]. Vijendra and Sharma (2015) [30] achieved a joint efficiency of 104.32% in bead-on-plate welds in 5 mm thick HDPE which proves the potential of this new method.

Banjare et al. (2017) [46] also proposed a new assisted heating tool that has an electric resistance inside with 50 W. This tool was created in order to avoid major changes

in the conventional tool design (see Figure 3.15c). With this new tool, these researches achieved improvements on tensile strength and impact strength while welding PP plates with 5 mm of thickness in butt joint configuration.

(a) (b) (c)

Figure 3.15. (a) Schematic illustration of the tool used on i-FSW. (b) Experimental set-up for i-FSW [30]. (c) Schematic illustration of a new heated tool by electric resistance [46].

Moochani et al. (2018) [47] also presented and tested a new heated tool with a stationary shoulder. This tool was heated with a hot air gun while the temperature was measured with an infrared sensor, Figure 3.16. According to this researcher, the advantage of using this tool is that the temperature can be maintained without changing other welding parameters. The effectiveness of this tool was proven for the union of PP since in this study a 96% of base material tensile strengths and 98% of base material percentage of elongation were obtained.

(a) (b)

Figure 3.16. (a) Schematic illustration of the new developed tool heated by a hot air gun. (b) Welding assembly during the process [47].

The composition and the coating of the stationary shoulder tools was also studied by different researches. Azarsa et al. (2012) [29] and Mostafapour and Azarsa (2012) [48] during the study of the FSW of 10 mm thick HDPE plates in butt joint configuration with a

stationary hot shoe, evaluated the effect of coating the shoe with polytetrafluoroethylene (PTFE) also known as Teflon. The experiments carried out revealed that when there was no coating on the shoulder, the molten material got stuck to the tool, which led to the formation of residual stresses at the top of the weld. This type of defects led the loss of tensile and flexural strengths. This problem was not verified in the tests carried out with PTFE shoulder coating and there was also an improvement in the quality of the surface finish with this solution as shown in Figure 3.17. Mostafapour and Asad (2016) [49], during the preliminary tests on FSW of PA 6 plates with 6 mm of thickness in butt joint configuration, also performed the comparison of the welding with and without coating of the hot shoe tool with Teflon and reached the same conclusions. According to Pirizadeh et al. (2014) [40], the choice of using a Teflon shoulder coat is usually due to its high chemical resistance, low friction coefficient and high melting temperature (327ºC) which is higher than most of the operating temperatures verified on FSW of polymeric materials.

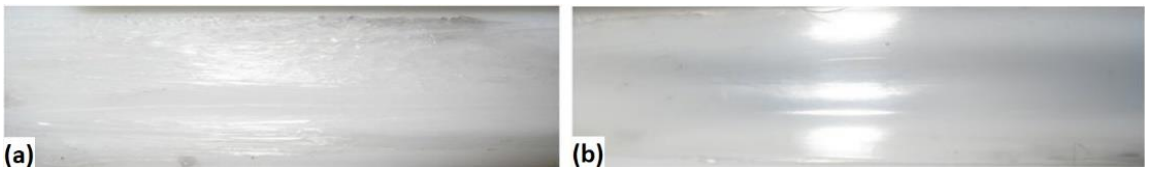

Figure 3.17. Effect on the surface finish of the weld with an hot shoe: (a) without coating and (b) with PTFE coating [48].

Eslami et al. (2015) [41] during the study of the FSW of dissimilar materials in lap joint configuration, joined PS and PP plates with 2.6 and 1.5 mm of thickness, respectively, and used stationary shoulders made from wood, aluminum, polycarbonate, Teflon and brass. The welds produced with the stationary shoulder made in Teflon achieved higher surface quality and therefore, the benefits of using this material were proven once again.

4. EFFECT OF DIFFERENT PARAMETERS ON FSW

4.1. Introduction

To better understand each of the parameters that are involved in the FSW, it is important to understand very well how the process works. FSW is a simple process that follows a set of 4 well-defined steps. Starting by ensuring the necessary rotational speed for the experiment, the first step consists in the progressive introduction of the tool in the material until reaching the desired depth, in order to allow the material to be heated and melted by friction. This first stage shown in is known as the plunging stage. Next, there is a waiting step in which the tool remains in rotation without moving forward, and the material reaches the necessary temperature and softening for a good performance of the welding. This phase is called the dwell stage. The third stage is called the welding stage, and in this phase the translation movement of the tool occurs, giving rise to the joining of the plates. After the tool reaches the end of the defined path, the translation movements stop. The tool must wait a few seconds in the material before being removed. The last step is therefore called the end of welding and tool retracting stage [1], [50]. After completing all the steps of the FSW process, the material must remain clamped to the structure for a few minutes to decrease the possibilities of distortions during cooling [48]. The welded joint usually presents a keyhole at the end of the welding path and material protrusion at the beginning [10].

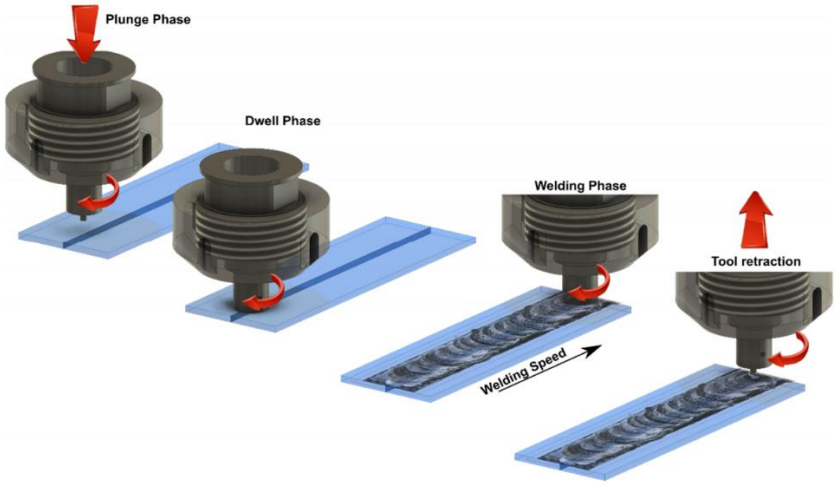

Figure 4.1. FSW stages [51].

Welding processes are inevitably associated with the existence of residual thermal stresses that causes distortions in the material, reducing the mechanical resistance of the weld [52]. Nateghi and Hosseinzadeh (2016) [52] studied the introduction of a cooling stage in an attempt to reduce the residual stresses that results from uncontrolled cooling in the FSW of 5 mm thick high density polyethylene (HDPE) plates in butt joint configuration. Cooling was carried out by applying CO_2 at 2 bar. The results showed that with the cooling stage the tensile strength improved, the residual stress and the angular distortion decreased. Therefore, the existence of five stages and not four must be considered.

Therefore, as Figure 4.2 shows, the FSW process is defined by five main parameters which are the rotational speed, welding speed, axial force, plunge depth and tilt angle.

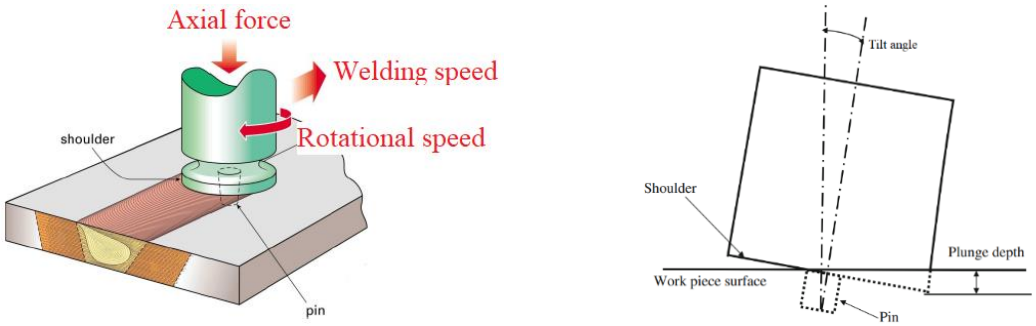

(a) (b)

Figure 4.2. Schematic illustration of: (a) rotational speed, welding speed and axial force, adapted from [53] and (b) plunge depth and tilt angle, adapted from [54].

The rotational speed quantifies the amount of rotation of the tool and is measured in revolutions per minute (rpm). The welding speed, also known as traverse speed or feed rate, corresponds to the speed of the translation movement of the tool along the joint and is measured in millimeters per second (mm/s) or in millimeters per minute (mm/min). Kiss and Czigány (2007) [55] and Hoseinlaghab et al. (2015) [56], affirmed that the effect of increasing the rotational speed is similar to the effect of reducing the welding speed. The justification for this phenomenon is that the increase in the rotational speed contributes to the increase in heat generated by friction and the reduction in the welding speed gives more time for the tool to heat the material, resulting in both cases in increasing the temperature of the material during welding. The axial force characterizes the amount of pressure exerted on the material during the welding process and is usually measured in Newton (N). The

evaluation of influence of axial force was initially ignored due to the inability to measure and control this parameter with the conventional milling machines. However, with the robotization of the process the axial force started to have a greater prominence because in robotic welding systems this parameter must be minimized due to cost and size of the robots [57]. Plunge depth, also known as penetration depth, is the parameter that defines the maximum depth reached by the shoulder relative to the material surface and is measured in millimeters (mm) [54]. In other words, the plunge depth allows to quantify the level of immersion of the shoulder in the material during FSW. The tilt angle, or attack angle, corresponds to the inclination of the tool in relation to the vector normal to the material surface during the welding stage and is measured on degrees (º).

The hold time is another important parameter and corresponds to the period between the moment the tool reaches the desired plunge depth and the start of the translation movement and is measured in seconds (s) [20], [29]. This period is important to ensure that the material around the tool is at the ideal temperature, allowing the formation of a pool of molten material before the beginning of the welding stage. Too short hold times lead to the formation of weak joints due to the lack of melting of the material. On the other hand, too long hold times can lead to degradation of the polymer by excess temperature [48]. The influence of this parameter is not usually discussed in weld optimization studies, as normally the initial part of the weld is neglected and only the central zone is studied. The geometry of the tool also influences the quality of the weld. Therefore, the profile and dimensions of the pin and of the shoulder also count as important parameters for FSW performance.

4.2. Rotational speed effect

Literature report many studies about the effect of rotational speed but considering that were used several materials, and the conclusions are not consensual, this analysis will be made according to the material used in each work developed.

4.2.1. Polyethylene (PE)

Squeo et al. (2009) [10] studied the FSW on 3 mm thick HDPE plates in butt joint configuration and tested rotational speeds between 3000 and 20000 rpm with pin diameters of 1 and 3 mm. In this study, they observed that without any pre-heating, an excessive rotational speed was responsible by joints with reduced strength and with a brittle

fracture mode. For the tests carried out with conventional FSW, an optimum value of 6000 rpm was found, while the highest tensile strength was achieved with the rotational speed of 5000 rpm when the material was pre-heated with a hot plate at 150ºC during 180 s.

Saeedy and Givi (2010) [23] studied the effect of double side pass on the FSW of HDPE plates with 8 mm of thickness in butt joint configuration with rotational speeds of 1200, 1400, 1600 and 1800 rpm. The maximum values of tensile strength and elongation were obtained with rotational speeds of 1600 rpm for single pass and 1400 rpm for double side pass, regardless the welding speed or the tilt angle used (see Figure 4.3).

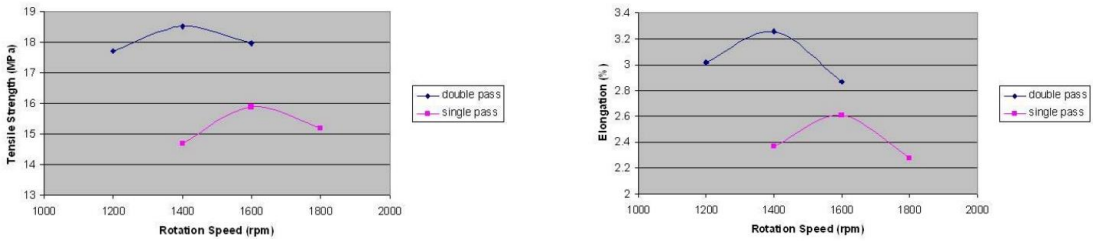

(a) (b)

Figure 4.3. Influence of different rotational speeds for single and double pass of the tool on: (a) tensile strength and (b) elongation [23].

Azarsa et al. (2012) [29] and Mostafapour and Azarsa (2012) [48] studied the FSW of HDPE plates with 10 mm of thickness in butt joint configuration with an hot shoe and used rotational speeds of 1000, 1250 and 1600 rpm. A rotational speed of 1600 rpm with a hot shoe temperature of 140ºC promoted the highest tensile and flexural strengths.

Bozkurt (2012) [58] used the Taguchi method to analyze the level of influence of different parameters on the conventional FSW of 4 mm thick HDPE plates in butt joint configuration. The parameters analyzed were the rotational speed, welding speed and tilt angle, and they observed that the first parameter has the highest importance followed by welding speed and title angle. Consequently, the tensile strength increases, and the optimum value was found for a rotational speed of 3000 rpm.

Azarsa and Mostafapour (2014) [59] also studied the FSW of HDPE plates with 10 mm of thickness in butt joint configuration and used a hot shoe tool. Rotational speeds of 710, 1120 and 1400 rpm were used, because they found, for lower values than 700 rpm, wormhole defects due to the low heat generation and, consequently, bad mixture of the material. Therefore, in this context, the joints produced in these conditions were easily

broken by hand. With rotational speeds above 1400 rpm, the material degradation was not only visible (see Figure 4.4), but the burned material could also be smelled during the process. The increase in rotational speeds from 700 and 1120 to 1400 rpm led to the increase in flexural strength.

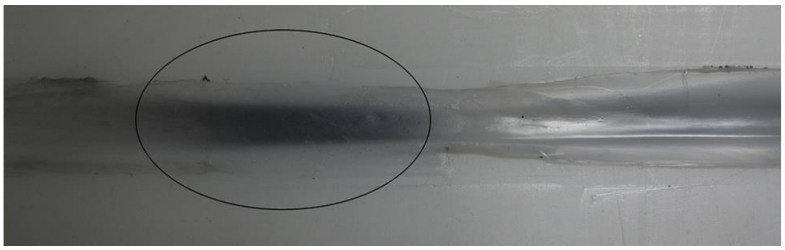

Figure 4.4. Burned material due to high rotational speeds used, adapted from [59].

Vijendra and Sharma (2015) [30], studied 5 mm thick HDPE plates welded by i-FSW, in bead-on-plate configuration, with rotational speeds of 1000, 2000 and 3000 rpm. An increase of the tensile strength was observed between 1000 and 2000 rpm, but higher values (between 2000 and 3000 rpm) promoted a decrease of the strength due to the formation of heavy flash. Joint efficiencies above 90% were reached for all rotational speeds, but the highest tensile strength was achieved with a rotational speed of 2000 rpm.

Hoseinlaghab et al. (2015) [56] studied the FSW of 8 mm thick HDPE plates and analysed the influence of the rotational speed on the creep behaviour and surface quality of the joints. The highest creep resistance was obtained by the authors with a rotational speed of 1120 rpm and welding speed of 31.5 mm/min.

Nateghi and Hosseinzadeh (2016) [52] studied the FSW of HDPE plates with 5 mm of thickness in butt joint configuration and, in this study, they introduced a cooling stage. They concluded that the rotational speed must be higher than 1000 rpm, to guarantee a good mixing of the material, and less than 2200 rpm to avoid excess temperature and, consequently, degradation and burning of the polymer. The formation of wormhole defects in RS was also observed. According to the authors, this defect occurred due to insufficient heat generation and consequent deficient mixing of the material, which is related with low rotational speeds. Rotational speeds of 1000, 1600 and 2200 rpm were used, and the highest tensile strength was achieved for 2200 rpm.

Moreno-Moreno (2018) [60] studied FSW of 8.5 mm thick HDPE plates in butt joint configuration with a stationary shoulder and rotational speeds of 1036 and 846 rpm. They conclude that higher rotational speeds promote higher tensile strength.

Mishra et al. (2019) [1] analyzed rotational speeds of 500, 600 and 800 rpm and with different welding speeds. A conventional tool was used. These authors found that, regardless of the welding speed, higher values of rotational speed are responsible by higher mechanical strength (see Figure 4.5). Therefore, the rotational speed of 800 rpm proved to be the optimum value.

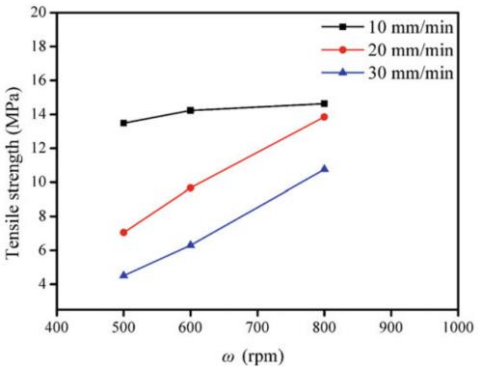

Figure 4.5. Effect of the rotational speed on the tensile strength for different welding speeds [1].

Aydin (2010) [2] developed studies of FSW in 4 mm thick UHMW-PE plates, with and without preheating of material, and they concluded that a excessive rotational speed, besides leading to the formation of defects, promote degradation of the polymer and projection of material from the pin and shoulder. In this study, rotational speeds of 960 and 1960 rpm were used. For excessive rotational speeds, burned zones were observed, due to high local temperatures, and an efficiency of 89% (compared with the base material strength) was achieved with a rotational speed of 960 rpm and a preheat of 50ºC.

Eslami et al. (2018) [22], studied the FSW of HMW-PE plates with 3 mm of thickness, using a stationary shoulder and rotational speeds of 1500, 2000 and 2500 rpm. They observed that higher rotations are beneficial to increase the tensile strength. With a rotational speed of 2500 rpm, it was possible to reach an efficiency more than 95% of the base material in terms of strength.

Arici and Sinmaz (2005) [27] studied the double side pass of the tool on FSW of 5 mm thick MDPE in butt joint configuration and used rotational speeds of 600, 800 and

1000 rpm. Only the highest value (1000 rpm) was responsible to soften the base material and, in this context, the other values were discarded from this study.

Saeedy and Givi (2010) [61], during the study of conventional FSW in MDPE plates with 6 mm of thickness in butt joint configuration, found that for a fixed welding speed of 15 mm/min, the value of 1600 rpm of rotational speed obtained the highest value of tensile strength and elongation compared to rotational speeds of 1400, 1800 and 2000 rpm. Later, Saeedy and Givi (2011) [62] also studied the FSW on MDPE plates but with 8 mm of thickness in butt join configuration and with the same rotational speeds. They found that for rotational speeds of 1000 and 1200 rpm the heat generated by friction was insufficient and, consequently, the joints present low resistance and the development of root defects. Figure 4.6 shows the existence of an optimal rotational speed of 1400 rpm, regardless of the welding speed or tilt angle used. With rotational speeds of 1600 and 1800 rpm there was a decrease in the tensile strength of welds promoted by the turbulence of flow and by the ejection of material out of the welds due to the excessive temperatures.

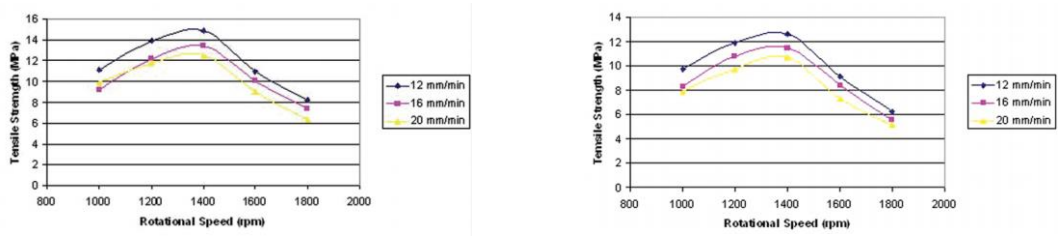

(a) (b)

Figure 4.6. Influence of different rotational speeds with different welding speeds for a tilt angle of: (a) 1º and (b) 2º [62].

Kiss and Czigány (2012) [26] during the study of the FSW in polyethylene terephthalate glycol (PETG) plates with 10 mm of thickness, using a stationary shoe, verified that the welding process occurs within the range of rotational speeds from 1200 to 1800 rpm to guarantee an acceptable quality. However, the maximum efficiency was achieved with a rotational speed of 2500 rpm. They also proposed a K factor that was proportional to the amount of heat generated and depending on rotational speed, welding speed and pin diameter (4.1).

$$K = \frac{rotational\ speed}{welding\ speed} * pin\ diameter. \quad (4.1)$$

According to these authors, a K factor between 150 and 400 is necessary to obtain a flexural strength close to the flexural strength of the base material. With a K factor bellow 150 the weld quality decreased because there was not enough molten material created during welding. With K factor values over 400, the low viscosity of the material led to the projection of the material out of the weld joint. The K factor presented an almost perfect linear proportionality to the width of the HAZ and proved to be close related to the temperature of the weld seam. Mendes et al. (2014) [45] reported that, despite the potential use of this factor, this K factor does not take into account the effect of introducing an external heat source or the amount of axial force used in the process, both of which are related to the formation of defects in the weld seam and, therefore, directly related to the welding resistance.

4.2.2. Polypropylene (PP)

Kiss and Czigány (2007) [55] developed studies with rotational speeds of 450, 630, 900, 1250 and 1800 rpm with the purpose to weld 15 mm thick PP plates in butt joint configuration by FSW. Although these authors did not discuss in detail the influence of each rotational speed, the highest value in terms of tensile strength was obtained for 1800 rpm.

Kiss and Czigány (2011) [63] studied the microstructure obtained by FSW in 10 mm thick PP plates. Two rotation speeds were used in this study and values of 2000 rpm (associated with a low tensile strength) and 3000 rpm (associated with a high strength) were analyzed. In both situations, a spherulitic structure similar to that of the base material was observed in the central zone of the weld, but with about half the diameter.

Panneerselvan and Lenin (2012) [64] for 10 mm thick PP plates found that rotational speeds below 1000 rpm were insufficient to generate heat by friction and for rotational speeds above 2500 rpm the material was projected out of the weld due to the turbulence of the flow. Therefore, rotational speeds between 1500 and 2500 rpm allowed a good amount of heat generated by friction and, consequently, a better mixing of the material. For similar material and thickness, Sharma and Singh (2013) [65] analyzed rotational speeds of 600, 750 and 900 rpm, and they found that higher rotational speeds promote higher values of tensile and impact strength. The increase observed in such properties was related with the higher values of heat generated by friction, which promote more homogeneous and strong joints. On the other hand, works developed by Lenin et al. (2014) [66] in 5 mm thick PP

plates studied rotational speeds of 1500, 1750, 2000 and 2250 rpm. Supported by the Taguchi method, the optimal mechanical performance was obtained for 1500 rpm.

Banjare et al. (2017) [46] welded 3 mm thick PP plates with rotational speeds of 360, 540, 720 and 840 rpm. According with this study, the maximum tensile strength was obtained for 720 rpm, while the highest elongation was observed for 360 rpm. Due to the similarity of results obtained in terms of strength, both rotational speeds are suggested for future studies.

Sahu et al. (2018) [35] developed welding studies with 6 mm thick PP plates, using square and cylindrical pin geometries, in order to analyze the rotational speed on the FSW process. Insufficient heat was generated for values below 500 rpm, while for rotational speeds above 1000 rpm occurred degradation of the material due to the high temperatures. Therefore, both conditions were responsible for low strength. For the rotational speeds in this range (500, 750 and 1000 rpm), the highest tensile strength was obtained 750 rpm, because a good mixing of the material was guaranteed without overheating the polymer. This conclusion was validated for both pin geometries analyzed. Simultaneously, higher values of rotational speed are responsible by lower axial loads during the process, which means that higher temperatures help the movement of the tool. Similar behavior was obtained by Moochani et al. (2018) [47] for the same range of rotational speeds (360, 565 and 950 rpm). As reported in Figure 4.7, increasing the rotational speed promotes a slight increase of the tensile strength, but a significant increase in terms of elongation. This phenomenon was explained by the improvement obtained in the polymeric mixture during the process.

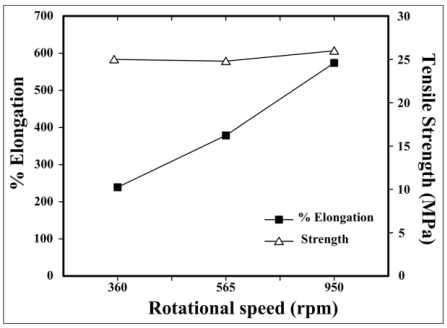

Figure 4.7. Effect of rotational speed on tensile strength and on percentage of elongation [47].

4.2.3. Acrylonitrile butadiene styrene (ABS)

Bagheri et al. (2013) [67] developed studies involving ABS plates with 5 mm of thickness and rotational speeds of 800, 1250 and 1600 rpm. Values above 1600 rpm were

neglected, because the polymer was burned due to the high temperatures generated in the welding process. On the other hand, for rotational speeds below 800 rpm, the joints have low mechanical strength due to insufficient frictional heat generation and consequent poor material mixing. Therefore, in the 800 to 1600 rpm range the tensile strength increased, and the maximum tensile strength was obtained for 1600 rpm.

Pirizadeh et al. (2014) [40] studied the potential of SRFSW to join ABS plates with 5 mm of thickness for rotational speeds of 400, 600 and 800 rpm. Similar to other studies, higher rotational speeds promote degradation of the material (polymers burn) and lower values (below 400 rpm) the heat generated is not enough to promote sufficient mixture of the material. Therefore, for the values mentioned above (400, 600 and 800 rpm), the highest tensile strength was obtained with the rotational speed of 400 rpm, because the best compromise between heat generated and the material mixture was obtained.

Mendes et al. (2014) [57] used rotational speeds of 1000, 1250 and 1500 rpm to join 6 mm thick ABS plates in butt joint configuration by FSW with a stationary shoe. With a rotational speed of 1000 rpm significant amount of cavities were displayed on the RS (see Figure 4.8a and Figure 4.9a). However, increasing the rotational speed up to 1250 rpm, the amount of defects on the RS decreased (see Figure 4.8b and Figure 4.9b), and with the rotational speed of 1500 rpm those defects visually disappeared (see Figure 4.8c and Figure 4.9c). However, even with rotational speeds of 1500 rpm a narrow region of poor mixture of the material was observed on the RS. Therefore, these authors concluded that the increase in the rotational speed contributed to the reduction of welding defects and to the improvement of the material mixing but was not enough to guarantee a perfect mixture of the molten material on the RS. Therefore, a minimum value of 1250 rpm must be applied to obtain defect free welds.

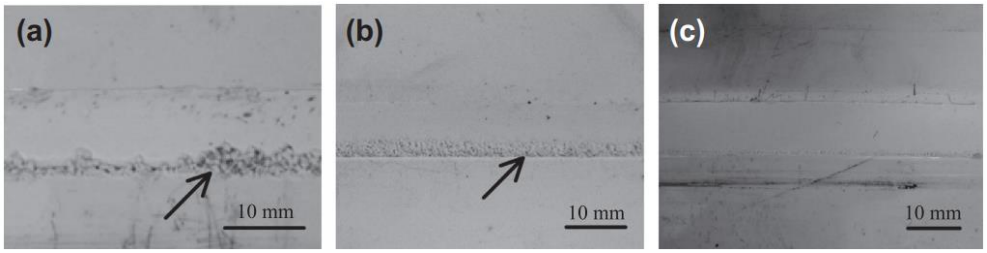

Figure 4.8. Morphology of the weld crown with rotational speeds of: (a) 1000 rpm, (b) 1250 rpm and (c) 1500 rpm [57].

Figure 4.9. Micrographs of the cross section of the welds produced with rotational speeds of: (a) 1000 rpm, (b) 1250 rpm and (c) 1500 rpm [57].

Mendes et al. (2014) [45] also studied the FSW on 6 mm thick ABS plates with a stationary hot shoe and rotational speeds of 1000, 1250 and 1500 rpm. They confirmed that for higher rotational speeds the defects significantly decrease and, consequently, an improvement of the mixture due to the higher temperatures observed. In this context, good quality of welds are obtained accompanied with improvements of tensile strength and strain.

Finally, Sadeghian and Givi (2015) [68] studied the FSW of ABS but in 8 mm thick plates. Conventional tapered and cylindrical tools were used to weld the ABS plates. In this context, two ideal rotation speeds were found by the authors for each pin geometry, and while a rotational speed of 1400 rpm was ideal for cylindrical pins, the best value for the conical pin was 900 rpm. In both cases, a tensile strength similar to that of the base material was achieved.

4.2.4. Polyamides (PA)

Husain et al. (2015) [69] developed studies of FSW in PA 66 plates with 8 mm of thickness, using cylindrical pins and rotational speeds of 780, 994, 1255, 1570 and 2000 rpm for different welding speeds. Depending on the welding speed used, rotational speeds of 1255 and 1570 rpm promoted the highest tensile strengths and impact strength, as reported in Figure 4.10. For example, the highest tensile strength obtained at 1570 rpm is around 54.7% of the value obtained for the base material. Therefore, rotational speeds of 1570 rpm are suggested for welding speeds higher than 27 mm/min.

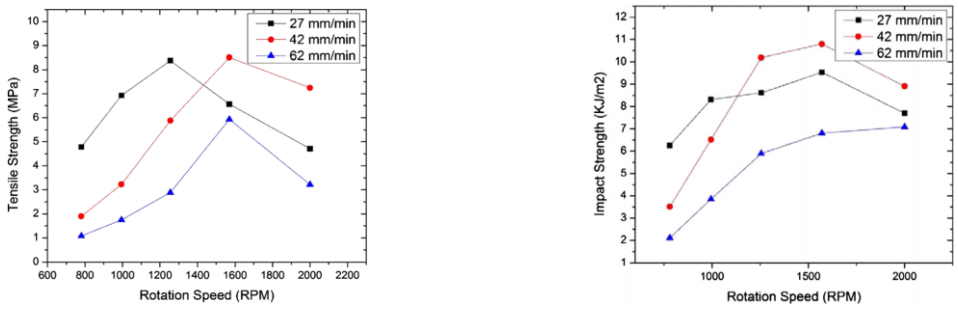

(a) (b)

Figure 4.10. Effect of rotational speed for different welding speeds on: (a) tensile strength and (b) impact strength [69].

Zafar et al. (2015) [70] and (2016) [71] studied the FSW process on 16 mm thick PA 6 plates with a threaded pin, welding speed of 25 mm/min and rotational speeds of 300, 400, 500 and 1000 rpm. In both studies, the rotational speed of 300 rpm was responsible for the highest tensile strength, regardless of the few flash defects observed and, as shown in Figure 4.11, without pores or cavities in the WN. However, higher values increase the temperature and, consequently, flash defects as well as and to the presence of pores, cavities and tunnel defects in the WN (see Figure 4.11b and 4.22c). Therefore, 300 rpm proved to be best rotational speed, despite the maximum tensile strength obtained being only 32% of the base material.

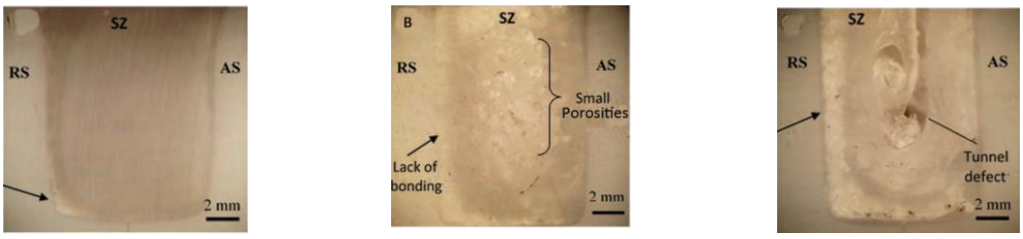

(a) (b) (c)

Figure 4.11. Cross section of the welds produced with rotational speeds of: (a) 300 rpm, (b) 400 rpm and (c) 500 rpm, adapted from [71].

Finnaly, Mostafapour and Asad (2016) [49] observed for the FSW of PA 6 plates with 6 mm that for rotational speeds below 500 rpm there was no welding, because the action of the tool led to the removal of the polymer. On the other hand, for rotational speeds above 800 rpm, polymer degradation was observed. Therefore, in this range they analyzed rotational speeds of 500, 630, 800 rpm and an efficiency (percentage of static strength of the

base material) of 98.1% was obtained for 630 rpm. However, they predicted the optimum value by response surface methodology (RSM) based on the three-factor Box–Behnken design (BBD), and a rotational speed of 730 rpm was reported as the ideal value with an ultimate tensile strength of 76.2 MPa (107.2% of base material strength).

4.2.5. Other materials

FSW on PC plates with 4 mm of thickness was studied by Derazkola et al. (2019) [72], and they found, regardless of the welding speed used, that an increase of the rotational speed promotes higher temperatures, greater stirred zone and heat affected zone and a decrease of the hardness. In terms of rotational speeds, they analyzed values of 1400, 1800, 2200 and 2600 rpm, and an increase up to 2200 rpm was observed in terms of tensile strength, flexural strength and impact strength. However, for higher values of rotational speed these properties decrease due to the excessive temperatures.

Derazkola and Simchi (2018) [73] studied conventional FSW on 4 mm thick PMMA plates using different tools and welding speeds but with rotational speeds of 810, 1250, 1600 and 1920 rpm. Regardless of the other parameters, the highest tensile and impact strength were obtained always for 1600 rpm. The increase in the rotational speed led to the increase of temperature and a decrease of the hardness. Similar study was developed by Adibeig et al. (2018) [74] on 4 mm thick PMMA plates, and the maximum tensile strength was achieved with a rotational speed of 250 rpm. Elyasi and Derazkola (2018) [17] studied conventional FSW on 4 mm thick PMMA plates in T-joint configuration, and rotational speeds of 1000, 1250 and 1600 rpm were analyzed. These authors observed that higher rotational speeds led to the increase of temperature, greater stirred zone and heat affected zone, as well as higher tensile strength and flexural strength.

Finally, Sharma et al. (2020) [75] studied the influence of the rotational speed on FSW of PLA plates with 6 mm of thickness in butt joint configuration. This study was carried out with rotational speeds of 700, 1400 and 2000 rpm and 3 different pin geometries. The results obtained from the tensile tests allowed to conclude that the highest values of strength were obtained with a rotational speed of 700 rpm for the conical pin and 1400 rpm for the cylindrical and threaded pin, as Figure 4.12 shows.

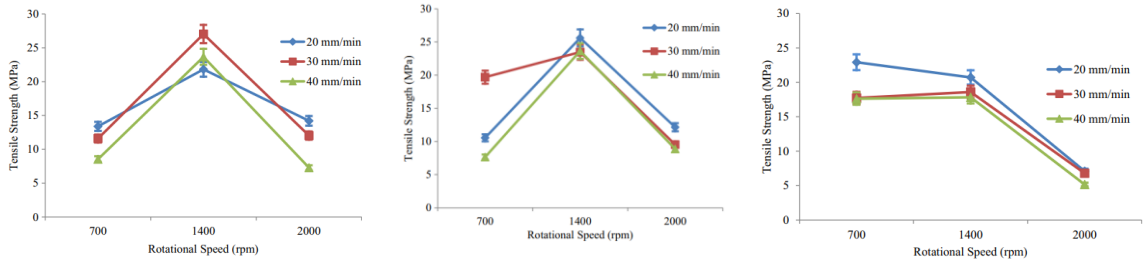

Figure 4.12. Effect of rotational speed for different welding speeds on the tensile strength with: (a) cylindrical pin, (b) threaded cylindrical pin and (c) conical pin [75].

4.2.6. Joints with dissimilar materials

Eslami et al. (2015) [36] and (2018) [76] studied FSW of PE and PP plates with 2 and 1.2 mm of thickness, respectively, in lap joint configuration with a stationary shoulder. Rotational speeds of 1500 and 2500 rpm were analyzed, and they concluded that higher rotational speeds led to higher values of tensile strength. In a similar study developed by Hajideh et al. (2017) [77], using 8 mm thick PP and PE plates in butt joint configuration, they observed that rotational speeds below 900 rpm led to a very irregular joint with low mechanical strength, while for speeds above 2920 rpm the base material melted and flow out of the weld seam due to the inability of the stationary shoulder to keep the polymer inside the weld crown. The highest values of tensile strength, elongation and hardness were obtained with the rotational speed of 1860 rpm, regardless of the welding speed or the pin geometry used.

Finally, Kumar and Roy (2019) [78] studied the FSW of ABS and PC plates with 6 mm of thickness. The study showed that the increase in the rotational speed, from 800 to 1600 rpm, resulted in an increase in the tensile strength and elongation. These improvements were explained on the fact that higher rotational speeds contribute to the improvement of the material mixture and to the increase in WN size (caused by the increased heat generated). On the other hand, with low rotational speeds, there was some difficulty in transporting the molten material from the AS to the RS. Above 1600 rpm there was the appearance of burned areas and the projection of the material out of the weld.

4.3. Welding speed effect

Similar to the previous point, literature report many studies about the effect of welding speed in different materials. Therefore, this analysis will be made according to the material used in each study.

4.3.1. Polyethylene (PE)

Squeo et al. (2009) [10] studied the FSW on 3 mm thick HDPE plates with pin diameters of 1 and 3 mm, with and without external heat application. This study evaluated welding speed of 10, 28 and 44 mm/min. The best tensile strength was always achieved with a welding speed of 28 mm/min for both pins for the welds made at room temperature. In optimum conditions, the welding speed of 10 mm/min achieved a strength close to the base material strength by preheating the material at 150ºC. Therefore, both welding speeds could be pointed as optimum values, depending on the situation.

Bozkurt (2012) [58] in his study related to the optimization of FSW on 4 mm thick HDPE plates found that the increasing the welding speed from 45 to 75 mm/min and from 75 to 115 mm/min led to the increase in tensile strength.

Azarsa et al. (2012) [29] and Mostafapour and Azarsa (2012) [48], during the FSW study on HDPE plates with 10 mm of thickness with an hot shoe tool, used welding speeds of 10, 25 and 40 mm/min. Only with welding speeds of 25 mm/min was possible to achieve joint efficiencies above 90%. Therefore, an optimum value for welding speed of 25 mm/min was found for this case of heat assisted friction stir welding. Azarsa and Mostafapour (2014) [59], during the study 10 mm thick HDPE with a hot shoe tool, found that the increase in welding speed from 25 to 50 and 100 mm/min led to the decrease in flexural strength. With welding speeds above 100 mm/s the formation of external voids and deformations on the welding surface occurred (see Figure 4.13) due to inadequate flow of the matrix and higher cooling rate. The welding speed of 25 mm/min achieved the best results on flexural strength.

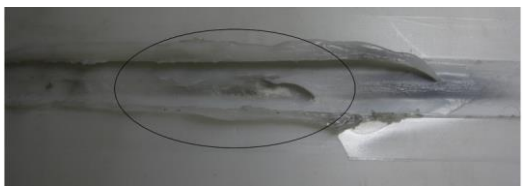

Figure 4.13. External voids and deformations on the weld surface, adapted from [59].

Vijendra and Sharma (2015) [30], studied the weldability of 5 mm thick HDPE plates by i-FSW in bead-on-plate configuration and tested welding speeds of 50 and 100 mm/min. The highest welding speed led to a poor mixture of the material and therefore, solid particles of the polymeric material were deposited on the seam. The rest of the experience was done with the lower welding speed of 50 mm/min and a maximum joint efficiency of 104.32% was achieved.

Nateghi and Hosseinzadeh (2016) [52], during the preliminary tests of the study on FSW in HDPE plates with 5 mm of thickness and with the introduction of a cooling stage, found that for welding speeds below 40 mm/min, material degradation occurred due to excess temperature. For welding speeds above 80 mm/min, the low operating temperature coupled with the deficient mixing of the material resulted in a reduction of the welding strength. Welding speeds of 40, 60 and 80 mm/min were used during the experience. The highest value of tensile strength was achieved with the welding speed of 40 mm/min.

Mishra et al. (2019) [1] during the study of FSW in HDPE plates with 6 mm of thickness, evaluated welding speeds of 10, 20 and 30 mm/min with different rotational speeds. These authors found that the decrease in welding speed contributed to the increase in mechanical strength regardless of the rotational speed used, as Figure 4.14 shows. Therefore, the welding speed of 10 mm/min proved to be the optimum value among the welding speeds studied. These researches also reported the occurrence of peeling on the surface of the polymer and observed that the increase of welding speed contributed to the increase of this defect, as reported in Figure 4.14b.

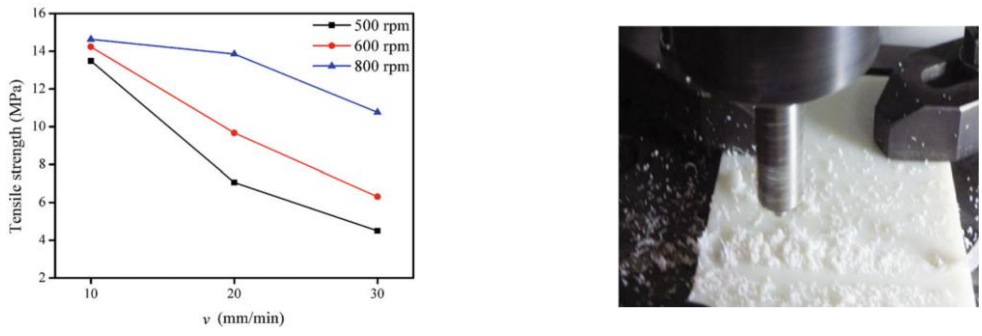

(a) (b)

Figure 4.14. (a) Effect of the welding speed on the tensile strength for different rotational speeds. (b) Peeling defect [1].

Aydin (2010) [2], during the study of FSW in 4 mm thick UHMW-PE plates with and without preheating the material, tested welding speeds of 10 and 20 mm/min. Both speeds allowed defect-free joints, but the highest welding speed led to the highest values of tensile strength.

Eslami et al. (2018) [22] during the study of FSW in HMW-PE plates with 3 mm of thickness, used welding speeds of 30, 50 and 70 mm/min. The increase in the welding speed allowed an increase in the tensile strength, thus the highest strength values were obtained with a welding speed of 70 mm/min.

Arici and Sinmaz (2005) [27] studied the double side pass of the tool on the FSW of 5 mm thick MDPE and used welding speeds of 12.5, 25 and 40 mm/min. The welding speed of 25 mm/min was pointed out as an optimal value for this case but the maximum tensile strength was achieved with the welding speed of 12.5 mm.

Arici and Selale (2007) [37] also studied the double side pass of the tool on the FSW of 5 mm thick MDPE with welding speeds of 12.5, 25 and 40 mm/min. The results demonstrated that the increase in welding speed led to reduction of tensile strength which justifies the fact that the highest tensile strength was achieved once again with a welding speed of 12.5 mm/min.

Saeedy and Givi (2011) [62], during the study on the FSW of MDPE plates with 8 mm of thickness, observed that at high welding speeds, the tool behaved similarly to a milling machine. Due to the lack of time to generate enough friction, the tool lost its ability to soften the polymer and milled the material collected by the pin, as shown in Figure 4.15. These authors also concluded that the increase in the welding speed was inversely proportional to the increase in the tensile strength of the joints. Therefore, the maximum tensile strength was always achieved with the slowest welding speed of 12 mm/min.

Figure 4.15. Milling effect during FSW due to the use of high welding speeds [62].

4.3.2. Polypropylene (PP)

Strand (2004) [5] studied the FSW of 6 mm thick PP plates in butt joint configuration with a hot shoe and used welding speeds of 51, 102, 203 and 305 mm/min. Results showed that the increase in welding speeds led to the decrease of the bending angle and of the weld strength. Therefore, the welding speed of 51 mm/min proved to be better for welding this material that the other speeds tested for the conditions of the experience.

Kiss and Czigány (2007) [55] used welding speeds of 20, 31.5, 40 and 63 mm/min to weld 15 mm thick PP plates in butt joint configuration by FSW. Although these researchers did not discuss in detail the influence of each speed, the welding speed of 20 mm/min led to the higher values of tensile strength, for the majority of the rotational speeds.

Sharma and Singh (2013) [65], during the study on the FSW of 10 mm thick PP plates in butt joint configuration, used welding speeds of 60, 70 and 80 mm/min and found that the welding speed of 60 mm/min was too slow, resulting in the degradation of the polymer by overheating. In turn, the welding speed of 80 mm/min proved to be excessive due to insufficient heat generated. Thus, the speed of 70 mm/min was considered the most suitable for the joining of this material since it resulted highest tensile and impact strength.

Lenin et al. (2014) [66] during the study of the optimization of different parameters in the FSW of 5 mm thick PP plates in butt joint configuration also evaluated welding speeds of 30, 40, 50 and 60 mm/min. By using the Taguchi method, it was possible to verify that the increase on welding speed let to the increase of tensile strength and that the optimum welding speed value was 60 mm/min.

Sahu et al. (2018) [35], during the study of FSW on 6 mm thick PP plates in butt joint configuration, used square and cylindrical pin geometries to study the influence of the welding speed on the welding performance. Preliminary tests showed that welding speeds below 5 mm/min led to the degradation of the material due to overheating. Welding speeds above 25 mm/min led to the formation of voids and weak welds due to the insufficient heat generated. The tests were then carried out with welding speeds of 5, 15 and 25 mm/min. For both geometries and for different rotational speeds, the intermediate welding speed of 15 mm/min obtained the higher tensile strengths (see Figure 4.16). The measurement of the evolution of the axial force showed that the reduction of the welding speed led to the reduction of the force exerted by the machine during the process, since the increase in the temperature of the material facilitated the movement of the tool (see Figure 4.16b).

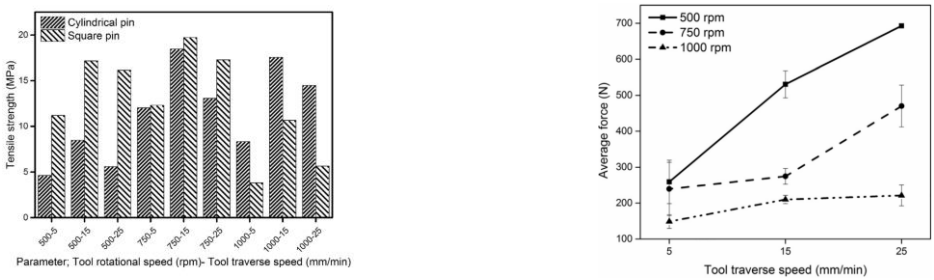

(a) (b)

Figure 4.16. (a) Effect of different rotational and welding speeds on: (a) the tensile strength and (b) average axial force [35].

Moochani et al. (2018) [47], during the study of FSW in PP plates with 4 mm of thickness in butt joint configuration with a new developed hot tool, tested welding speeds of 24, 40 and 60 mm/min. The results obtained revealed that the increase in the welding speed resulted in a slight loss of the tensile strength of the welds. On the other hand, increasing the welding speed resulted in a marked decrease in the percentage of elongation, specially from 40 tom 60 mm/min. The welding speed of 24 mm/min proved to lead to better welds, but good results were also achieved with a welding speed of 40 mm/min, as shown in Figure 4.17.

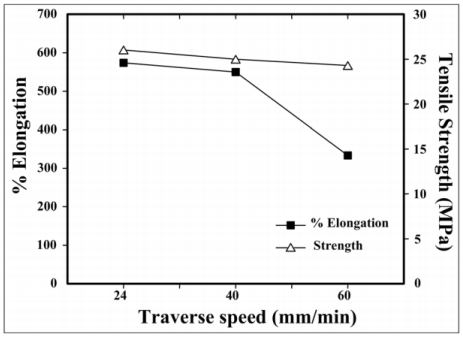

Figure 4.17. Effect of welding speed on tensile strength and on the percentage of elongation [47].

4.3.3. Acrylonitrile butadiene styrene (ABS)

Bagheri et al. (2013) [67] in the study on the FSW of 5 mm thick ABS plates in butt joint configuration with hot shoe found that welding speeds above 80 mm/min led to the formation of external voids and deformations on the weld surface, as reported in Figure 4.18. By decreasing the welding speed, the mean of tensile strength increased. The best results in the tensile strength tests were obtained with the lowest welding speed of 20 mm/min. Despite the good results, the authors argue that this speed was too slow and that

future studies should focus on obtaining the same tensile strength with higher welding speeds to increase the efficiency of this welding process.

Figure 4.18. External voids and deformations produced under high welding speeds [67].

Pirizadeh et al. (2014) [40], studied the potential of SRFSW to join ABS plates with 5 mm of thickness in butt joint configuration and observed that welding speeds above 60 mm/min result in the formation of cavities and superficial deformations on the weld line area. The welding speed of 40 mm/min proved to be the optimum value among all that were used during the study because led to the highest values of tensile strength.

Mendes et al. (2014) [57] studied the optimization of FSW of 6 mm thick ABS plates in butt joint configuration and used a stationary shoe, a rotational speed of 1250 rpm and a axial force between 2 and 3.75 kN to tested welding speeds of 50, 100 and 200 mm/min. The welds made with welding speeds of 50 and 100 mm/min presented an excellent surface quality without voids or porosity, while the welds produced with a welding speed of 200 mm/min presented a rough surface (see Figure 4.19). These authors analyzed the influence of the ratio rotational/welding speed and found that ratios higher than 10 led to good surface quality. These researchers also found that the highest tensile strength was obtained with welding speeds of 50 mm/min.

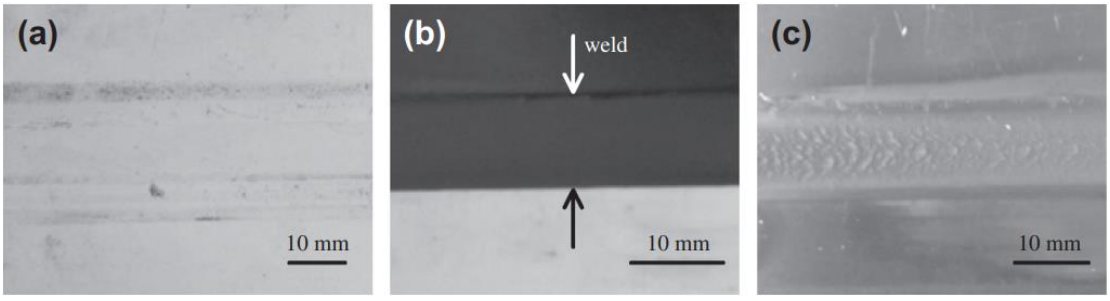

Figure 4.19. Morphology of the weld crown with rotational speeds of : (a) 50 mm/min, (b) 100 mm/min and (c) 200 mm/min [57].

Mendes et al. (2014) [45] also studied the FSW on 6 mm thick ABS plates in butt joint configuration but with a hot stationary shoe. Once again, welding speeds of 50, 100 and 200 mm/min were tested. In this study, the researchers found it difficult to establish a pattern of influence of this parameter. Even so, it was possible to verify that the increase in the welding speed contributed to the increase of the tensile strength when the process presented low operating temperature due to insufficient rotation or axial pressure. However, when welding conditions favored higher operating temperatures, the increase in welding speed has shown to have little influence on the strength of the joint and in some cases, eventually led to the loss of strength of the weld (see Figure 4.20). This study also revealed that the decrease in welding speed favored the increase in strain at brake during tensile tests (see Figure 4.20b). Low welding speeds allowed better weld quality and therefore a value between 50 and 100 mm/min should be used according to these researchers.

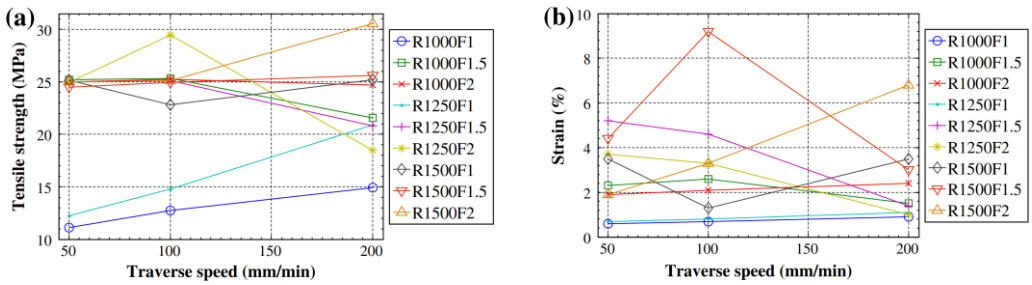

Figure 4.20. Effect of welding speed on: (a) tensile strength and (b) strain at brake [45].

Sadeghian and Givi (2015) [68] studied the FSW of 8 mm thick ABS plates in butt joint configuration and used welding speeds of 6, 16 and 25 mm/min. These researchers found that welding speeds of 16 and 25 mm/min achieved tensile strengths similar to the base material strength for conical and cylindrical pin, respectively.

4.3.4. Polyamide (PA)

Husain et al. (2015) [69], studied the FSW of 8 mm thick PA 66 plates in butt joint configuration and used welding speeds of 27, 42 and 62 mm/min. The results showed that by increasing the welding speed, the optimum rotational speed value also increased. The highest tensile strength for rotational speeds up to 1255 rpm were achieved with a welding speed of 27 mm/min. With higher rotational speeds, a welding speed of 42 mm/min led to higher tensile strengths. The highest values of tensile and impact strength were achieved

with 42 mm/min of welding speed. For those reasons, this welding speed proved to be more suitable for this experience, but the welding speed of 27 mm/min also achieved good results.

Mostafapour and Asad (2016) [49], during the preliminary tests of FSW on 6 mm thick PA 6 plates in butt joint configuration, used a stationary hot shoe and verified that a welding speed between 20 and 30 mm/min must be used. Higher welding speeds led to the formation of lots of porosity and large cavities, as shown in Figure 4.21a. With welding speeds below 20 mm/min occurred material degradation due to the excessive pin stirring action, as shown in Figure 4.21b. Joint efficiencies above 90% were only achieved with a welding speed of 20 mm/min.

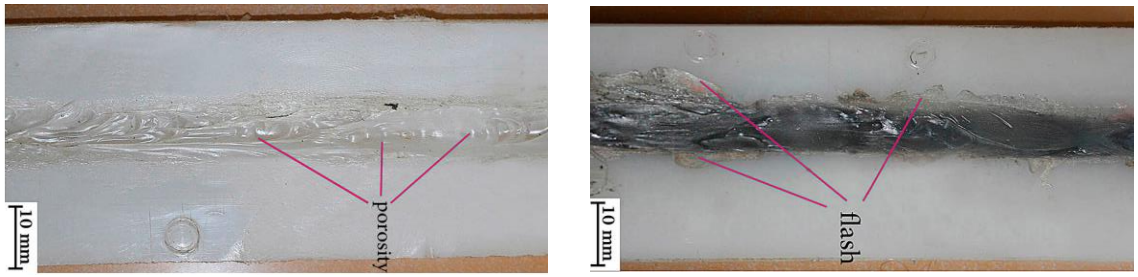

(a) (b)

Figure 4.21. Defects produced with welding speeds: (a) above 30 mm/min and (b) below 20 mm/min [49].

4.3.5. Other materials

Derazkola et al. (2019) [72] during the study of the FSW on PC plates with 4 mm of thickness in butt joint configuration, verified that the increase of the welding speed from 70 to 105 and 170 mm/min contributed to the decrease of the operating temperature, the dimension of the SZ, the thickness of the HAZ and for the decrease in hardness, regardless of the rotational speed used. At high welding speeds of 170 mm/min the formation of small cracks that easily resulted in the formation of planar cracks led to the decrease of tensile, flexural and impact strengths. According with these researchers, this defect appeared due to the interaction of the tool with cold material. The speed of 105 mm/min proved to be the most adjusted to this study since it resulted in the highest values of tensile strength, flexural strength and impact energy, as reported in Figure 4.22.

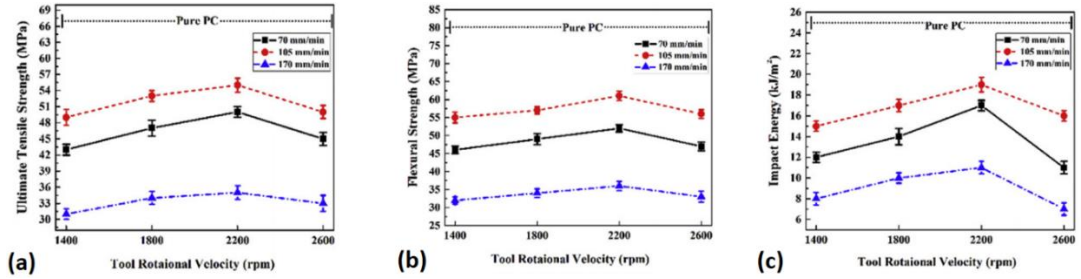

Figure 4.22. Effect of welding speed during conventional FSW of PP plates on: (a) tensile strength, (b) flexural strength and (c) impact energy, adapted from [72].

Lambiase et al. (2020) [79] during the study of the FSW in 3 mm thick PC plates in butt joint configuration, studied the influence of the welding speed variation on the tensile strength. The results obtained with a rotational speed of 2000 rpm and a tilt angle of 0º demonstrated that the increase in the rotational speed from 20 to 60 mm/min resulted in an increase in tensile strength from 10 to 37 MPa. In turn, increasing the welding speed to 100 and 200 mm/min resulted in a decrease of tensile strength values, as shown in Figure 4.23.

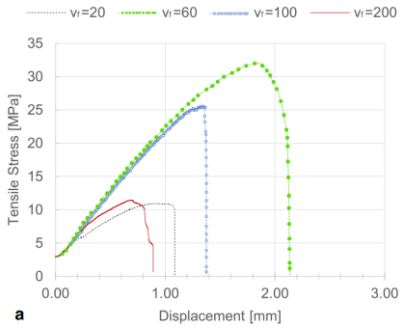

Figure 4.23. Force-displacement curves of PP joint made by conventional FSW for different values of welding speed [79].

Derazkola and Simchi (2018) [73] studied the conventional FSW on 4 mm thick PMMA plates in butt joint configuration and used welding speeds of 25 and 50 mm/min. Although three different tools and four rotational speeds were used, the decrease in welding speed from 25 to 50 mm/min led to the increase of material temperature, of tensile and impact strength and to the decrease in hardness values.

Elyasi and Derazkola (2018) [17] also studied the FSW on 4 mm thick PMMA plates and used welding speeds of 25 and 50 mm/min but in T-joint configuration. The decrease on welding speed led to the increase of material temperature, of SZ and HAZ dimensions, of tensile strength and of flexural strength, for all the rotational speeds used.

Adibeig et al. (2018) [74] also studied conventional FSW on 4 mm thick PMMA plates in butt joint configuration. The preliminary tests showed that at welding speeds above 25 mm/min occurred the formation of welds with external voids and tunnel defects. Therefore, the study was carried out with welding speeds of 16 and 20 mm/min. The welding speed of 16 mm/min achieved higher values of tensile strength due to the higher heat generated which led to better material flow in the weld zone.

Sharma et al. (2020) [75] studied the influence of welding speed during FSW on 6 mm thick PLA plates in butt joint configuration. The study was carried out with welding speeds of 20, 30 and 40 mm/min and allowed to verify that with the use of a cylindrical pin the increase in the rotational speed led to a decrease in the tensile strength of the welding, except for the rotational speed of 1400 rpm in which there was an increase in tensile strength with an increase in welding speed from 20 to 40 mm/min. With the threaded cylindrical pin there was also a loss of strength with the increase in welding speed except with the speed of 700 rpm where once again there was an increase in tensile strength with an increase in welding speed from 20 to 40 mm/min. For the conical pin, the increase in the welding speed resulted in the loss of tensile strength for all the rotational speeds tested. The highest value of tensile strength was achieved with a welding speed of 30 mm/min with the cylindrical pin and a rotational speed of 1400 rpm, as shown in Figure 4.24.

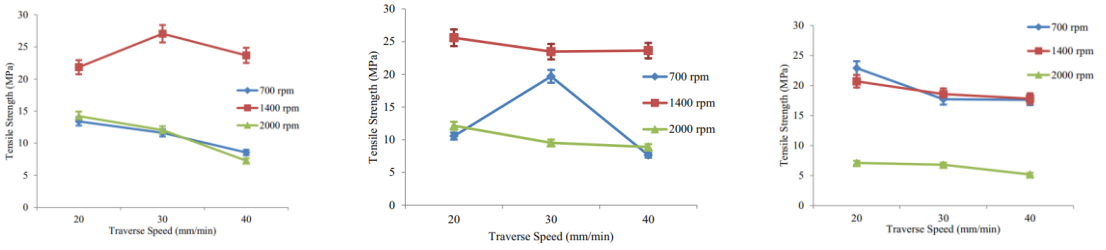

Figure 4.24. Effect of welding speed for different rotational speeds on the tensile strength of welds obtained with: (a) cylindrical pin, (b) threaded cylindrical pin and (c) conical pin [75].

4.3.6. Joints with dissimilar materials

Hajideh et al. (2017) [77], during the study of FSW on PP and PE plates with 8 mm of thickness in butt joint configuration, verified that the welding speed for the union of these polymers should be above 8 mm/min and below 12.5 mm/min in order to avoid the excess or lack of heat generated, respectively. The increase in these welding speeds led to an increase in the tensile strength, elongation and hardness of the material. The variation in

the welding speed has also influenced the microstructure since the decrease in the welding speed and the consequent increase in the temperature and fluidity of the material resulted in a less homogeneous microstructure than at higher welding speeds, as shown in Figure 4.25.

(a) (b)

Figure 4.25. Microstructure obtained with welding speeds of: (a) 12.5 mm/min and (b) 8 mm/min [77].

Eslami et al. (2015) [36], studied the FSW of PE and PP plates with 2 and 1.2 mm of thickness, respectively, in lap joint configuration, with a stationary shoulder and used two welding speeds of 20 and 100 mm/min and two pin geometries with 6 mm of diameter. The welding speed of 20 mm/min led to material degradation and to the consequent color change of the polymer due to the excessive heat generated. On the other hand, the welding speed of 100 mm/min proved to be more suitable for the process as it obtained the highest tensile strength value. Later, Eslami et al. (2018) [76] studied the same material in the same conditions but with pin diameters of 3 and 6 mm. This time, with the smallest pin diameter the welding speed of 20 mm/min did not occur material degradation and were achieved better results that with the largest pin with the welding speed of 100 mm/min. These two results prove that the optimum welding speed value depends on the geometry and size of the tool.

Kumar and Roy (2019) [78] during the study on the FSW of ABS and PC plates with 6 mm of thickness in butt joint configuration, verified that at high welding speeds the tensile strength was low due to the bad mixture of the molten material and due to the appearance of defects in the RS. Therefore, there was an increase in the strength of the joint by decreasing the welding speed from 18 to 12 mm/min. In turn, decreasing the welding speed from 12 to 6 mm/min led to the reduction of the tensile strength due to the occurrence of overheating and due to the formation of burned areas. However, the decrease in welding speed contributed to the increase of elongation.

4.4. Axial force effect

As reported in previous chapter, the axial force was initially devalued due to the inability of the machines to measure it during the process. However, nowadays, there is interest in studying the influence of axial force in the process.

Eslami et al. (2018) [22] during the study of FSW in HMW-PE plates with 3 mm of thickness in butt joint configuration, evaluated the influence of the axial force on the tensile strength. For different axial forces of 800, 950 and 1100 N, they found that an intermediate value of force allowed higher values of tensile strength.

Mendes et al. (2014) [57] studied the influence and optimization of the axial force on FSW of 6 mm thick ABS plates with a stationary shoulder, and according to them, the pressure is a parameter that has more representativity. However, the choice of evaluating the force instead of pressure is related to the fact that FSW equipment is usually parameterized by force. These authors investigated the effect of axial forces of 0.75, 2.25 and 4 kN with a rotational speed of 1500 rpm and a welding speed of 100 mm/min. With axial forces of 0.75 and 2.25 kN a good surface quality and a seam free from defects was obtained. With an axial force of 4 kN the increase of friction between the material and the shoulder led to the formation of a rough surface, but the weld crown stayed defect-free. The increase on axial force showed to lead to the increase the plastic strain but had no significant effect on the tensile strength.

Mendes et al. (2014) [45] also studied the FSW of 6 mm thick ABS with hot stationary shoe and found that axial force plays an important role in FSW performance, especially for reduced rotational speeds (1000 and 1250 rpm). The increase in axial force, mainly from 1 to 1.5 kN, allowed the increase in the tensile strength of the weld for these rotational speeds. On the other hand, with higher rotational speeds (1500 rpm), the increase in axial force from 1 to 2 kN did not evidence major changes in the welding strength,(see Figure 4.26a). This result is in agreement with the results obtained by Mendes et al. (2014) [57]. The influence of axial force is more noticeable in terms of strain, because the values obtained for 1.5 and 2 kN were usually higher than those obtained with 1 kN of axial force (Figure 4.26b). The results also demonstrate that an increase of the axial force was responsible by lower porosity but higher surface roughness and the occurrence of plastic deformation in the AS due to the higher concentration of heat in this region (see Figure 4.27).

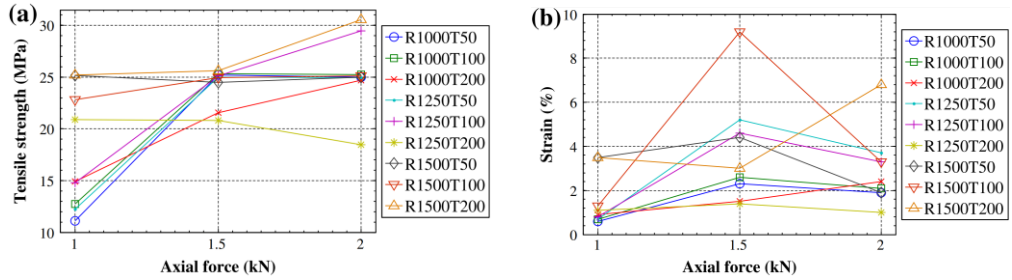

Figure 4.26. Effect of axial force on: (a) tensile strength and (b) strain at brake [45].

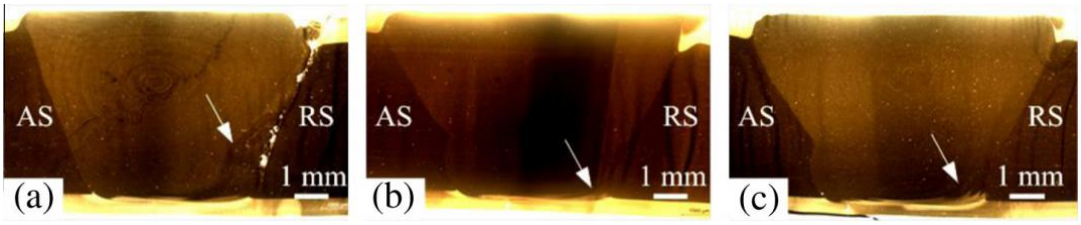

Figure 4.27. Effect of axial force on the macrostructure of the weld cross section with values of: (a) 1 kN, (b) 1.5 kN and (c) 2 kN [45].

4.5. Plunge depth effect

The influence of the plunge depth of the tool was also little discussed in the works related to FSW of polymeric materials. Most studies did not report the amount of plunge depth used, which makes it difficult to analyze this parameter. Despite this, the few studies carried out on the optimization of this parameter have found that the variation of the plunge depth has a great influence on the quality of the welding.

Azarsa et al. (2012) [29] and Mostafapour and Azarsa (2012) [48], during the study on the FSW of HDPE plates with 10 mm of thickness in butt joint configuration with an hot shoe, found in preliminary studies that the plunge depth optimum value was 0.5 mm. Higher plunge depths led to a significant increase in the amount of flash produced and to the reduction of the thickness of the weld. With lower plunge depths the shoulder rode on a cushion of molten material which decreased the contact pressure.

Adibeig et al. (2018) [74] studied conventional FSW on 4 mm thick PMMA plates in butt joint configuration and used a double step shoulder. Plunge depths of 0.5 and 1 mm of the first shoulder were tested. The average tensile strength of the welds was higher with the plunge depth of 0.5 mm because with the plunge depth of 1 mm the loss of material was too high. However, the maximum tensile strength value was achieved with a plunge depth of 1 mm.

Derazkola et al. (2019) [72] during the study of FSW on 4 mm thick PC plates in lap joint configuration, evaluated plunge depths of 0.3, 0.6, 0.9, 1.2, 1.5 and 1.8 mm. These researchers found that the increase in the plunge depth led to the increase of the peak temperature, of the width of HAZ and the decrease in the hardness. The increase on plunge depth between 0.3 and 1.2 mm led to the increase of the SZ dimension. Above this plunge depth, the size of the SZ decreases due to material expelling from the weld seam caused by the high temperature and fluidity of the material (see Figure 4.28). The plunge depth of 1.2 mm allowed the best results in tensile strength, flexural strength and impact energy, as reported in Figure 4.29.

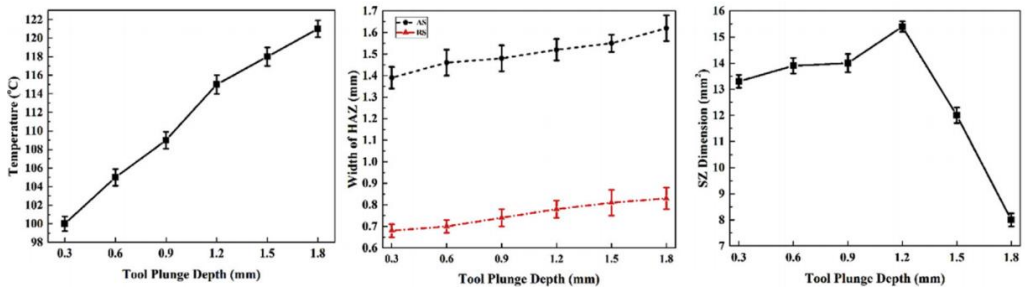

(a) (b) (c)

Figure 4.28. Effect of plunge depth during conventional FSW of PP plates on: (a) temperature, (b) thickness of HAZ and (c) SZ dimension, adapted from [72].

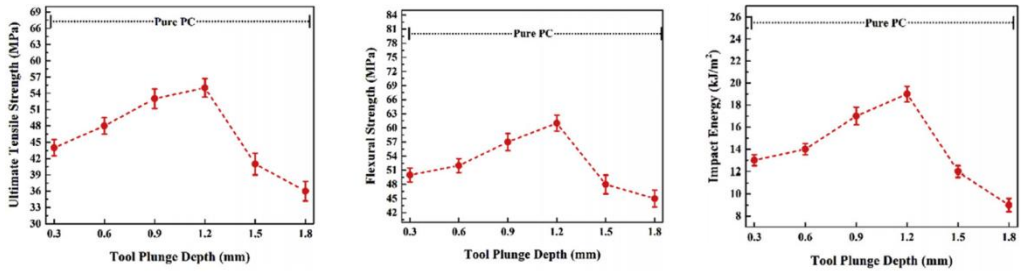

(a) (b) (c)

Figure 4.29. Effect of plunge depth during conventional FSW of PP plates on: (a) tensile strength, (b) flexural strength and (c) impact energy, adapted from [72].

4.6. Tilt angle effect

Contrary to what was seen in the case of the study of axial force and plunge depth, the study of the tilt angle was carried out by several researchers. However, the parameter was only evaluated for rotating shoulder tools. In the case of stationary shoulder tools, only the use of 0º tilt angles was reported.

Hoseinlaghab et al. (2015) [56] studied the conventional FSW of 8 mm thick HDPE plates and analyzed the influence of the tilt angle on the creep resistance and on surface quality of the joints. According to these researchers, the increase of the tilt angle from 0 to 2º resulted in the decrease of the creep resistance and in the drop of the quality of the welds. Therefore, a tilt angle of 0º was recommended.

Bozkurt (2012) [58] in the study related to the optimization of FSW on 4 mm thick HDPE plates in butt joint configuration found that between tilt angles of 1, 2 and 3º the highest tensile strength was obtained with a tilt angle of 2º.

Arici and Sinmaz (2005) [27] studied the influence two different tilt angles on the conventional FSW of 5 mm thick MDPE plates in butt joint configuration. The study was carried out with tilt angles of 0 and 1º. By analyzing the results, the authors of this study concluded that the tilt angle of 1º obtained better weld surfaces since the material was not expelled out of the weld as it happened with a tilt angle of 0º. No voids or cracks were observed with an angle of 1º and the increase in tilt angle also led to the increase of the tensile strength.

Arici and Selale (2007) [37] also studied the FSW with double side pass of the tool in 5 mm thick MDPE plates with tilt angles of 0, 1, 2, 3, 4 and 5º. Once again, the joints that showed the best tensile strength were produced with the tilt angle of 1°. Increasing the tilt angle above 1º led to the decrease on tensile strength values due to the reduction of the welding zone thickness.

Saeedy and Givi (2010) [61], during the study of FSW in 6 mm thick MDPE plates in butt joint configuration, found that the increase on the tilt angle from 1º to 2º led to the decrease in the tensile strength and on the percent of elongation regardless of the rotational speed used, as reported in Figure 4.30.

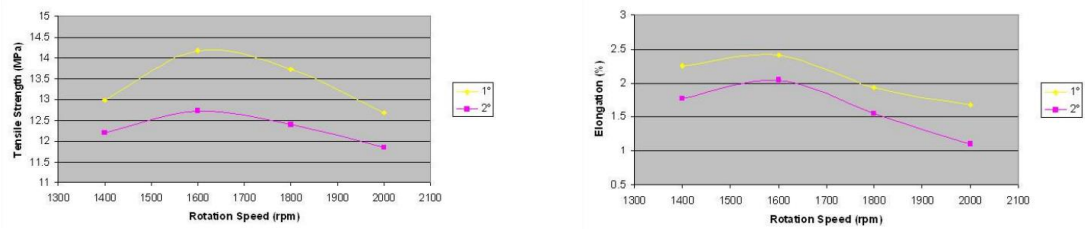

(a) (b)

Figure 4.30. Influence of different tilt angles with different rotational speeds on: (a) tensile strength and (b) percent of elongation [61].

Saeedy and Givi (2011) [62], during the study on the FSW of 8 mm thick MDPE plates in butt joint configuration, confirmed that increasing the tilt angle from 1º to 2º resulted in the loss of tensile strength of the welds. The loss of mechanical strength was justified by the fact that the increase in the tilt angle led to the formation of tunnel defects.

Sadeghian and Givi (2015) [68] studied the FSW of 8 mm thick ABS plates with tilt angles of 0, 1 and 2º and with different rotational speeds, welding speeds and tool geometries. According the authors increasing the tilt angle led to the increase of heat generated but led to the increase of the instability of the process. With the optimization of the different parameters it was possible to obtain tensile strengths close to the base material strength with tilt angles of 1º for the cylindrical pin tool and of 2º for conical pin tool.

Zafar et al. (2015) [70] and Zafar et al. (2016) [71] studied the FSW process on 16 mm thick PA 6 plates in butt joint configuration with a threaded pin. This study compared welds produced with tilt angles of 0º and 3º and rotational speeds of 300 rpm. The tilt angle of 3º led to the formation off bubble like flash defect which was an indicator of the high temperature of the material. According to these researchers, by increasing the tilt angle, the compressive force of the shoulder on the material increases which leads to the increasing of the friction and of the heat generated.

Derazkola et al. (2019) [72] during the study of the FSW on PC boards with the 4 mm of thickness in butt joint configuration, studied the variation of the tilt angle of 0.5, 1.0, 1.5, 2.0, 2.5, 3.0, 3.5 and 4º. The increase in the tilt angle led to an increase in the material temperature and thickness of the HAZ and a decrease in hardness values. The SZ also increased with the increase of the angle up to 2.5º, (see Figure 4.31). Above this angle there was a decrease in SZ due to the projection of material out of the weld. The 2.5º angle led to higher tensile strength, flexural strength and impact energy, as shown in Figure 4.32.

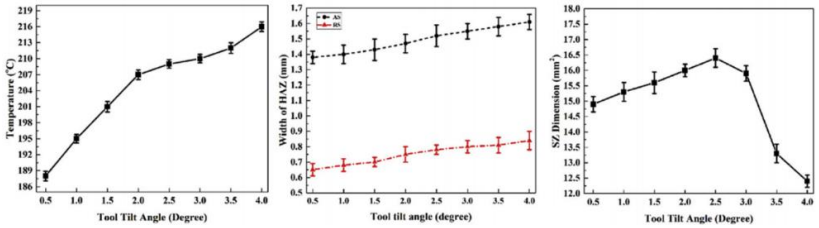

(a) (b) (c)

Figure 4.31. Effect of tilt angle during conventional FSW of PP plates on: (a) temperature, (b) thickness of HAZ and (c) SZ dimension, adapted from [72].

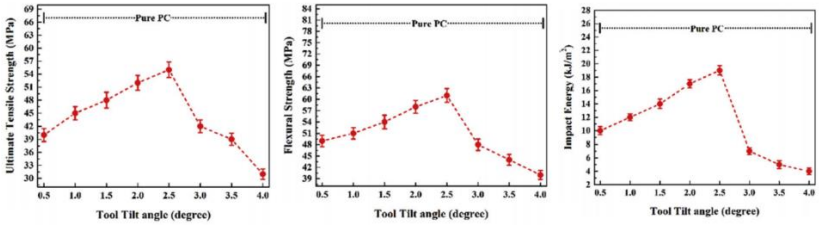

(a) (b) (c)

Figure 4.32. Effect of tilt angle during conventional FSW of PP plates on: (a) tensile strength, (b) flexural strength and (c) impact energy, adapted from [72].

Lambiase et al. (2020) [79] during the study of FSW in PC plates with 3 mm of thickness in butt joint configuration, studied the influence of the tilt angle variation using angles of 0, 2, 4 and 6º. Once again, an increase in the tilt angle has shown to lead to an increase in the plunge depth, in the operating temperature, in the amount of flash defect, in the turbulence of the mixture and in the reduction of the thickness of the weld. The maximum tensile strength was obtained with the tilt angle of 2º, but the maximum elongation was achieved with the tilt angle of 4º.

Kumar and Roy (2019) [78] also evaluated the influence of the tilt angle on the FSW of ABS and PC plates with 6 mm of thickness in the butt joint configuration. This study revealed that an increase in the tilt angle from 0 and 1 to 2º resulted in an increase in the tensile strength and elongation of the joint because it contributed to the increase of pressure on the molten material and thus allowed an improvement in the mixture of material. Above the 2º of tilt angle, it was found that reducing the height of the weld by expelling the material out of the seam led to the loss of mechanical strength.

4.7. Pin geometry and size effect

Changing the pin geometry and size is one of the ways to achieve better FSW results without making major changes in other welding parameters. Since the pin is the element responsible for most of the heat generated and for the mixing of the material, it is easy to see that the change in its geometry has a great impact on the performance of the FSW process.

Squeo et al. (2009) [10] studied the FSW on 3 mm thick HDPE plates in butt joint configuration with pin diameters of 1 and 3 mm with and without preheating the tool and the material. In both cases, the highest values of tensile strength were achieved with the smallest pin diameter.

Hoseinlaghab et al. (2015) [56] studied the FSW of 8 mm thick HDPE plates and analyzed the influence of the pin geometry on the creep resistance and on surface quality of the joints. These researchers compared cylindrical and conical pin geometries with pin diameters of 6, 7 and 8 mm and pin lengths of 5 and 7 mm. For both pin geometries, the pin diameter of 6 mm and the pin length of 7 mm resulted in best appearance of the welds. Therefore, the study was carried out with these dimensions.

Eslami et al. (2018) [22] used 3 different double-groove pin diameters in the study of FSW in HMW-PE plates with 3 mm of thickness in butt joint configuration. Comparing the results obtained with the pin diameters of 3, 4 and 5 mm it was possible to verify that the increase in the pin diameter led to an increase in the tensile strength of the weld.

Strand (2004) [5] used pin diameters of 6.4, 9.5 and 12.7 mm in the study of FSW of 6 mm thick PP plates in butt joint configuration with an hot shoe tool. The increase of pin diameter led to the increase of flexural strength and to welds with a spherulitic structure more similar to the spherulitic structure of the base material. Thus, maximum flexural strength was achieved with a pin diameter of 12.5 mm.

Sharma and Singh (2013) [65], during the study on FSW with 10 mm thick PP plates in butt joint configuration, evaluated the influence of the variation of the tool pin diameter between 8, 10 and 12 mm. The study showed that the increase in diameter from 8 to 10 mm led to the improvement on tensile and impact strength due to the improvement in heat generation associated with to the increase in surface area of contact. In turn, increasing the pin diameter to 12 mm led to a drop in these values due to the formation of flash defects.

Sadeghian and Givi (2015) [68] studied the influence of tool geometry on the FSW of 8 mm thick ABS plates in butt joint configuration. For this, the researchers used 5 cylindrical pin tools and 5 conical pin tools. Pins with 5, 6 and 8 mm in diameter were used. For both pin geometries used, the pin diameter of 6 mm led to tensile strengths values similar to the base material strength when the other parameters were optimized.

Kiss and Czigány (2007) [55] stated that there is a need for the pin to contain at least one groove to collect the material behind the tool instead of accumulating it. When studying the FSW of PP plates with 15 mm of thickness in butt joint configuration with conventional milling tools (see Figure 4.33) these authors found that the increase in the groove slope, i.e., the increase in density of the grooves allowed to obtain welds with better mechanical properties. A groove slope of 45º allowed a better intermeshing of the materials than the tool with a groove slope of 15º.

Figure 4.33. Conventional milling tools used in the FSW of PP plates [54].

Panneerselvan and Lenin (2014) [80] studied the effect of the rotation on clockwise and counterclockwise directions with the threaded pin in FSW in PA 6 plates with 10 mm of thickness in butt joint configuration. A left hand threaded pin was used for welding in clockwise (see Figure 4.34a) and counterclockwise directions (see Figure 4.34b).

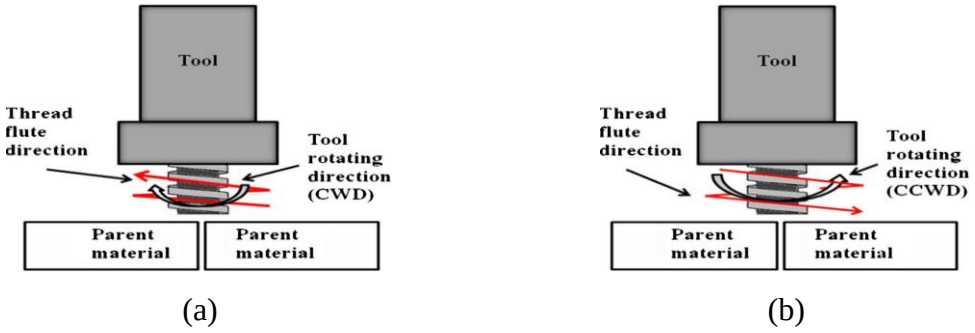

(a) (b)

Figure 4.34. Schematic illustration of the process with left hand threaded pin with: (a) clockwise and (b) counterclockwise rotation [80].

When the left had threaded pin rotated in the clockwise direction, the material was extruded through the flute gap in the granular form due to the upward flow promoted by this direction of rotation. The weld seam presented less material consolidated and less material entered in the colloidal form (see Figure 4.35a) Many cavities and voids were found by analyzing the cross section obtained. With counterclockwise direction the downward flow promoted by the flute direction led to an improvement of the heat produced by friction and the material became colloidal more easily. With the counterclockwise direction there was no material extrusion which allowed to reduce the number and size of the defects formed in comparison with clockwise direction (see Figure 4.35b). For these reasons, the authors of this study concluded that the direction of the rotation in threaded pins must be opposite to the orientation of the thread direction in order to promote the downward flow of the molten material.

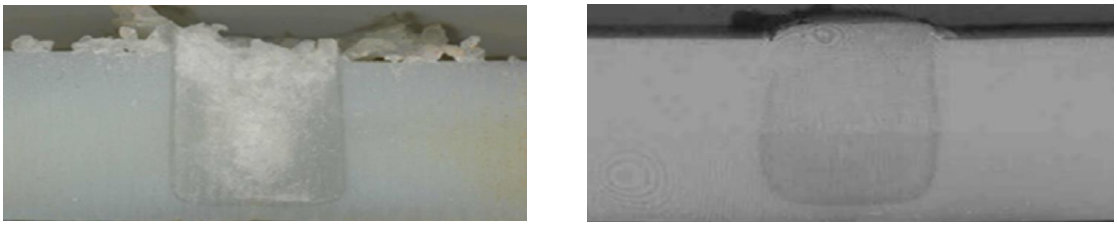

(a) (b)

Figure 4.35. Cross section of the welds produced with a left hand threaded pin with: (a) clockwise direction and (b) counterclockwise direction, adapted from [80].

Kumar and Roy (2019) [78] also evaluated the influence of the direction of rotation of a threaded pin tool during the FSW on ABS and PC plates with 6 mm thickness in the butt joint configuration. These researchers used a right-hand threaded pin. Once again, the results demonstrated the need to promote the downward flow of molten material. The joints made by turning the tool counterclockwise led to the projection of material out of the weld.

Panneerselvan and Lenin (2012) [64] investigated the effect of 6 geometries during the FSW study of 10 mm thick PP plates in the butt joint configuration. The pins used in this study were the straight cylindrical, taper cylindrical, square, triangular, threaded cylindrical and the grooved with square. The results obtained demonstrate that the threaded cylindrical pin requires less linear force than the others to complete the welding, for any welding speed used, followed by the triangular pin, the grooved with square pin, the square

pin, the taper cylindrical pin and finally the straight cylindrical pin. The study also shows that the linear force is higher at the beginning of the process, decreasing gradually with the advance of the welding.

Panneerselvan and Lenin (2013) [81] continued the study on FSW of 10 mm thick PP plates in butt joint configuration and evaluated the effect of 4 different pins on the microstructure and on the welding hardness. These researchers found that the threaded cylindrical pin obtained welds free from defects and with the highest hardness values. The square pin also revealed a good surface finish, but some defects were visible that could compromise the strength of the weld. Even with a good surface quality, the triangular pin was the one that showed to lead to the greatest number of internal defects. Finally, the tapered pin did not obtain good welds for the conditions of the experiment.

Lenin et al. (2014) [66] used the Taguchi method to evaluate the level of influence of the variation of the pin geometry, the welding speed and the rotational speed in the conventional FSW of PP plates with 5 mm of thickness in butt joint configuration. The pin geometries studied were the square pin, the tapered pin, the triangular pin and the threaded pin. The results showed that the pin geometry had a level of influence of about 50% on the final value of the welding quality. This study also reveals that the threaded pin led to higher values of tensile strength and the taper pin the lowest.

Sadeghian and Givi (2015) [68] studied the influence of tool geometry on the FSW of 8 mm thick ABS plates in butt joint configuration. For this, the researchers used 5 cylindrical pin tools and 5 conical pin tools with different pin and shoulder diameters. The results of the welds showed that the conical pin achieved strongest joints. On the other hand, by analyzing the average tensile strength value for each geometry, the cylindrical pin tools had better results. The tensile strength values of the material reflect excellent results, since efficiencies of 99.1% and 100.6% were achieved for the cylindrical and conical pin tools, respectively. The study also shows that the increase in the ratio shoulder/pin diameters contributed to higher the strength of the welds.

Hoseinlaghab et al. (2015) [56] studied the FSW of 8 mm thick HDPE plates and compared cylindrical and conical pin geometries and observed that the use of a cylindrical pin was preferable because this geometry led to higher creep resistances.

Hajideh et al. (2017) [77], during the study of the dissimilar materials joining by FSW in PP and PE plates with 8 mm of thickness in butt joint configuration, used 4 different

pin geometries to evaluate their influence on the tensile strength and the maximum elongation of the weld. A threaded cylindrical pin, a square pin, a triangular pin and a simple cylindrical pin were used. The highest values of tensile strength, elongation and hardness were obtained using the threaded cylindrical pin. The square pin and the triangular pin showed lower results despite guaranteeing a better mixing of the material. The loss of resistance was attributed to the fact that these pins do not allow to obtain a microstructure as uniform as that obtained with the threaded cylindrical pin. Once again, the cylindrical pin proved to be the one that gave the worst resistance and elongation results due to the inability to guarantee a good mixing of the material, which also led to an irregular microstructure.

Eslami et al. (2015) [36] studied the FSW of PP with PE with 1.2 and 2 mm of thickness, respectively, in lap joint configuration and with a stationary shoulder. The study was carried out with a flat face pin and a triangular pin, both with 6 mm of diameter. The results showed that the triangular pin obtained higher lap shear strength values due to its more aggressive geometry which allowed a better mixing of the material. These researches also studied two pin lengths of 2.4 and 2.8 mm and observed that the larger pin led to better results.

Later, Eslami et al. (2018) [76] also studied the FSW of PP with PE with 1.2 and 2 mm of thickness, respectively, in lap joint configuration, with a stationary shoulder and with a flat face pin and a triangular pin but with pin diameters of 3 and 6 mm. By changing the diameter of the pin, these researchers concluded that the with the smallest pin diameter better results were achieved and that the flat face pin was preferable.

Sahu et al. (2018) [35] during the study of FSW in 6 mm thick PP plates in butt joint configuration, evaluated a conical, a square and a cylindrical pin geometries. The conical pin revealed some difficulties in welding this material with the formation of large defects leading to joints easily breakable by hand, as shown in Figure 4.36. However, welds made with square and cylindrical pins showed better appearance, less defects and higher tensile strengths. The maximum strength value of about 56% of the base material strength was obtained with the square pin because there was a best mixture of the molten material with this geometry.

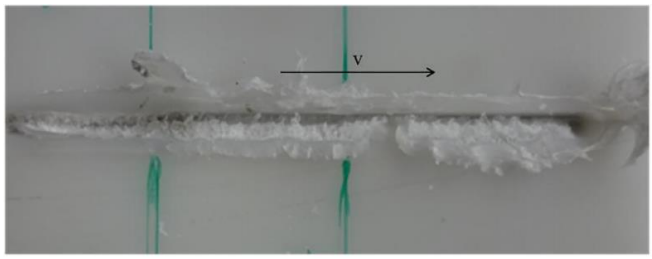

Figure 4.36. Weld with poor finish and reduced tensile strength obtained by FSW with conical pin tool [35].

Derazkola and Simchi (2018) [73] studied the FSW in PMMA plates with 4 mm of thickness in butt joint configuration and used 3 different pin tools. The study used cone frustum, square frustum and triangle frustum pin geometries (see Figure 4.37). The results showed that the cone frustum pin geometry used allowed the best results in the tests of tensile and impact strength. The other two tools obtained worst results due to the formation of more defects in the SZ of the welds.

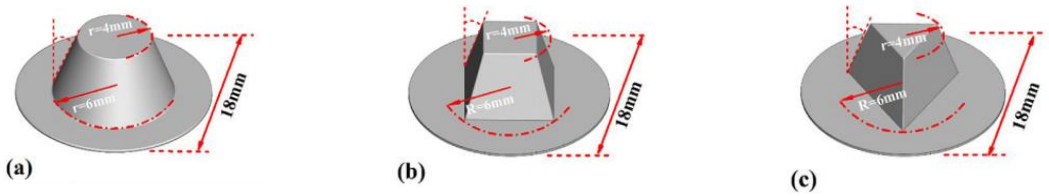

Figure 4.37. Pin geometries used to weld PMMA plates with conventional FSW: (a) cone frustum, (b) square frustum and (c) triangle frustum [73].

Sharma et al. (2020) [75] during the study of FSW in PLA plates with 6 mm of thickness in butt joint configuration, analyzed the influence cylindrical, threaded and conical pins (see Figure 4.38). The highest values of tensile strength and the best surface finish with minimum flash were obtained with the cylindrical pin. In turn, the conical pin led to the formation of severe flash and wormhole defects, indicating that this geometry is not suitable for FSW in this material. The threaded cylindrical pin led to the formation of some internal voids at high rotational speeds justified by the turbulent mixture.

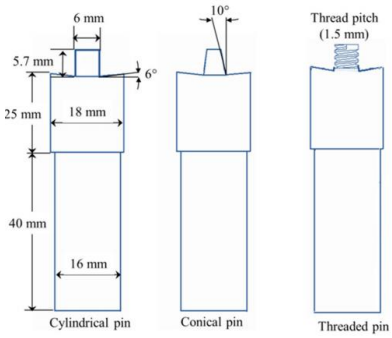

Figure 4.38. Tools used to weld 6 mm thick PLA in butt joint configuration by FSW [75].

4.7.1. SRFSW – pin geometry

Pirizadeh et al. (2014) [40], studied the potential of SRFSW to join ABS plates with 5 mm of thickness in butt joint configuration and evaluated two pin geometries: a simple form pin (see Figure 4.39a) and a convex form pin (see Figure 4.39b). From the analysis of the results obtained, it was possible to verify that the convex pin provides greater tensile strength than the simple pin for any of the combinations of rotational speed and welding speed used, as shown in Figure 4.39c.

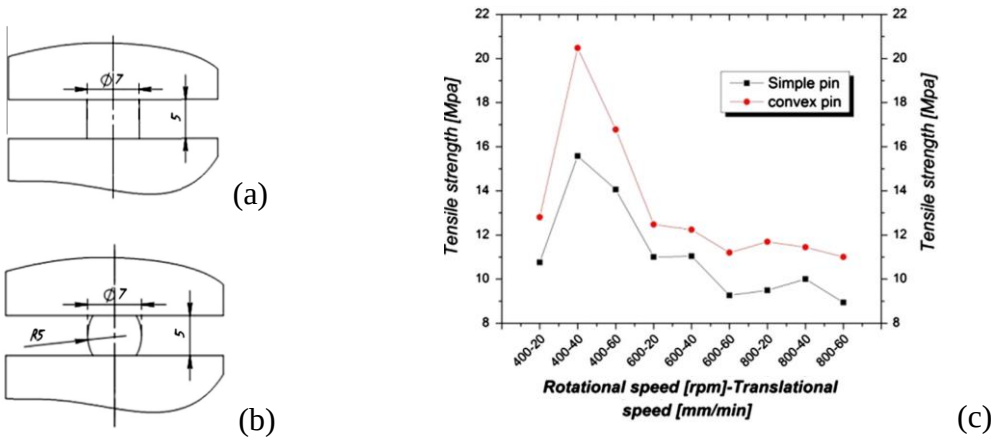

Figure 4.39. Pin geometry: (a) simple and (b) convex. (c) Effect of pin geometry on the tensile strength of the material in the SRFSW [40].

4.8. Shoulder geometry and size effect

Sadeghian and Givi (2015) [68] studied the influence of tool geometry on the FSW of 8 mm thick ABS plates in butt joint configuration and used 5 cylindrical pin tools and 5 conical pin tools. Concave shoulders with 10, 15 and 20 mm in diameter were used. The concave shoulder was used in order to trap the material under the shoulder during the

process. The maximum values of tensile strength were achieved with both pin geometries for the largest shoulder.

Nateghi and Hosseinzadeh (2016) [52] analyzed the influence of different shoulder diameters during the study of FSW in HDPE plates with 5 mm of thickness in butt joint configuration and with the introduction of a cooling stage. Shoulder diameters of 18, 20 and 22 mm were tested. Preliminary studies proved that a shoulder diameter lower than 18 mm led to the formation of a weld nugget with low width which was associated with a reduced weld strength. Shoulder diameters higher than 22 mm resulted in high angular distortion due to the excessive increase in thermal energy. Between the dimensions tested, the shoulder diameter of 22 mm allowed higher values of tensile strength. The increase on the diameter of the shoulder led to a more uniform thermal density and prevented the burn of material.

Banjare et al. (2017) [46], during the preliminary tests of a new heated tool for the FSW of 3 mm thick PP plates in butt joint configuration, found that the 18 mm shoulder diameter was insufficient to retain the molten material within the weld. The use of a larger shoulder with 20 mm resulted in the elimination of this problem and in the increase of the area affected by the heat, which resulted in the improvement of the mechanical strength.

Sahu et al. (2018) [35] during the study of FSW in PP plates with 6 mm of thickness in butt joint configuration, compared the results obtained of conventional tools with rotating shoulders of 16 and 12 mm of diameter. In these conditions, the largest shoulder obtained a lot of distortion, as reported in Figure 4.40. The use of the smallest shoulder led to the reduction of the distortion due to less material shrinkage during the cooling stage. However, with the smallest shoulder, the stirred zone narrowed. Based on these results, the authors concluded that the problems found could be solved by adapting the conventional tool with a stationary shoulder, since the rotation of the shoulder proved to be detrimental to the welding performance.

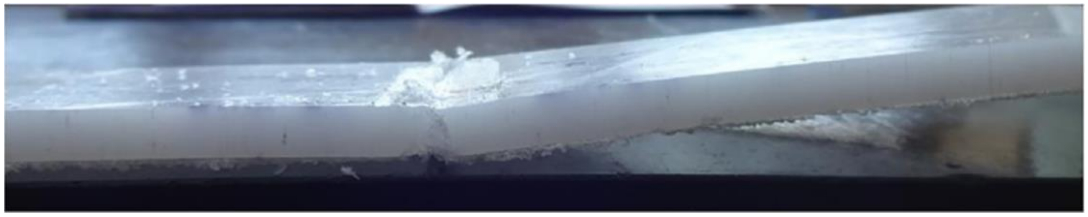

Figure 4.40. Distortion of the welded material [35].

Mishra et al. (2019) [1], during the study on FSW of 6 mm thick HDPE plates in butt joint configuration, used tools with shoulder diameters of 14, 18 and 24 mm and found that increasing the shoulder diameter led to the increase of the stirred volume of the molten material. Despite this, the 24 mm shoulder led to the loss of material from the weld zone. This appended because the greater contact area leads to an increase in the heat generated by friction between the shoulder and the polymer. The increase in the diameter of the shoulder was also related to the degradation of the material on the surface of the polymer. Therefore, the researchers concluded that the use of smaller shoulders was necessary for the success of the welding and for that reason they followed the study only with the shoulder of 14 mm in diameter.

4.9. Material preheating temperature effect

Squeo et al. (2009) [10] studied the potential of preheating the material with a heater plate at 100, 125 and 150ºC with contact times between 0 and 180 s in the FSW of 3 mm thick HDPE plates in butt joint configuration. For a contact time of 180 seconds with the plate at 150ºC, a tensile strength value close to base material strength was obtained, proving that by preheating the material led to substantial improvements on joint strength.

Aydin (2010) [2], during the study of FSW in 4 mm thick plates of UHMW-PE in butt joint configuration, evaluated three different situations. First, conventional FSW tests were carried out with the material at room temperature. Thus, the material presented partial burned areas with high rotational speeds which meant that this material cannot be welded at high rotational speeds. The tensile tests showed a joint efficiency between 56-59%, in relation to the base material strength. For this reason, experiments were carried out using a heater plate on the base of the polymer, allowing to evaluate the effect of preheating the material at two different temperatures of 50 and 80 ºC. Contrary to what the welds made at room temperature showed, some of the joints produced with an external heat source showed a defect-free microstructure. According to this researcher, the preheating of the material made it possible to obtain a more stable operating temperature, favoring the mixing of the material and the formation of smother surfaces. The tensile tests carried out on specimens preheated to 50 and 80 ºC resulted in joint efficiencies of 78-89% and 56-72%, respectively, when compared with the base material strength. The loss of efficiency with preheating to

80ºC was attributed to the excessive approach to the polymer melting temperature during the process.

4.10. Tool temperature effect

Squeo et al. (2009) [10] studied the potential of preheating the pin with a hot air gun between 60 and 100ºC on the FSW of 3 mm thick HDPE plates in butt joint configuration and used two pin diameters. The joints welded with the 1 mm diameter pin showed only residual improvements with preheating due to the fast cooling of the pin. On the other hand, the joints welded with the 3 mm diameter pin achieved more significant improvements but with lower strengths than those obtained with the smaller pin.

Azarsa et al. (2012) [29] and Mostafapour and Azarsa (2012) [48] studied the FSW on 10 mm thick HDPE plates in butt joint configuration with an hot shoe. In both studies, hot shoe temperatures of 80, 110 and 140ºC were tested. The results obtained by the exclusive variation of the shoe temperature demonstrated that the welds obtained with the shoe at 140ºC present better tensile and flexural strength. According to these researchers, at high rotational speeds of 1600 rpm with the hot shoe temperature of 80ºC, polymer degradation occurred, due to the pin stirring action. By increasing the tool temperature to 110ºC, the material degraded was reduced and with a tool temperature of 140ºC the problem of material degradation disappeared. This phenomenon was justified by the fact that under these conditions there is only a partial melting of the material, which associated with the low conductivity of the polymers results in the concentration of thermal energy in the WN and, consequently, in the degradation of the material in this area. In other words, the increase in rotation must be followed by an increase in the temperature of the shoe in order to avoid heat concentration on the WN.

Azarsa and Mostafapour (2014) [59], during the study of FSW in HDPE plates with 10 mm of thickness in butt joint configuration, found that the use of shoe temperatures below 70ºC result in low flexural strength due to the lack of molten material in the seam, as shown in Figure 4.41. Shoulder temperatures above 150ºC led to burr production and to thickness reduction due to the excess fluidity of the material. The increase in shoulder temperature from 70 to 110ºC led to an increase in flexural strength but increasing the temperature to 150ºC led to the lower values of mean of flexural strength.

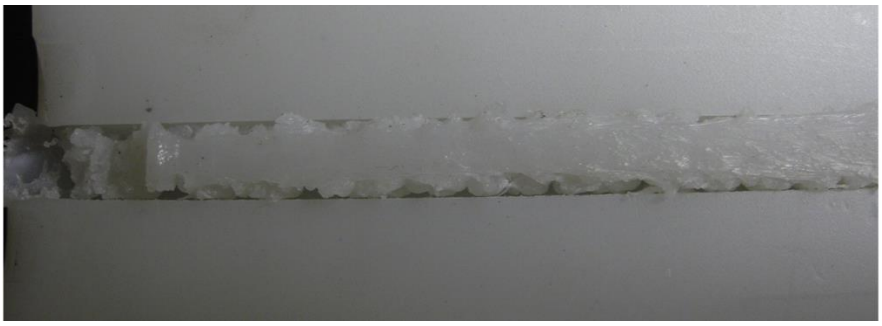

Figure 4.41. Result of welding performed with shoe temperature below 70ºC, adapted from [59].

Vijendra and Sharma (2015) [30], studied the weldability of 5 mm thick HDPE plates by i-FSW in bead-on-plate configuration. These researchers observed that for a tool temperature above 55ºC, a heavy flash occurred and the degradation and burn of the polymer, visible due to the material change to a yellowish color. Tensile strength efficiency above 95% for different temperature settings and different rotational speeds demonstrated the potential of the i-FSW. With a rotational speed of 2000 rpm and a tool temperature of 45ºC, the highest joint efficiency of 104.32% was obtained, as shown in Figure 4.42.

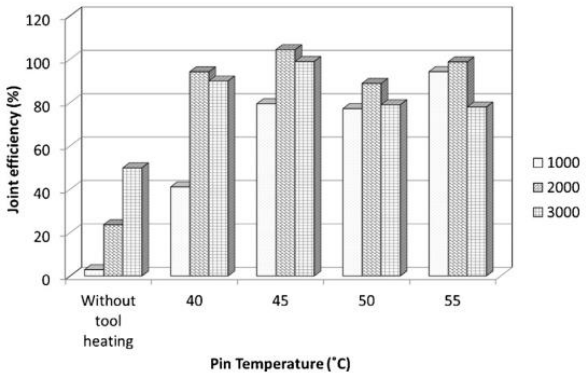

Figure 4.42. Join efficiency for different values of rotational speed and tool temperatures with i-FSW [30].

Strand (2004) [5] studied the FSW of 6 mm thick PP plates in butt joint configuration and used hot shoe temperatures of 110, 127, 143, 160 and 177ºC. The analysis of the results demonstrated that the increase in temperature led to the increase of weld strength and to better microstructural properties. The maximum flexural strength was achieved with the hot shoe temperature of 177ºC.

Banjare et al. (2017) [46] used a new tool heated with an electric resistance for welding 3 mm thick PP plates in butt joint configuration by FSW. The results demonstrated that the use of this heated tool at 110ºC brings advantages to the process, since the values of tensile strength and elongation were always superior in comparison to those obtained by the non-heated tool at the same rotational speeds (see Figure 4.43). The welds obtained without heating the tool showed a higher tendency for the formation of cavities within the seam and irregular surfaces with pronounced burr defects. On the other hand, the welds obtained with hot tool presented few or no defects and a better surface finish.

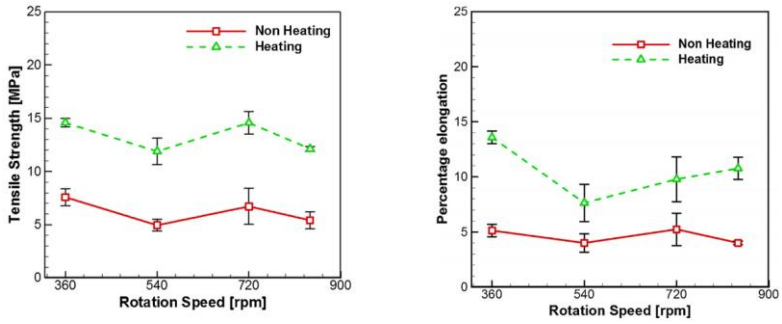

(a) (b)

Figure 4.43. Efect of rotational speed with and without heating the tool on: (a) tensile strength and (b) Percentage of elongation [46].

Moochani et al. (2018) [47], during the study of FSW in PP plates with 4 mm of thickness in butt joint configuration, studied the application of a new stationary shoulder tool heated by a hot air gun during the process. In the preliminary testing phase, the researchers compared the FSW process with and without heating the tool with a rotational speed of 950 rpm and a welding speed of 24 mm/min. Welding with tool heating resulted in joints with better surface finish and higher mechanical strength, (see Figure 4.44). Welds produced without heating the tool could be separated manually. The tensile tests also revealed that the increase in the temperature of the tool during the welding process from 130 to 150 ºC resulted in the improvement of the tensile strength and in the increase of the maximum elongation, justified by the improvement of the material mixture promoted by the greater fluidity of the polymer. In turn, the increase in the temperature of the tool to 170ºC led to a slight reduction in tensile strength and in the big drop in maximum elongation caused by the excessive reduction of crystallinity and consequently by the reduction of the mechanical properties of

the material, as reported in Figure 4.44c. Therefore, an optimum tool temperature of 150ºC was pointed.

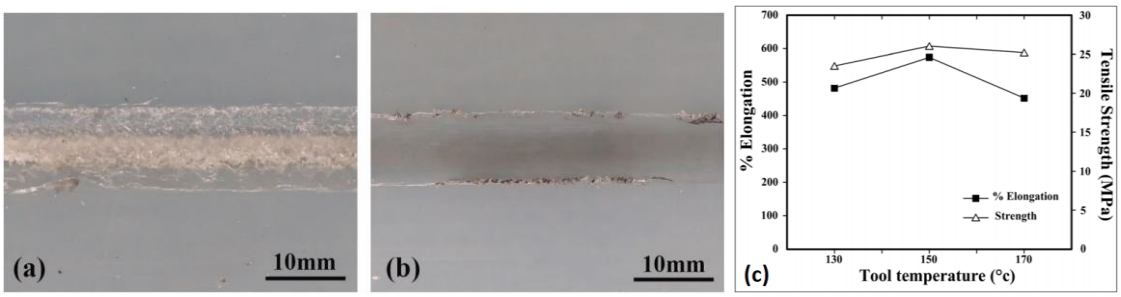

Figure 4.44. Weld surface of PP plates welded with: (a) non-heated tool and (b) heated tool. (c) Effect of tool temperature on tensile strength and on the percentage of elongation of joints [47] .

Bagheri et al. (2013) [67] also studied the influence of different heating temperatures of the hot shoe during the FSW of ABS plates with 5 mm of thickness on butt joint configuration with shoe temperatures of 50, 80 and 100ºC. Once again, the increase in the shoe temperature proved to be beneficial to the process, allowing to reach a maximum tensile strength of 88% in relation to the strength of the base material for the highest shoe temperature tested (100ºC) with a rotational speed of 1600 rpm and a welding speed of 20 mm/min.

Mendes et al. (2014) [45], in the study on the FSW of 6 mm thick ABS plates in butt joint configuration with and hot shoe used shoe temperatures of 90, 115 and 130ºC with 5 degrees of tolerance. Welds made with an average temperature of 90ºC showed a low quality surface finish, making it possible to identify porosity and burr defects in the RS (see Figure 4.45a). The higher roughness was an indicator of the lack of fusion during the process. In turn, the welds carried out with an average temperature of 130ºC also demonstrated low quality in the surface finish of the crown, with notes of burnt polymer, indicating that this temperature is excessive for the union of this polymer (see Figure 4.45c). The welds carried out with an average temperature of 115ºC showed a smooth surface finish and pore-free cross section (see Figure 4.45b). It was concluded that the operating temperature of the FSW must be adjusted so that it is close to the glass transition temperature of the polymer.

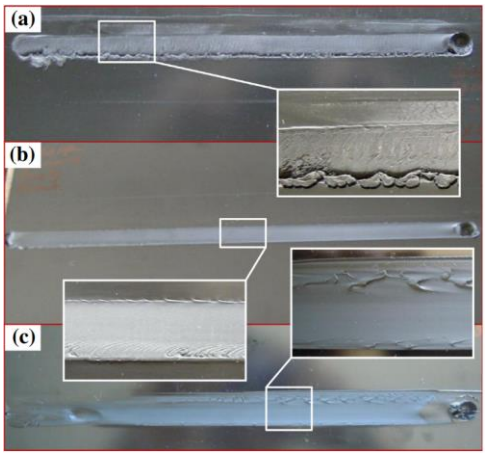

Figure 4.45. Surface finish of welds produced with hot shoe temperatures of: (a) 90ºC, (b) 115ºC and (c) 130ºC [45].

Mostafapour and Asad (2016) [49], in the study of FSW in PA 6 plates with 6 mm of thickness in the butt joint configuration, confirmed that with the increase of rotational speed an increase in the temperature of the shoe must occur in order to avoid the degradation of the polymer and the consequent loss of mechanical strength of the weld. These researchers also found that the increase in the temperature of the hot shoe up to the optimum value of 150ºC allowed an increase in the tensile strength of the joint. Above this value, the excess temperature of the shoe led to a drop in material strength due to the formation of flash defects and due to the reduction of the thickness of the weld. Shoe temperatures above 150ºC not only led to the degradation and projection of molten material out of the weld, but also to the degradation of the Teflon shoe coating. As a consequence of the degradation of the coating, the material showed a greater tendency to stick to the shoe leading into the loss of quality in the surface finish of the weld, as shown in Figure 4.46.

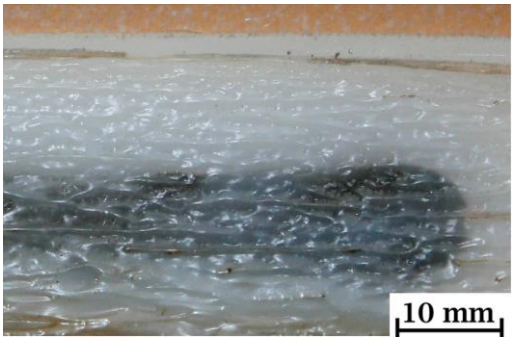

Figure 4.46. Poor surface wiring resulting from excessive operating temperature and loss of shoe coating quality [49].

5. CONCLUSIONS AND SUGGESTIONS FOR FUTURE WORKS

The Table 5.1 was developed in order to synthesize the information related to the optimization of different parameters from the different researches related with the FSW of polymeric materials. Each line corresponds to the resume of one different study and contains information about the technique used, the thickness and the materials welded, the evaluated parameters and the respective optimum values determined. Based on the analysis of this table and on what was described in the previous chapters, it was possible to reach to some important conclusions related to the joining of polymeric materials by FSW.

Table 5.1. Resume of the researches carried out on FSW in polymeric materials

Authors (year) [reference]	Technic, material (thickness) and joint configuration	Welding parameters used	Optimum welding parameters found
Strand (2004) [5]	FSW with hot shoe, PP (6 mm) and butt welded	Pin geometry: tapered threaded; Pin diameter: 6.4, 9.5 and 12.7 mm; Rotational speed: 1080 rpm; Welding speed: 51, 102, 203 and 305 mm/min; Shoe temperature: 110, 127, 143, 160 and 177 ºC.	The performance of the welds was improved with pin diameters of 12.5 mm, a welding speed of 51 mm/min and a shoe temperature of 160 to 177ºC.
Arici and Sinmaz (2005) [27]	Single and double side FSW, MDPE (3 and 5 mm) and butt welded	Shoulder diameter: 16 mm; Pin diameter: 5 mm; Pin length: 2.8 mm; Rotational speed: 600, 800 and 1000 rpm; Welding speed: 12.5, 25, 40 and 60 mm/min; Tilt angle: 0 and 1º.	A tensile strength close to the material base strength was achieved with a rotational speed of 1000 rpm, a welding speed of 12.5 mm/min and a tilt angle of 1º and with double side pass of the tool in the 5 mm thick plates.
Kiss and Czigány (2007) [55]	Conventional FSW, PP (15 mm) and butt welded	Tool geometry: traditional milling tool with 6 and 8 grooves; Groove slope: 15º, 30º and 45º; Tool diameter: 8 mm; Rotational speed: 450, 630, 900, 1250 and 1800 rpm; Welding speed: 20, 31.5, 40 and 63 mm/min.	Better results were obtained with 6 grooves and a groove slope of 45º, a rotational speed of 1800 rpm and a welding speed of 20 mm/min.
Arici and Selale (2007) [37]	Double side FSW, MDPE (5 mm) and butt welded	Shoulder diameter: 16 mm; Pin diameter: 5 mm; Pin length: 2.8 mm; Rotational speed: 1000 rpm; Welding speed: 12.5, 25 and 40 mm/min; Tilt angle: 0, 1, 2, 3, 4 and 5º	A tensile strength of 87% of the base material strength was obtained with a welding speed of 12.5 mm/min and a tilt angle of 1º.
Squeo et al. (2009) [10]	FSW with preheating the pin by hot air gun or the plate with a heater plate, HDPE (3 mm) and butt welded	Shoulder diameter: 6 mm; Pin diameter: 1 and 3 mm; Rotational speed: 3000 to 20000 rpm; Welding speed: 10, 28 and 44 mm/min; Preheating temperature of the pin: room temperature and 70ºC; Heater plate temperature: 100, 125 and 150ºC; Contact time between the heater plate and the material: 0 to 180 s.	A tensile strength close to the strength of the base material was achieved with a pin diameter of 1 mm, a rotational speed of 5000 rpm, a welding speed of 10 mm/min and a contact time of 180 s with a heater plate at 150ºC.

Authors (year) [reference]	Technic, material (thickness) and joint configuration	Welding parameters used	Optimum welding parameters found
Aydin (2010) [2]	FSW with and without preheating the plates, UHMW-PE (4 mm) and butt welded	Shoulder diameter: 20 mm; Pin geometry: M4; Pin length: 3.8 mm; Rotational speed: 960 and 1960 rpm; Welding speed: 10 and 20 mm/min; Preheating temperatures: room temperature, 50ºC and 80ºC.	A tensile strength of 89% compared with the tensile strength of the base material was achieved with a rotational speed of 960 rpm, a welding speed of 20 mm/min and a preheating temperature of 50 ºC.
Rezgui et al. (2010) [20]	FSW with stationary shoulder, HDPE (15 mm) and butt welded	Pin geometry: Cylindrical threaded; Pin size: M10, M12 and M14; Rotational speed: 900, 1280 and 1700 rpm; Welding speed: 16, 29 and 44 mm/min; Hold time: 9, 15 and 20 s	In this case, optimum welding parameters were not discussed
Saeedy and Givi (2010) [23]	Single and double side FSW, HDPE (8 mm) and butt welded	Number of tools: 2; Shoulder diameter: 10 and 15 mm; Pin diameter: 5 and 6 mm; Pin length: 4.5 and 7.8; Rotational speed: 1200, 1400, 1600 and 1800 rpm; Welding speed: 12 mm/min; Tilt angle: 1º.	Maximum elongation percentage and maximum tensile strength of 18.52 MPa (80% of the base material strength) were obtained with double side pass and a rotational speed of 1400 rpm.
Saeedy and Givi (2010) [61]	Conventional FSW, MDPE (6 mm) and butt welded	Shoulder diameter: 12 mm; Pin geometry: cylindrical; Pin diameter: 5 mm; Pin length: 5.7 mm; Rotational speed: 1400, 1600, 1800 and 2000 rpm; Welding speed: 15 mm/min; Tilt angle: 1 and 2º.	A tensile strength of 14.18 MPa (70% of the base material strength) was achieved with a rotational speed of 1600 rpm and a tilt angle of 1º.
Saeedy and Givi (2011) [62]	Conventional FSW, MDPE (8 mm) and butt welded.	Shoulder diameter: 12 mm; Pin geometry: cylindrical; Pin diameter: 6 mm; Pin length: 7.7 mm; Rotational speed: 1000, 1200, 1400, 1600 and 1800 rpm; Welding speed: 12, 16 and 20 mm/min; Tilt angle: 1 and 2º;	A tensile strength of 14.9 MPa (75% of the base material strength) was obtained with a rotational speed of 1400 rpm, a welding speed of 12 mm/min and a tilt angle of 1º.
Kiss and Czigány (2011) [63]	FSW with stationary shoulder, PP (10 mm) and butt welded	Tool geometry: milling cutter with 8-tooth; Tool diameter: 8 mm; Rotational speed: 2000 and 3000 rpm; Pin depth: 9.6 mm; Welding speed: 60 mm/min.	The maximum tensile strength of 86% of the base material strength was achieved with a rotational speed of 3000 rpm.
Azarsa et al. (2012) [29]	FSW with hot shoe, HDPE (10 mm) and butt welded	Shoulder dimensions: 28 mm x 250 mm; Shoulder coating: PTFE; Pin geometry: cylindrical threaded; Pin diameter: 10 mm; Rotational speed: 1000, 1250 and 1600 rpm; Plunge depth: 0.5 mm; Welding speed: 10, 25 and 40 mm/min; Shoulder temperature: 80, 110 and 140ºC.	An ultimate tensile strength above 90% of the base material strength and the higher flexural strength were obtained with a hot shoe temperature of 140ºC, a rotational speed of 1600 rpm and a welding speed of 25 mm/min.
Mostafapour and Azarsa (2012) [48]	FSW with hot shoe, HDPE (10 mm) and butt welded	Shoulder dimensions: 28 mm x 250 mm; Shoulder coating: PTFE; Pin geometry: cylindrical threaded; Pin diameter: 10 mm; Rotational speed: 1000, 1250 and 1600 rpm; Plunge depth: 0.5 mm; Welding speed: 10, 25 and 40 mm/min; Shoulder temperature: 80, 110 and 140ºC.	Ultimate tensile strength above 90% of the base material strength and the higher flexural strength were obtained with a hot shoe temperature of 140ºC, a rotational speed of 1600 rpm and a welding speed of 25 mm/min.
Panneerselvan and Lenin (2012) [64]	Conventional FSW, PP (10 mm) and butt welded	Shoulder diameter: 24 mm; Pin geometry: straight cylindrical, taper cylindrical, square, triangular, threaded cylindrical and grooved with square; Pin diameter: 6 mm; Rotational speed: 1000, 1500 and 2500 rpm; Welding speed: 15, 30, 45 and 60 mm/min.	In this case, optimum welding parameters were not discussed
Bozkurt (2012) [58]	Conventional FSW, HDPE (4 mm) and butt welded	Shoulder diameter: 18 mm; Pin diameter: 6 mm; Pin length: 3.8 mm; Rotational speed: 1500, 2100 and 3000 rpm; Welding speed: 45, 75 and 115 mm/min; Tilt angle: 1, 2 and 3º.	Maximum tensile join efficiency of 86.2% was obtained with a rotational speed of 3000 rpm, a welding speed of 115 mm/min and a tilt angle of 2º.
Kiss and Czigány (2012) [26]	FSW with stationary shoe, PETG (10 mm) and butt welded	Pin geometry: conventional milling cutter with 4 and 8 edges; Tool diameter: 8 and 12 mm; Rotational speed: 750, 900, 1200 and 2250 rpm; Welding speed: 50, 75, 90 and 100 mm/min.	In this research it was found that a new K factor between 150 and 400 was needed to obtain proper quality welded joints on this material.

Authors (year) [reference]	Technic, material (thickness) and joint configuration	Welding parameters used	Optimum welding parameters found
Bagheri et al. (2013) [67]	FSW with hot shoe, ABS (5 mm) and butt welded	Pin geometry: threaded; Pitch length: 7 mm; Pin diameter: 10 mm; Rotational speed: 800, 1250 and 1600 rpm; Welding speed: 20, 40 and 80 mm/min; Shoe temperature: 50, 80 and 100ºC;	A maximum joint efficiency of 88% in relation to the base material strength was achieved with a shoe temperature of 100ºC, a rotational speed of 1600 rpm and a welding speed of 20 mm/min.
Inaniwa et al. (2013) [21]	Conventional FSW, HDPE, PA 6 and PVC (5 mm) but welded	Shoulder diameter: 20 mm; Din geometry: cylindrical threaded M10;Pin length:4.8 mm; Gap between the shoulder and the plate: 0.1 mm; Rotational speed: 800 and 1240 rpm for HDPE, 380, 440 and 500 rpm for PA 6 and 1600 and 1800 rpm for PVC; Welding speeds: 15, 30 and 45 mm/min for HDPE, 40 and 50 mm/min for PA 6 and 10, 20 and 30 mm/min for PVC; Tilt angle: 0º.	A joint efficiency of 70%, 45% and 35% were obtained for HDPE (with 1240 rpm and 15 mm/min), PVC (with 1800 rpm and 10 mm/min) and PA 6 (with 440 rpm and 40 mm/min), respectively.
Panneerselvan and Lenin (2013) [81]	Conventional FSW, PP (10 mm) and butt welded	Shoulder diameter: 24 mm; Pin geometry: square, taper; triangular and threaded; Pin diameter: 6 mm; Pin length: 10 mm; Rotational speed: 1500, 1750, 2000 and 2250 rpm; Welding speed: 30, 40, 50 and 60 mm/min.	The optimum geometry was the threaded tool which achieved welds with good quality and defect free cross sections.
Sharma and Singh (2013) [65]	Conventional FSW, PP (10 mm) and butt welded	Tool diameter: 8, 10 and 12 mm; Rotational speed: 600, 750 and 900 rpm; Welding speed: 60, 70 and 80 mm/min.	A tensile strength of 80% of the base material strength was achieved with a tool diameter of 10 mm, a rotational speed of 900 rpm and a welding speed of 70 mm/min.
Azarsa and Mostafapour (2014) [59]	FSW with hot shoe, HDPE (10 mm) and butt welded	Shoe dimensions: 28 mm x 250 mm; Shoulder coating: PTFE; Pin geometry: cylindrical threaded M10x1; Pin length: 9.5 mm; Rotational speed: 710, 1120 and 1400 rpm; Welding speed: 25, 50 and 100 mm/min; Shoe temperature: 70, 110 and 150ºC.	A maximum value of flexural strength of 33.78 MPa which is about 95% of the base material flexural strength was achieved with a rotational speed of 1400 rpm, a welding speed of 25 mm/min and a shoe temperature of 110ºC.
Panneerselvan and Lenin (2014) [80]	Conventional FSW, PA 6 (10 mm) and butt welded	Shoulder diameter: 24 mm; Pin geometry: Left hand threaded; Tool rotation direction: clockwise and counterclockwise; Pitch length: 1 mm; Pin diameter: 6 mm; Pin length: 10 mm; Gap between the shoulder and the plate: 0.5 mm; Rotational speed: 1000 rpm; Welding speed: 10 mm/min.	These researchers concluded that the left-hand threaded pin must operate in counterclockwise direction which also means that a right-hand threaded pin must operate in clockwise direction.
Pirizadeh et al. (2014) [40]	SRFSW, ABS (5 mm) and butt welded	Shoulder coating: PTFE; Pin shape: simple and convex; Pin diameter: 7 mm; Rotational speed: 400, 600 and 800 rpm; Welding speed: 20, 40 and 60 mm/min;	The highest tensile strength of 20.7 MPa which is 60.63% of the base material strength was achieved with the convex pin, a rotational speed of 400 rpm and a welding speed of 40 mm/min.
Lenin et al. (2014) [66]	Conventional FSW, PP (10 mm) butt welded	Shoulder diameter: 24 mm; Pin geometry: square, taper, triangular and threaded; Pin diameter: 6 mm; Pin length: 9.8 mm; Rotational speed: 1500, 1750, 2000 and 2250 rpm; Welding speed: 30, 40, 50 and 60 mm/min.	The optimum parameters found were a threaded pin geometry, a rotational speed of 1500 rpm and a welding speed of 60 mm/min.
Mendes et al. (2014) [57]	FSW with a stationary shoe, ABS (6 mm) and butt welded	Shoulder dimensions: 25 mm x 177 mm; Pin geometry: conical threaded; Pin diameter: 10 mm at the base and 6 mm at the tip; Pin length: 5.9 mm; Rotational speed: 1000, 1250 and 1500 rpm; Welding speed: 50, 100 and 200 mm/min; Axial force: 0.75, 2.25, 3.75 and 4 kN.	Minimal values of rotational speed of 1250 rpm and of axial force of 1.5 kN are required to achieve a defect free weld. The optimum parameters found were a rotational speed of 1500 rpm, a welding speed of 50 mm/min and a axial force of 4 kN.
Mendes et al. (2014) [45]	FSW with hot shoe, ABS (6 mm) and butt welded	Shoulder dimensions: 25 mm x 177 mm; Pin geometry: conical threaded; Pin diameter: 10 mm at the base and 6 mm at the tip; Pin length: 5.9 mm; Rotational speed: 1000, 1250 and 1500 rpm; Welding speed: 50, 100 and 200 mm/min; Axial force: 1, 1.5 and 2 kN; Shoe temperature: 90, 115 and 130ºC.	Good quality welds were achieved with rotational speeds above 1250 rpm, welding speeds between 50 and 100 mm/min, a minimum value of axial force of 1.5 kN and ahoe temperatures of 115ºC

Authors (year) [reference]	Technic, material (thickness) and joint configuration	Welding parameters used	Optimum welding parameters found
Sadeghian and Givi (2015) [68]	Conventional FSW, ABS (8 mm) and butt welded	Shoulder geometry: concave cylindrical; Shoulder diameter: 10, 15 and 20 mm; Pin geometry: conical and cylindrical; Pin diameter: 5, 6 and 8 mm; Rotational speed: 900, 1400 and 1800 rpm; Welding speed: 6, 16 and 25 mm/min; Tilt angle: 0, 1 and 2º.	An efficiency of 100.6% was achieved with a conical pi with 6 mm of diameter and a concave shoulder of 20 mm and with a rotational speed of 900 rpm, a welding speed of 25 mm/min and a tilt angle of 2º.
Zafar et al. (2015) [70]	Conventional FSW, PA 6 (16 mm) and butt welded	Shoulder geometry: double step shoulder; First shoulder diameter: 18 mm; Second shoulder diameter: 25 mm; Pin geometry: M8; Rotational speed: 300, 400, 500 and 1000 rpm; Welding speed: 25 mm/min; Tilt angle: 0º;	A tensile strength of 32% of the base material strength was achieved with a rotational speed of 300 rpm.
Husain et al. (2015) [69]	Conventional FSW, PA 66 (8 mm) and butt welded	Shoulder diameter: 18 mm; Pin geometry: cylindrical; Pin diameter: 4 mm; Pin length: 7.8 mm; Rotational speed: 780, 994, 1255, 1570 and 2000 rpm; Welding speed: 27, 42 and 62 mm/min;	The maximum tensile strength of 8.52 MPa which is 54.7% of the base material strength and the maximum impact strength was achieved with a rotational speed of 1570 rpm and a welding speed of 42 mm/min.
Vijendra and Sharma (2015) [30]	i-FSW, HDPE (5 mm) and bead on plate welded	Shoulder diameter: 10 mm; Pin geometry: taper threaded; Major and minor diameter: 6 and 5 mm, respectively; Pin length: 3.83 mm; Rotational speeds: 1000, 2000 and 3000 rpm; Welding speed: 50 and 100 mm/min; Pin temperatures: 40, 45, 50 and 55ºC;	The highest joint efficiency of 104.32% was obtained with a rotational speed of 2000 rpm, a welding speed of 50 mm/min and a tool temperature of 45ºC
Eslami et al. (2015) [36]	FSW with stationary shoulder, PE (2 mm) with PP (1.2 mm)	Shoulder geometry: stationary shoulder in PTFE with a highly conductive bronze sleeve; Pin geometry: flat face and triangular; Pin diameter: 6 mm; Pin length: 2.4 and 2.8 mm; Rotational speed: 1500 and 2500 rpm; Welding speed: 20 and 100 mm/min.	Higher values of tensile strength were achieved with triangular pin, a pin length of 2.8 mm, a rotational speed of 2500 rpm and a welding speed of 100 mm/min.
Eslami et al. (2015) [41]	FSW with and without stationary shoulder, PS (2.6 mm) with PP (1.5 mm)	Conventional shoulder diameter: 8, 10, 15 and 20 mm; Stationary shoulder material: PC, PTFE, aluminum, wood and brass; Pin geometry: cylindrical with two flat surfaces, triangular and square; Pin length: 2 to 3.6 mm; Pin diameter: 3 to 7 mm; Rotational speed: 800 to 3000 rpm; Welding speed: 10 to 70 mm/min	By comparing results, the researchers concluded that the stationary shoulder made in PTFE led to better surface quality that the rest of the stationary shoulder and that the conventional tools. The optimization of other parameter were not discussed.
Zafar et al. (2016) [71]	Conventional FSW, PA 6 (16 mm) and butt welded	Shoulder geometry: double step shoulder; First shoulder diameter: 18 mm; Second shoulder diameter: 25 mm; Shoulder diameter: 25 mm; Pin geometry: M8; Rotational speed: 300, 400, 500 and 1000 rpm; Welding speed: 25 mm/min; Tilt angle: 0 and 3º;	A tensile strength of 32% of the base material strength was achieved with a rotational speed of 300 rpm and a tilt angle of 0º.
Hoseinlaghab et al. (2015) [56]	Conventional FSW, HDPE (8 mm) and butt welded	Shoulder diameter: 10, 15 and 20 mm; Pin geometry: cylindrical and conical; Pin diameter: 5, 6, 7 and 8 mm; Pin length: 5 and 7 mm; Rotational speed: 450, 560, 710, 900, 1120, 1400 and 1800 rpm; Welding speed: 10, 12.5, 16, 20, 25] 31.5 mm/min, tilt angle: 0, 1 and 2º.	The highest creep resistance was achieved with a shoulder diameter of 20 mm, a cylindrical pin geometry, a pin diameter of 6 mm, a pin length of 7 mm, a rotational speed of 1120 rpm, a welding speed of 20 mm/min and a tilt angle of 0º.
Nateghi and Hosseinzadeh (2016) [52]	FSW with application of cooling, HDPE (5 mm) and butt welded	Pin geometry: threaded; Shoulder diameter: 18, 20 and 22 mm/min; Rotational speed: 1000, 1600 and 2200; Welding speed: 40, 60 and 80 mm/min; Cooling: with and without; Cooling pressure: 2 bar.	The highest value of tensile strength was obtained with a cooling stage and with a rotational speed of 2200 rpm, a welding speed of 40 mm/min and a shoulder diameter of 22 mm.
Mostafapour and Asad (2016) [49]	FSW with hot shoe, PA 6 (6 mm) and butt welded	Shoe dimensions: 28 mm x 250 mm; Pin geometry: M10; Shoe coating: PTFE; Rotational speed: 500, 630 and 800 rpm; Welding speed: 20, 25 and 30 mm/min; Shoe temperature: 100, 125 and 150ºC.	A joint efficiency of 98.06% was achieved with a rotational speed of 630 rpm, a shoulder temperature of 150ºC and a welding speed of 20 mm/min, but an optimum value of rotational speed of 730 rpm was calculated.

Authors (year) [reference]	Technic, material (thickness) and joint configuration	Welding parameters used	Optimum welding parameters found
Banjare et al. (2017) [46]	FSW with and without heated tool, PP (3 mm) butt welded	Shoulder diameter: 18 and 20 mm; Pin geometry: threaded cylindrical; Pin diameter: 3.5 mm; Pin length: 2.75; Rotational speed: 360, 540, 720 and 840 rpm; Welding speed: 20 and 30 mm/min; Tilt angle: 2º; Tool temperature: room temperature and 110ºC.	A maximum joint efficiency of 55.51% was achieved with a tool temperature of 110ºC, a shoulder diameter of 20 mm and a rotational speed of 720 rpm. Nothing was said about the optimum welding speed.
Hajideh et al. (2017) [77]	FSW with stationary shoulder, PP-PE (8 mm) and butt welded	Pin geometry: Square, Threaded cylindrical, Triangular and straight cylindrical; Pin diameter: 10 mm; Rotational speed: 900, 1860 and 2920 rpm; Welding speed: 8, 10 and 12.5 mm/min.	A tensile strength of 98% of the PE resistance was achieved with the threaded cylindrical pin and with a rotational speed of 1860 rpm and a welding speed of 12.5 mm/min.
Sahu et al. (2018) [35]	Conventional FSW, PP (6 mm) and butt welded	Shoulder diameter: 12 and 16 mm; Pin geometry: conical (15º), square and cylindrical; Pin diameter: 6 mm; Pin length: 5.6 mm; Rotational speed: 500, 750 and 1000 rpm; Welding speed: 5, 15 and 25 mm/min; Tilt angle: 1º.	A maximum joint efficiency of 59.82% was achieved with a shoulder diameter of 12 mm, a square pin geometry, a rotational speed of 750 rpm and a welding speed of 15 mm/min.
Eslami et al. (2018) [76]	FSW with stationary shoulder, PE (2 mm) with PP (1.2 mm) and lap welded	Shoulder geometry: stationary shoulder in PTFE with a highly conductive bronze sleeve; Pin geometry: flat face and triangular; Pin diameter: 3 and 6 mm; Pin length: 2.4 and 2.8 mm; Rotational speed: 1500 and 2500 rpm; Welding speed: 20 and 100 mm/min.	A joint efficiency of 76% of the PP tensile strength was achieved with flat face pin, a pin length of 2.8 mm, a rotational speed of 2500 rpm and a welding speed of 20 mm/min.
Eslami et al. (2018) [22]	FSW with stationary shoe, HMW-PE (3mm) and butt welded	Pin geometry: double-grooved; Pin diameter: 3, 4 and 5 mm; Pin length: 2.95 mm; Rotational speed: 1500, 2000 and 2500 rpm; Welding speed: 30, 50 and 70 mm/min; Axial Force: 800, 950 and 1100 N.	Joint efficiencies above 90% were achieved with different experiments and the optimum values found were a pin diameter of 5 mm, a welding speed of 2500 rpm, a rotational speed of 70 mm/min and an axial force of 950 N.
Moochani et al. (2018) [47]	FSW with new heated stationary shoulder, PP (4 mm) and butt welded	Rotational speed: 360, 565 and 950 rpm; Welding speed: 24, 40 and 60 mm/min; Tool temperature: 130, 150 and 170ºC.	Tensile strengths and percentage of elongation above 90% were achieved with different conditions but the optimum parameters found were a rotational speed of 950 rpm, a welding speed of 24 mm/min and a tool temperature of 150ºC.
Romero et al. (2018) [42]	FSW with and without stationary shoulder, HDPE (8.5 mm) and butt welded	Tool 1: threaded conical with rotational shoulder; Tool 2: threaded cylindrical with stationary shoulder; Rotational speed: 846 and 1036 mm/min; Welding speed: 14 and 25 mm/min	These researchers found that the tool 2 achieved welds with better surface quality. Optimum parameters were not discussed.
Derazkola and Simchi (2018) [73]	Conventional FSW, PMMA (4 mm) and butt welded	Shoulder diameter:18 mm; Pin geometry: cone frustum, square frustum and triangle frustum; Pin upper diameter: 12 mm; Pin lower diameter: 8 mm; Pin height: 3.6 mm; Rotational speed: 810, 1250, 1600 and 1920 rpm; Welding speed: 25 and 50 mm/min; Plunge depth: 0.2 mm; Tilt angle: 2º;	Maximum tensile strength of 59MPa (84% of PMMA strength) was achieved with a cone frustum pin geometry, a rotational speed of 1600 rpm and a welding speed of 25 mm/min.
Elyasi and Derazkola (2018) [17]	Conventional FSW, PMMA (4 mm) and T-joined	Shoulder diameter: 20 mm; Pin geometry: frustum; Pin length: 4.8 mm; Rotational speed: 1000, 1250 and 1600 rpm; Welding speed: 25 and 50 mm/min; Plunge depth: 0.2 mm; Tilt angle: 2º.	Maximum tensile strength (84% of PMMA strength) and flexural strength (93% of PMMA strength) were achieved with a rotational speed of 1600 rpm and a welding speed of 25 mm/min.
Adibeig et al. (2018) [74]	Conventional FSW, PMMA (4 mm) and butt welded	Shoulder geometry: conventional and double step shoulder; Lower shoulder diameter: 16 mm; Upper shoulder diameter: 24 mm; Shoulder concavity angle: 3º; Pin geometry: cylindrical threaded M6; Pin length: 2.5 mm; Rotational speed: 250, 315, 400 and 500 rpm; Welding speed: 16 and 20 mm/min; Plunge depth: 0.5 and 1 mm;	The highest tensile strength was achieved with a rotational speed of 250 rpm, a welding speed of 16 mm/min and a plunge depth of 1 mm, but the mean of tensile strength values was higher with rotational speeds of 315 rpm and plunge depths of 0.5 mm.

Authors (year) [reference]	Technic, material (thickness) and joint configuration	Welding parameters used	Optimum welding parameters found
Moreno-moreno et al. (2018) [60]	FSW stationary shoulder, HDPE (8.5 mm) and butt welded	Shoulder: pinewood scraper; Pin geometry: cylindrical threaded; Rotational speed: 846 and 1036 rpm; Welding speed: 14 and 25 mm/min; Tilt angle: 0º;	Maximum tensile strength was achieved with a rotational speed of 1036 rpm and a welding speed of 14 mm/min.
Mishra et al. (2019) [1]	Conventional FSW, HDPE (6 mm) and butt welded	Shoulder diameter: 14, 18 and 24 mm; Pin diameter: 5 mm; Pin length 5.6 mm; Rotational speed: 500, 600 and 800 rpm; Welding sped: 10, 20 and 30 mm/min; Tilt angle: 1º; Plunge depth: 0.1 mm;	The maximum tensile strength of 14.63 MPa which is about 44.34% of the base material strength was achieved with a shoulder diameter of 14 mm; a rotational speed of 800 rpm and a welding speed of 10 mm/min.
Derazkola et al. (2019) [72]	Conventional FSW, PC (4 mm) and lap welded	Shoulder diameter: 18 mm; Pin diameter: 6 mm; Pin length: 3.8 mm; Rotational speed: 1400, 1800, 2200 and 2600 rpm; Welding speed: 70, 105 and 170 mm/min; Plunge depth: 0.3, 0.6, 0.9, 1.2, 1.5 and 1.8 mm; Tilt angle: 0.5, 1, 1.5, 2, 2.5, 3, 3.5 and 4º.	The highest tensile strength (55 MPA) and flexural strength (61 MPa) were achieved with a rotational speed of 2200 rpm, a welding speed of 105 mm/min, a plunge depth of 1.2 mm and a tilt angle of 2.5º.
Kumar and Roy (2019) [78]	Conventional FSW, ABS-PC (6 mm) and butt welded	Shoulder geometry: double step shoulder; First shoulder diameter: 24 mm; Second shoulder diameter: 16 mm; Shoulder concavity angle: 3º; Pin geometry: threaded; Pin diameter: 6 mm; Pin length: 4.8 mm; Rotational speed: 800, 1200 and 1600; Welding speed: 6, 12 and 18 mm/min; Tilt angle: 0, 1 and 2º.	Maximum joint efficiency of 73% of the base material strength was achieved with a rotational speed of 1600 rpm, a welding speed of 12 mm/min and a tilt angle of 2º.
Lambiase et al (2020) [79]	Conventional FSW, PC (3 mm) and butt welded	Pin geometry: cylindrical; Pin diameter: 4 mm; Rotational speed: 2000 rpm; Welding speed: 20, 60, 100 and 200 mm/min; Plunge depth: 0.05 mm; Tilt angle: 0, 2, 4 and 6º	Maximum tensile strength of 45 MPa, which is 78% of base material strength was achieved with a welding speed of 60 mm/min and a tilt angle of 2º.
Sharma et al. (2020) [75]	Conventional FSW, PLA (6 mm) and butt welded	Shoulder diameter: 18 mm; Shoulder concavity angle: 6º; Pin geometry: cylindrical, conical and threaded; Pin diameter: 6 mm; Pin length: 5.7 mm; Rotational speed; 700, 1400 and 2000 rpm; Welding speed: 20, 30 and 40 mm/min;	Maximum highest tensile strength of 27.04 MPa which is 65.95% of the base material strength was achieved with the cylindrical pin, a rotational speed of 1400 rpm and a welding speed of 30 mm/min.

5.1. Conclusions

With several authors reporting the success of the technique with very high joint efficiencies, it appears that the FSW may come to replace other joining techniques currently used, especially in the industry with the help of robotization. Because the FSW proved to be more difficult in polymeric materials than in metallic ones, there was a need to introduce some innovations to the conventional process. Even with some authors reporting good results with conventional tools, the use of stationary shoulder tools and the development of different heated tools, or even by heating the base material, were some of the solutions found that allowed the improvement of the efficiency of the process for this group of materials. The tool that stood out most among the studies was the hot stationary shoe.

Most of the studies related with the optimization of the process were focused mainly on the optimization of rotational speeds and welding speeds. The optimal values of these and other parameters vary widely from study to study, even within the same materials and the same techniques. For this reason, it was impossible to set an optimal value for each of these parameters. On the other hand, it is possible to point out ranges of values based on what was found on the literature.

The optimum values of rotational speed determined for PP and PE were between 900 and 3000 rpm. For the PP, optimal rotational speeds of 720 and 750 were determined but the joint efficiency achieved with these speeds was less than 60% so it was decided not to include them in the interval. For PE, an optimal rotational speed of 5000 rpm was also found, but it was obtained with a 1 mm diameter pin, which may justify the need to have used a speed so much higher than the other studies. ABS, PA 6 and PA 66 presented optimal rotational speeds between 300 and 1600 rpm. For the remaining polymers it was decided to refer only to the ideal values obtained due to the fact that the number of studies is insufficient to point other conclusions. The optimal rotational speeds found for the PC were 2000 and 2200 rpm, for the PMMA were 1600 and 350 rpm, for PVC were 1800 rpm and for the PLA were 1400 rpm.

Regarding the welding speed, the range of optimum values determined for PP and PE is between 10 and 70 mm/min and for ABS, PA 6 and PA 66 between 10 and 50 mm/min. In the case of the remaining polymers, the optimal values found for PC were 60 and 105 mm/min, for PMMA 16 and 25 mm/min, for PVC 10 mm/min and for PLA 30 mm/min.

The axial force and the plunge depth are two parameters that have been poorly evaluated in the literature. Despite this, the studies that evaluated the influence of these parameters found that the variation of the axial force and plunge depth have a great impact on the final quality of the welding. The researchers who approached the study of axial force found that the increase in pressure on the material favors the reduction of the number of defects within the weld seam. On the other hand, excessive values of axial force have been shown to be detrimental to the quality of the weld. The values indicated as optimum for the union of polymeric materials by FSW ranged between 950 and 1500 N and were only determined for stationary shoulder tools. From the plunge depth study, it was found that the optimum plunge depth values were between 0.5 mm and 1 mm. For welds in lap joint

configuration, the ideal value was found at 1.2 mm. For both these parameters, due to the lack of information, is expected that optimum values different from these could be determined in the future.

The study of influence of the tilt angle proved to be important on the optimization of the FSW process but was only evaluated for rotating shoulder tools. In the case of stationary shoulder tools, only the use of angles of 0º was reported. Among the studies that evaluated different tilt angles, most of these found that the optimum value was between 1 and 2º. The increase of the tilt angle from 0 to 1 or 2º led to the increase of the temperature, of the pressure on the molten material and of the SZ size. This increase was therefore related with the reduction of the number and size of the defects and with the improvement of the mechanical properties. Tilt angles above these values led to the formation of excessive flash defect and to the reduction of the weld thickness which led to the weakening of the joints.

Regarding the pin size, it was found that most studies used pin diameters close to the thickness of the material to be joined. However, there were also good results with diameters very different from this dimension. Thus, it was not possible to draw conclusions about the optimal value or its proportion in relation to other dimensions. The comparison between different pin geometries for the welding of polymers showed that in most cases the best results were obtained with threaded or grooved pins because these tools facilitate the transport of the material and guarantee a better mixture of the polymer. In the case of threaded pins, the direction of rotation should always favor the downward movement of the material to ensure a good welding. On the other hand, sometimes the application of these tools has led to the formation of too turbulent flows. For this reason, in certain cases the use of cylindrical and conical straight pins was preferable.

The study of traditional tools also focused on the study of the shoulder diameter and geometry. The optimization of the shoulder diameter was also not easy to do, since small shoulders cannot retain the material and large shoulders lead to the degradation of the polymer and the formation of large distortions during the cooling phase. These phenomena justify why so many studies used stationary shoulders and why other researcher recommended the use of this solution after facing difficulties with conventional tools. For conventional tools, the use of concave shoulders helped in the task of securing the material within the weld.

Regarding the study of the influence of the heating temperature of the tool, it was found that the optimal heating temperatures are between 100 and 177ºC. PE was also tested with induction heating of the tool and it was found that the temperature of 45ºC was ideal for this technique. In the case of PE, the heating of the material was also studied, resulting in an optimum preheating temperature of 50ºC or a contact time of 180 s with a heating plate at 150ºC. In all of these cases, the introduction of heat has always improved compared to the process at room temperature

5.2. Suggestions for future works

FSW of polymeric materials is a recent welding technique with many parameters involved and the amount of studies is not yet enough to characterize the process well. Thus, it is suggested that in the future more studies should be carried out to optimize the FSW in polymeric based materials.

From the information collected in this bibliographic review, it was possible to verify that parameters related with the axial force and plunge depth have been poorly studied, although their influence on the final quality of welding has been proven. Therefore, it is also suggested that in future studies greater importance should be given to the influence of these two parameters.

Since the heated and stationary tools have shown to bring advantages to the welding of polymeric materials by FSW, it is also suggested to continue to study the improvement of the different existing tools and the creation of new solutions.

The study of the quality of the union by FSW focused almost exclusively on tests on impact and static loads. Thus, it is still necessary to better understand the behavior of welded materials under fatigue loads.

Most studies neglect the analysis of the first centimeters of the weld because it appears that this initial zone has less quality. Since several authors have reported tensile and flexural strengths similar to that of the base material after zone of the welding, it is justified that in future works there is also an emphasis on improving the quality of the initial welding centimeters.

BIBLIOGRAPHY

[1] D. Mishra, S. K. Sahu, R. P. Mahto, S. K. Pal, and K. Pal, "Friction Stir Welding for Joining of Polymers," Springer, Singapore, 2019, pp. 123–162.

[2] M. Aydin, "Effects of welding parameters and pre-heating on the friction stir welding of UHMW-polyethylene," *Polym. - Plast. Technol. Eng.*, vol. 49, no. 6, pp. 595–601, Jan. 2010, doi: 10.1080/03602551003664503.

[3] S. Strand, "Joining plastics - Can Friction Stir Welding compete?," in *Electrical Insulation Conference and Electrical Manufacturing and Coil Winding Conference and Exhibition*, Sep. 2003, pp. 321–326, doi: 10.1109/eicemc.2003.1247904.

[4] N. Amanat, N. L. James, and D. R. McKenzie, "Welding methods for joining thermoplastic polymers for the hermetic enclosure of medical devices," *Medical Engineering and Physics*, vol. 32, no. 7. Elsevier, pp. 690–699, Sep. 01, 2010, doi: 10.1016/j.medengphy.2010.04.011.

[5] S. Strand, "Effects of Friction Stir Welding on Polymer Microstructure," *Theses Diss.*, Feb. 2004, Accessed: Jun. 01, 2020. [Online]. Available: https://scholarsarchive.byu.edu/etd/42.

[6] A. Rudawska, "Adhesive joint strength of hybrid assemblies: Titanium sheet-composites and aluminium sheet-compositesExperimental and numerical verification," *Int. J. Adhes. Adhes.*, vol. 30, no. 7, pp. 574–582, Oct. 2010, doi: 10.1016/j.ijadhadh.2010.05.006.

[7] A. Pramanik *et al.*, "Joining of carbon fibre reinforced polymer (CFRP) composites and aluminium alloys – A review," *Compos. Part A Appl. Sci. Manuf.*, vol. 101, pp. 1–29, Oct. 2017, doi: 10.1016/J.COMPOSITESA.2017.06.007.

[8] A. Yousefpour, M. Hojjati, and J. P. Immarigeon, "Fusion bonding/welding of thermoplastic composites," *Journal of Thermoplastic Composite Materials*, vol. 17, no. 4. pp. 303–341, Jul. 19, 2004, doi: 10.1177/0892705704045187.

[9] C. Ageorges, L. Ye, and M. Hou, "Advances in fusion bonding techniques for joining thermoplastic matrix composites: A review," *Compos. - Part A Appl. Sci. Manuf.*, vol. 32, no. 6, pp. 839–857, Jun. 2001, doi: 10.1016/S1359-

835X(00)00166-4.

[10] E. A. Squeo, G. Bruno, A. Guglielmotti, and F. Quadrini, “FRICTION STIR WELDING OF POLYETHYLENE SHEETS,” *Ann. “DUNĂREA JOS” Univ. Galati Fascicle V, Technol. Mach. Build.*, pp. 241–246, 2009.

[11] W. M. Thomas, E. D. Nicholas, J. C. Needham, M. G. Murch, P. Templesmith, and C. J. Dawes, “Friction Stir Butt Welding,” GB Patent 9125978.8, International Patent PCT/GB92/02203, 1991.

[12] W. Thomas and E. Nicholas, “Friction stir welding for the transportation industries,” *Mater. Des.*, vol. 18, no. 4–6, pp. 269–273, Dec. 1997, doi: 10.1016/S0261-3069(97)00062-9.

[13] W. M. Thomas, K. I. Johnson, and C. S. Wiesner, “Friction Stir Welding – Recent Developments in Tool and Process Technologies,” *Adv. Eng. Mater.*, vol. 5, no. 7, pp. 485–490, Jul. 2003, doi: 10.1002/adem.200300355.

[14] G. H. Payganeh, N. B. Mostafa Arab, Y. Dadgar Asl, F. A. Ghasemi, and M. Saeidi Boroujeni, “Effects of friction stir welding process parameters on appearance and strength of polypropylene composite welds,” *Int. J. Phys. Sci.*, vol. 6, no. 19, pp. 4595–4601, Sep. 2011, doi: 10.5897/IJPS11.866.

[15] R. S. Mishra and Z. Y. Ma, “Friction stir welding and processing,” *Mater. Sci. Eng. R Reports*, vol. 50, no. 1–2, pp. 1–78, Aug. 2005, doi: 10.1016/J.MSER.2005.07.001.

[16] R. Nandan, T. DebRoy, and H. K. D. H. Bhadeshia, “Recent advances in friction-stir welding – Process, weldment structure and properties,” *Prog. Mater. Sci.*, vol. 53, no. 6, pp. 980–1023, Aug. 2008, doi: 10.1016/J.PMATSCI.2008.05.001.

[17] M. Elyasi and H. A. Derazkola, “Experimental and thermomechanical study on FSW of PMMA polymer T-joint,” *Int. J. Adv. Manuf. Technol.*, vol. 97, no. 1–4, pp. 1445–1456, Jul. 2018, doi: 10.1007/s00170-018-1847-7.

[18] Y. Huang, X. Meng, Y. Wang, Y. Xie, and L. Zhou, “Joining of aluminum alloy and polymer via friction stir lap welding,” *J. Mater. Process. Technol.*, vol. 257, pp. 148–154, Jul. 2018, doi: 10.1016/J.JMATPROTEC.2018.02.043.

[19] M. T.S.M. Sai *et al.*, “Experimental Study on Effect of Welding Parameters of Friction Stir Welding (FSW) on Aluminium AA5083 T-joint,” *Inf. Technol. J.*, vol. 15, no. 4, pp. 99–107, Sep. 2016, doi: 10.3923/itj.2016.99.107.

[20] M. A. Rezgui, M. Ayadi, A. Cherouat, K. Hamrouni, A. Zghal, and S. Bejaoui, "Application of Taguchi approach to optimize friction stir welding parameters of polyethylene," *EPJWC*, vol. 6, p. 07003, 2010, doi: 10.1051/EPJCONF/20100607003.

[21] S. Inaniwa, Y. Kurabe, Y. Miyashita, and H. Hori, "Application of friction stir welding for several plastic materials," in *Proceedings of the 1st International Joint Symposium on Joining and Welding*, Elsevier, 2013, pp. 137–142.

[22] S. Eslami, J. F. Miranda, L. Mourão, P. J. Tavares, and P. M. G. P. Moreira, "Polyethylene friction stir welding parameter optimization and temperature characterization," *Int. J. Adv. Manuf. Technol.*, vol. 99, no. 1–4, pp. 127–136, Aug. 2018, doi: 10.1007/s00170-018-2504-x.

[23] S. Saeedy and M. K. B. Givi, "Experimental investigation of double side friction stir welding (FSW) on high density polyethylene blanks," in *ASME 2010 10th Biennial Conference on Engineering Systems Design and Analysis, ESDA2010*, Dec. 2010, vol. 4, pp. 845–848, doi: 10.1115/ESDA2010-25346.

[24] K. Kumar and S. V. Kailas, "The role of friction stir welding tool on material flow and weld formation," *Mater. Sci. Eng. A*, vol. 485, no. 1–2, pp. 367–374, Jun. 2008, doi: 10.1016/j.msea.2007.08.013.

[25] T. Machniewicz, P. Nosal, A. Korbel, and M. Hebda, "Effect of FSW traverse speed on mechanical properties of copper plate joints," *Materials (Basel).*, vol. 13, no. 8, p. 1937, Apr. 2020, doi: 10.3390/MA13081937.

[26] Z. Kiss and T. Czigány, "Effect of welding parameters on the heat affected zone and the mechanical properties of friction stir welded poly(ethylene-terephthalate-glycol)," *J. Appl. Polym. Sci.*, vol. 125, no. 3, pp. 2231–2238, Aug. 2012, doi: 10.1002/app.36440.

[27] A. Arici and T. Sinmaz, "Effects of double passes of the tool on friction stir welding of polyethylene," in *Journal of Materials Science*, Jun. 2005, vol. 40, no. 12, pp. 3313–3316, doi: 10.1007/s10853-005-2709-x.

[28] E. T. Akinlabi, "Characterisation of dissimilar friction stir welds between 5754 Aluminium alloy and C11000 copper." 2010.

[29] E. Azarsa, A. M. Asl, and V. Tavakolkhah, "Effect of process parameters and tool coating on mechanical properties and microstructure of heat assisted friction stir

welded polyethylene sheets," *Adv. Mater. Res.*, vol. 445, pp. 765–770, 2012, doi: 10.4028/www.scientific.net/AMR.445.765.

[30] B. Vijendra and A. Sharma, "Induction heated tool assisted friction-stir welding (i-FSW): A novel hybrid process for joining of thermoplastics," *J. Manuf. Process.*, vol. 20, pp. 234–244, Oct. 2015, doi: 10.1016/J.JMAPRO.2015.07.005.

[31] J. Y. Sheikh-Ahmad, D. S. Ali, S. Deveci, F. Almaskari, and F. Jarrar, "Friction stir welding of high density polyethylene—Carbon black composite," *J. Mater. Process. Technol.*, vol. 264, pp. 402–413, Feb. 2019, doi: 10.1016/J.JMATPROTEC.2018.09.033.

[32] F. Lambiase, A. Paoletti, V. Grossi, and A. Di Ilio, "Analysis of loads, temperatures and welds morphology in FSW of polycarbonate," *J. Mater. Process. Technol.*, vol. 266, pp. 639–650, Apr. 2019, doi: 10.1016/J.JMATPROTEC.2018.11.043.

[33] F. Lambiase, A. Paoletti, and A. Di Ilio, "Mechanical behaviour of friction stir spot welds of polycarbonate sheets," *Int. J. Adv. Manuf. Technol.*, vol. 80, no. 1–4, pp. 301–314, Sep. 2015, doi: 10.1007/s00170-015-7007-4.

[34] B. Kusharjanta, W. P. Raharjo, and Triyono, "Temperature comparison of initial, middle and final point of polypropylene friction stir welded," in *AIP Conference Proceedings*, Mar. 2016, vol. 1717, no. 1, p. 040011, doi: 10.1063/1.4943454.

[35] S. K. Sahu *et al.*, "Friction stir welding of polypropylene sheet," *Eng. Sci. Technol. an Int. J.*, vol. 21, no. 2, pp. 245–254, Apr. 2018, doi: 10.1016/J.JESTCH.2018.03.002.

[36] S. Eslami, T. Ramos, P. J. Tavares, and P. M. G. P. Moreira, "Effect of Friction Stir Welding Parameters with Newly Developed Tool for Lap Joint of Dissimilar Polymers," in *Procedia Engineering*, Jan. 2015, vol. 114, pp. 199–207, doi: 10.1016/j.proeng.2015.08.059.

[37] A. Arici and S. Selale, "Effects of tool tilt angle on tensile strength and fracture locations of friction stir welding of polyethylene," *Sci. Technol. Weld. Join.*, vol. 12, no. 6, pp. 536–539, Aug. 2007, doi: 10.1179/174329307X173706.

[38] R. W. Carter, "Auto-adjustable tool for self-reacting and conventional friction stir welding," United States Patent, US6758382 B1, May 02, 2004.

[39] G. Bjorkman and M. Cantrell, "Self-Reacting Friction Stir Welding for Aluminum Alloy Circumferential Weld Applications," Jan. 2003. Accessed: Jul. 20, 2020.

[Online]. Available: https://ntrs.nasa.gov/search.jsp?R=20030061190.

[40] M. Pirizadeh, T. Azdast, S. Rash Ahmadi, S. Mamaghani Shishavan, and A. Bagheri, "Friction stir welding of thermoplastics using a newly designed tool," *Mater. Des.*, vol. 54, pp. 342–347, Feb. 2014, doi: 10.1016/j.matdes.2013.08.053.

[41] S. Eslami, T. Ramos, P. J. Tavares, and P. M. G. P. Moreira, "Shoulder design developments for FSW lap joints of dissimilar polymers," *J. Manuf. Process.*, vol. 20, pp. 15–23, Oct. 2015, doi: 10.1016/J.JMAPRO.2015.09.013.

[42] Y. M. Romero, M. Moreno Moreno, B. Arrieta Cardozo, W. Plata Rueda, S. Consuegra Pacheco, and J. Unfried-Silgado, "Weldability of high-density polyethylene using friction stir welding with a non-rotational shoulder tool," *Weld. Int.*, vol. 32, no. 9, pp. 640–649, Sep. 2018, doi: 10.1080/09507116.2017.1347353.

[43] S. H. Dashatan, T. Azdast, S. R. Ahmadi, and A. Bagheri, "Friction stir spot welding of dissimilar polymethyl methacrylate and acrylonitrile butadiene styrene sheets," *Mater. Des.*, vol. 45, pp. 135–141, Mar. 2013, doi: 10.1016/j.matdes.2012.08.071.

[44] T. W. Nelson, C. D. Sorenson, and C. J. Johns, "Friction stir welding of polymeric materials," US Papent 6811632 B2, 2004.

[45] N. Mendes, A. Loureiro, C. Martins, P. Neto, and J. N. Pires, "Morphology and strength of acrylonitrile butadiene styrene welds performed by robotic friction stir welding," *Mater. Des.*, vol. 64, pp. 81–90, Dec. 2014, doi: 10.1016/j.matdes.2014.07.047.

[46] P. N. Banjare, P. Sahlot, and A. Arora, "An assisted heating tool design for FSW of thermoplastics," *J. Mater. Process. Technol.*, vol. 239, pp. 83–91, Jan. 2017, doi: 10.1016/J.JMATPROTEC.2016.07.035.

[47] A. Moochani, H. Omidvar, S. R. Ghaffarian, and S. M. Goushegir, "Friction stir welding of thermoplastics with a new heat-assisted tool design: mechanical properties and microstructure," *Weld. World*, vol. 63, no. 1, pp. 181–190, Jan. 2019, doi: 10.1007/s40194-018-00677-x.

[48] A. Mostafapour and E. Azarsa, "A study on the role of processing parameters in joining polyethylene sheets via heat assisted friction stir welding: Investigating microstructure, tensile and flexural properties," *Int. J. Phys. Sci.*, vol. 7, no. 4, pp. 647–654, 2012, doi: 10.5897/ijps11.1653.

[49] A. Mostafapour and F. Taghizad Asad, "Investigations on joining of Nylon 6 plates

via novel method of heat assisted friction stir welding to find the optimum process parameters," *Sci. Technol. Weld. Join.*, vol. 21, no. 8, pp. 660–669, Nov. 2016, doi: 10.1080/13621718.2016.1169669.

[50] S. Kang, J. Kim, Y. Jang, and K. Lee, "Welding Deformation Analysis, Using an Inherent Strain Method for Friction Stir Welded Electric Vehicle Aluminum Battery Housing, Considering Productivity," *Appl. Sci.*, vol. 9, no. 18, p. 3848, Sep. 2019, doi: 10.3390/app9183848.

[51] F. Lambiase, H. A. Derazkola, and A. Simchi, "Friction stir welding and friction spot stir welding processes of polymers-state of the art," *Materials*, vol. 13, no. 10. MDPI AG, May 01, 2020, doi: 10.3390/ma13102291.

[52] E. Nateghi and M. Hosseinzadeh, "Experimental investigation into effect of cooling of traversed weld nugget on quality of high-density polyethylene joints," *Int. J. Adv. Manuf. Technol.*, vol. 84, no. 1–4, pp. 581–594, Apr. 2016, doi: 10.1007/s00170-015-7663-4.

[53] "friction-stir-welding - TechMiny." https://techminy.com/friction-stir-welding/friction-stir-welding-2/ (accessed Aug. 31, 2020).

[54] R. Jain *et al.*, "Friction Stir Welding: Scope and Recent Development," in *Modern Manufacturing Engineering*, Springer International Publishing Switzerland, 2015, pp. 179–229.

[55] Z. Kiss and T. Czigány, "Applicability of friction stir welding in polymeric materials," *Period. Polytech. Mech. Eng.*, vol. 51, no. 1, pp. 15–18, 2007, doi: 10.3311/pp.me.2007-1.02.

[56] S. Hoseinlaghab, S. S. Mirjavadi, N. Sadeghian, I. Jalili, M. Azarbarmas, and M. K. Besharati Givi, "Influences of welding parameters on the quality and creep properties of friction stir welded polyethylene plates," *Mater. Des.*, vol. 67, pp. 369–378, Feb. 2015, doi: 10.1016/J.MATDES.2014.11.039.

[57] N. Mendes, A. Loureiro, C. Martins, P. Neto, and J. N. Pires, "Effect of friction stir welding parameters on morphology and strength of acrylonitrile butadiene styrene plate welds," *Mater. Des.*, vol. 58, pp. 457–464, Jun. 2014, doi: 10.1016/j.matdes.2014.02.036.

[58] Y. Bozkurt, "The optimization of friction stir welding process parameters to achieve maximum tensile strength in polyethylene sheets," *Mater. Des.*, vol. 35, pp. 440–

445, Mar. 2012, doi: 10.1016/j.matdes.2011.09.008.

[59] E. Azarsa and A. Mostafapour, "Experimental investigation on flexural behavior of friction stir welded high density polyethylene sheets," *J. Manuf. Process.*, vol. 16, no. 1, pp. 149–155, Jan. 2014, doi: 10.1016/j.jmapro.2013.12.003.

[60] M. Moreno-Moreno, Y. Macea Romero, H. Rodríguez Zambrano, N. C. Restrepo-Zapata, C. R. M. Afonso, and J. Unfried-Silgado, "Mechanical and thermal properties of friction-stir welded joints of high density polyethylene using a non-rotational shoulder tool," *Int. J. Adv. Manuf. Technol.*, vol. 97, no. 5–8, pp. 2489–2499, Jul. 2018, doi: 10.1007/s00170-018-2102-y.

[61] S. Saeedy and M. K. B. Givi, "Experimental application of friction stir welding (FSW) on thermo plastic medium density polyethylene blanks," in *ASME 2010 10th Biennial Conference on Engineering Systems Design and Analysis, ESDA2010*, Jan. 2010, vol. 4, pp. 841–844, doi: 10.1115/ESDA2010-25344.

[62] S. Saeedy and M. K. B. Givi, "Investigation of the effects of critical process parameters of friction stir welding of polyethylene," in *Proceedings of the Institution of Mechanical Engineers, Part B: Journal of Engineering Manufacture*, Aug. 2011, vol. 225, no. 8, pp. 1305–1310, doi: 10.1243/09544054JEM1989.

[63] Z. Kiss and T. Czigány, "Microscopic analysis of the morphology of seams in friction stir welded polypropylene," *Express Polym. Lett.*, vol. 6, no. 1, pp. 54–62, Jan. 2012, doi: 10.3144/expresspolymlett.2012.6.

[64] K. Panneerselvam and K. Lenin, "Investigation on effect of tool forces and joint defects during FSW of polypropylene plate," in *Procedia Engineering*, Jan. 2012, vol. 38, pp. 3927–3940, doi: 10.1016/j.proeng.2012.06.450.

[65] R. Sharma and O. P. Singh, "Effect of FSW Process Parameters on Mechanical Properties of Polypropylene: An Experimental Study," *Int. J. Innov. Res. Sci. Eng. Technol.*, vol. 2, pp. 7792–7798, 2013.

[66] K. Lenin, H. A. Shabeer, K. Suresh Kumar, and K. Panneerselvam, "Process parameters optimization for friction stir welding of Polypropylene material using Taguchi's approach," 2014.

[67] A. Bagheri, T. Azdast, and A. Doniavi, "An experimental study on mechanical properties of friction stir welded ABS sheets," *Mater. Des.*, vol. 43, pp. 402–409, Jan. 2013, doi: 10.1016/J.MATDES.2012.06.059.

[68] N. Sadeghian and M. K. Besharati Givi, “Experimental optimization of the mechanical properties of friction stir welded Acrylonitrile Butadiene Styrene sheets,” *Mater. Des.*, vol. 67, pp. 145–153, Feb. 2015, doi: 10.1016/j.matdes.2014.11.032.

[69] I. M. Husain, R. K. Salim, T. Azdast, S. Hasanifard, S. M. Shishavan, and R. E. Lee, “Mechanical properties of friction-stir-welded polyamide sheets,” *Int. J. Mech. Mater. Eng.*, vol. 10, no. 1, pp. 1–8, Dec. 2015, doi: 10.1186/s40712-015-0047-6.

[70] A. Zafar, M. Awang, S. R. Khan, and S. Emamian, “Effect of Double Shoulder Tool Rotational Speed on Thermo-Physical Characteristics of Friction Stir Welded 16mm Thick Nylon6,” *Appl. Mech. Mater.*, vol. 799–800, pp. 251–255, 2015.

[71] A. Zafar, M. Awang, S. R. Khan, and S. Emamian, “Investigating Friction Stir Welding on Thick Nylon 6 Plates,” *Weld. J.*, vol. 95, no. 6, pp. 210–218, Jun. 2016.

[72] H. Aghajani Derazkola, A. Simchi, and F. Lambiase, “Friction stir welding of polycarbonate lap joints: Relationship between processing parameters and mechanical properties,” *Polym. Test.*, vol. 79, p. 105999, Oct. 2019, doi: 10.1016/J.POLYMERTESTING.2019.105999.

[73] H. Aghajani Derazkola and A. Simchi, “Experimental and thermomechanical analysis of the effect of tool pin profile on the friction stir welding of poly(methyl methacrylate) sheets,” *J. Manuf. Process.*, vol. 34, pp. 412–423, Aug. 2018, doi: 10.1016/J.JMAPRO.2018.06.015.

[74] M. R. Adibeig, S. Hassanifard, F. Vakili-Tahami, and J. H. Hattel, “Experimental investigation of tensile strength of friction stir welded butt joints on PMMA,” *Mater. Today Commun.*, vol. 17, pp. 238–245, Dec. 2018, doi: 10.1016/J.MTCOMM.2018.09.009.

[75] A. K. R. Sharma, M. Roy Choudhury, and K. Debnath, “Experimental investigation of friction stir welding of PLA,” *Weld. World*, pp. 1–11, Mar. 2020, doi: 10.1007/s40194-020-00890-7.

[76] S. Eslami, M. A. V. de Figueiredo, P. J. Tavares, and P. M. G. P. Moreira, “Parameter optimisation of friction stir welded dissimilar polymers joints,” *Int. J. Adv. Manuf. Technol.*, vol. 94, no. 5–8, pp. 1759–1770, Feb. 2018, doi: 10.1007/s00170-017-0043-5.

[77] M. Rezaee Hajideh, M. Farahani, S. A. D. Alavi, and N. Molla Ramezani,

"Investigation on the effects of tool geometry on the microstructure and the mechanical properties of dissimilar friction stir welded polyethylene and polypropylene sheets," *J. Manuf. Process.*, vol. 26, pp. 269–279, Apr. 2017, doi: 10.1016/j.jmapro.2017.02.018.

[78] S. Kumar and B. S. Roy, "Novel study of joining of acrylonitrile butadiene styrene and polycarbonate plate by using friction stir welding with double-step shoulder," *J. Manuf. Process.*, vol. 45, pp. 322–330, Sep. 2019, doi: 10.1016/J.JMAPRO.2019.07.013.

[79] F. Lambiase, V. Grossi, and A. Paoletti, "Effect of tilt angle in FSW of polycarbonate sheets in butt configuration," *Int. J. Adv. Manuf. Technol.*, vol. 107, no. 1–2, pp. 489–501, Mar. 2020, doi: 10.1007/s00170-020-05106-2.

[80] K. Panneerselvam and K. Lenin, "Joining of Nylon 6 plate by friction stir welding process using threaded pin profile," *Mater. Des.*, vol. 53, pp. 302–307, Jan. 2014, doi: 10.1016/J.MATDES.2013.07.017.

[81] K. Panneerselvam and K. Lenin, "EFFECTS AND DEFECTS OF THE POLYPROPYLENE PLATE FOR DIFFERENT PARAMETERS IN FRICTION STIR WELDING PROCESS," *IJRET Int. J. Res. Eng. Technol.*, Accessed: Jul. 20, 2020. [Online]. Available: http://www.ijret.org.